UC Irvine
UC Irvine Electronic Theses and Dissertations

Title
Strategies to Achieve Magnetic Orientation with a Photoreceptor-based Chemical Compass

Permalink
https://escholarship.org/uc/item/8bv6w641

Author
Ma, Timothy

Publication Date
2017

Peer reviewed|Thesis/dissertation

eScholarship.org Powered by the California Digital Library
University of California

UNIVERSITY OF CALIFORNIA,
IRVINE

Strategies to Achieve Magnetic Orientation with a Photoreceptor-based Chemical Compass

DISSERTATION

submitted in partial satisfaction of the requirements
for the degree of

DOCTOR OF PHILOSOPHY

in Physics

by

Timothy Ma

Dissertation Committee:
Associate Professor Thorsten Ritz, Chair
Professor Zuzanna Siwy
Assistant Professor Jun Allard

2017

© 2017 Timothy Ma

DEDICATION

To mom and dad.
And to my sister, at this moment I have one more degree than you.

TABLE OF CONTENTS

LIST OF FIGURES

LIST OF TABLES

ACKNOWLEDGMENTS

I would like to thank my committee chair, Professor Thorsten Ritz, for his instruction as a mentor and teacher throughout my various projects.

I would like to thank Zuzanna Siwy for allowing me workspace in her lab and the encouraging environment to be surrounded by other biophysics students.

I would like to thank my lab beginning with the graduate student before me, Greg Zicarelli, for teaching me everything about fruit flies and previous research on our topic. Post-doc Gabriella Maria Procopio spent many hours reviewing the quantum physics with me. Phillise Todd underwent the same graduate student schedule alongside me.

I would like to thank John Phillips and his lab in Virginia Tech for allowing me to spend a summer learning their biological techniques.

I would like to thank UC Irvine and the DARPA Human Frontier Science Grant for their funding.

CURRICULUM VITAE

Timothy Ma

EDUCATION

Doctor of Philosophy in Physics **2017**
University of California, Irvine *Irvine, California*

Masters of Science in Physics **2011**
University of California, Irvine *Irvine, California*

Bachelors of Arts in Physics **2010**
University of California, Berkeley *Berkeley, California*

Bachelors of Arts in Astronomy **2010**
University of California, Berkeley *Berkeley, California*

RESEARCH EXPERIENCE

Graduate Research Assistant **2011–2017**
University of California, Irvine *Irvine, California*

Undergraduate Research Assistant **2009–2010**
University of California, Berkeley *Berkeley, California*

Research Intern **2008**
Alameda Applied Sciences Corporation *San Leandro, California*

Research Intern **2007**
General Atomics *San Diego, California*

TEACHING EXPERIENCE

Teaching Assistant **2010–2011**
University of California, Irvine *Irvine, California*

Service

President, Associated Graduate Students **2015–2016**
University of California, Irvine *Irvine, California*

Vice President of External Affairs, Associated Graduate Student **2014–2015**
University of California, Irvine *Irvine, California*

Board Member, UC Irvine Alumni Association **2015–2016**
University of California, Irvine *Irvine, California*

Legislative Liaison, Associated Graduate Students **2013–2014**
University of California, Irvine *Irvine, California*

Board Member, UC Student Association **2013–2015**
University of California *Oakland, California*

Environmental Liaison, UC Student Association **2013–2014**
University of California *Oakland, California*

Member, Physics Grad Caucus **2010–2017**
University of California, Irvine *Irvine, California*

REFEREED CONFERENCE PUBLICATIONS

M. Krishnan, J. Wright, and T. Ma, A Fast, Electromagnetically Driven Supersonic Gas Jet Target For Laser Wakefield Acceleration **Jun 2009**
AIP Conf. Proc. 1086, 264

ABSTRACT OF THE DISSERTATION

Strategies to Achieve Magnetic Orientation with a Photoreceptor-based Chemical Compass

By

Timothy Ma

Doctor of Philosophy in Physics

University of California, Irvine, 2017

Associate Professor Thorsten Ritz, Chair

Researchers have found a wide range of organisms to possess the ability to detect, align, and navigate using magnetic fields. While this biophysical mechanism is unknown in most species, there are two leading theories. The first is ferromagnetism which involves either giving animals a physical torque towards the magnetic field, or a cellular channel that is sensitive to magnetic fields. The second theory involves the use of the radical pair mechanism where a spin-correlated pair of radical electrons reacts to the magnetic field through a combination of the hyperfine and Zeeman interactions. The radical electrons are then able to proceed to a spin-selective reaction that may produce a nervous signal.

Under the premise that many photoreceptors on the retina of an eye contain a radical pair magnetic sensor, a procedure is formed to collect the magnetic signal and use it to align or orient oneself. The model must take into account the various angles associated with the magnetic field and surface of the retina, along with possible rotations that the eye can make. The process of orienting involves a simple control loop, and noise is introduced to test the overall robustness of the system to a wide variety of possible pitfalls. A virtual reality simulation using Google Cardboard was created to show what magnetic vision could look like to a human and to birds.

Many experiments were performed on Drosophila melanogaster under a series of different

gradient and uniform magnetic fields in horizontal and vertical conditions in a Hirsh maze. The fruit flies exhibited a naïve avoidance of magnetic fields at ten times Earth strength fields and were affected by very low intensity magnetic fields.

Chapter 1

Introduction

Magnetoreception is the sensory ability to perceive magnetic fields. The extent and purpose for this ability varies greatly from contributing to circadian rhythms to possibly creating mental map for direction and navigation objectives. The mechanism for magnetoreception for some basic bacteria is well understood, but the mechanisms for larger, more complex animals such as insects and mammals have not yet been confirmed. To get to the current state of magnetoreception, I want to answer a few questions. How do we get to where we are now? What is the basic model? What are the steps to get to the current model? What are the alternate processes for all of these steps? Are these alternates feasible?

1.1 Earth's Magnetic Field

Different information can be pieced from Earth's magnetic field. There are different levels of magnetic perception and how it can affect an animal. On the most basic level, Drosophilae Melanogaster can at least simply detect the presence of Earths magnetic field [14]. By changing the duration of exposure to the magnetic field, the circadian rhythm of Drosophila

were affected so that their period of being awake was both shifted and elongated.

The next level of magnetic information to be perceived from the Earth is similar to the simple compass. This can work in different ways. Like a bar magnet, its possible to have a compass that always points North, even in the southern hemisphere. Theres another type of compass such as a paperclip that will point towards North in the northern hemisphere or south in the southern hemisphere. It does not feel the polarity of the magnetic field but simply points in the direction of the strongest field.

The next level of information is both the use of an inclination compass and detection of strength of the magnetic field. This is closely related to the last compass in that it points in the direction of the strongest magnetic field. Because the world is round, the strongest magnetic field is made some angle into the Earth. At the magnetic North pole, the field direction is straight down, but at the equator, the field is parallel with Earths surface. Being able to detect the inclination of the magnetic field means being able to tell the users latitude. Earths magnetic field has a strength of roughly 0.5 Gauss, but it can vary from 0.25 Gauss to 0.6 Gauss.

1.2 Biology & Possible Mechanisms

1.2.1 Observational Biology

The earliest experiments start with the Wilschkos in the 1960's. They tested various animals including molluscs, arthropods, fish, birds, and mammals. They tested these animals for the different kinds of compasses they could have whether they be polarity or inclination compasses. Polarity compasses will tell which way is north, and inclination compasses will tell what direction the strongest field occurs in.

The most prominent experiments put migratory European robins into large paper funnels and found a few things. They can sense Earths magnetic field, they have an inclination compass, and they can only sense it under blue/green light, but not yellow-red or no light [52]. Red Foxes [9] have an increased success rate of 60% catching unseen prey underneath a layer of snow by hunting when traveling north-east. When hunting in other directions, their success rate is 15%. These foxes mostly hunt using their sense of hearing, and they can possibly use the magnetic field to figure out the distance to the prey.

Dogs have been observed to defecate with not only a preference of being aligned with the magnetic field, [18] but an avoidance of the east west line. Bees do a waggle dance which is their language of communication [50]. On a honeycomb they are found to orient themselves with the eight cardinal directions. However, when the magnetic field is disrupted by being zeroed out or increased too much, then they lose their orientation sense.

1.2.2 Magnetite as a Method of Magnetoreception

Bacteria have been shown to have ferromagnetic particles. These magnetite crystals (Fe_3O_4) have dipoles that align themselves with the north south axis. With their flagellum, they can control their depth in water [22]. This use of magnetite does not require response because the bacteria will be natural aligned.

Magnetite mechanisms have been proposed for larger animals as one sense of many to make decisions on navigation. Magnetite is the most dense and conductive biogenic solid known to exist. The molecule at temperatures above 120K are ordered in a structure that creates ordered magnetic moments [19]. Mollusks teeth are capped with magnetite. Honey bees and birds have been found to have organic magnetite. Both single-domain and superparamagnetic magnetite crystals have been found within the ethmoid region and upper beak of migratory birds and homing pigeons [3], [51]. There are many strategies for this to work.

One would be a cell membrane that has a magnetite material. The cell can spin somewhat freely like a compass, and when the cell is oriented in a certain direction with the rest of the body, then a short circuit can happen and a signal occurs. There are different energies for this elongated ellipsoid that need to be accounted for which include the magnetostatic energy, bending energy, energy to change the volume and stretching elastic energy [43].

Another method is called a torque receptor. If many of these magnetite molecules are oriented together in a straight line, their magnetic moments will add up. If this rod is externally on the skin and connected to hair cells, the animal could feel a slight tug in one direction from all the hairs getting tugged towards the magnetic field. The torque is given by the simple formula:

$$\mathbf{D}_m = m \times \mathbf{H} \tag{1.1}$$

where m is the permanent magnetic moment and H is the external magnetic field.

This paramagnetic mechanism has been hypothesized to occur in three different ways, notably by single-domain magnetite particles [23], fixed super-paramagnetic magnetite particles, and magnetite-containing liquid crystals [13]. Single domain magnetite are materials that once magnetized by an external field, will lose their dipole moment once the external field is gone. Super-paramagnetic materials can keep their dipole moment long after the external field is gone. There is a hypothesis that the magnetite-containing liquid crystals can modulate the intensity of light. For a superparamagnetic collective crystal with shape anisotropy, the type II torque is given by

$$\mathbf{D}_\chi = V(\chi \cdot \mathbf{H}) \times \mathbf{H} \tag{1.2}$$

where χ is the tensor of the apparent magnetic susceptibility of the particle collective and V is its volume.

Permanent magnets attached to the head of birds resulted in loss of ability to orient. Further tests have been done in which the ophthalmic nerve, which connects the upper beak to the brain, was cut. Birds could no longer tell the difference between natural and perturbed fields, but they could still navigate in the testing facility. One more additional test was done where birds were subjected to a strong magnetic pulse in order to magnetize the particles in a different way. They found little change in their ability to orient. This would indicate that they were either using visual cues or an alternate magnetoreceptor mechanism such as photopigments [4].

1.2.3 Electrical Induction as a Method of Magnetoreception

Fish have been shown to have sensitivity to electrical/magnetic materials. Catfish avoid metallic rods that are largely exposed to water, but will nibble on metallic rods that are only slightly exposed to water. Catfish show no reaction to glass rods in water. In the same paper, sharks were able to use electrical fields to navigate for food [20]. The mechanism for this effect is called ampullae of Lorenzi. Throughout the nose and head of a shark, there are little pores that are connected to each other. These pores detect voltages, and the shark can tell the direction of a difference in voltage change. They can detect as low as 0.1 $\mu V/cm$. At this voltage, the current along the tubes is 5×10^{-11} A. These pores are not found in birds, nor do they seem to be sensitive to magnetic fields [31]. Birds do not have these ampullae of Lorenzi. Also there is not much variation in electric field strengths over ground, so birds and other land animals would not be able to use this for navigation anyway.

1.2.4 Experimental Biology

There has been a great deal of lab experiments on animals that probe the magnetic sense in a controlled environment. These range from insects, reptiles, birds, to mammals. I'll only

be going through a few significant ones.

In the 1960's, European robins [52] were tested in a paper funnel structure (Kramer cages). They caught birds in the spring and autumn time and put them in the assay. They put these birds in for one night and would look at their scratching on the paper funnel the next day. With high significance during the spring, they would scratch north. When the horizontal component of the magnetic field was changed, they would scratch towards the new north, but when they reversed the vertical component of the magnetic field, the birds would scratch south. Also they found that birds would only exhibit this behavior under green through violet light. Under no light or red-yellow light, the birds exhibit no magnetic behavior.

The most convincing experiments done on Drosophila melanogaster are ones in which flies are trained under certain magnetic conditions, and in a new setting, these flies move along their trained direction. In one experiment [36] flies were put in one of four training boxes where they learned to associate a light motivation with an angle of the magnetic field. Then in the testing facility, they were put in a radial assay where they moved around within the magnetic field. The lab found that male flies, under an Earth strength magnetic field, moved in their trained direction significantly, indicating they use the magnetic field as a compass. However, females did not show any sort of behavior.

Another test in a T-maze [15] trained flies in a five gauss magnetic field. Their naïve response is to naturally avoid the field, but after being trained to associate the magnetic field with a sucrose reward, flies moved significantly towards a strong magnetic field. Differing from the above experiment, most males and females showed this behavior. They found the most significance happened under a full spectrum of light. There was still significance under short wavelength length, but flies lost their magnetic sense under long wavelength light.

Mice [37] were trained inside a water assay where one of four directional arms has a small hidden platform that a mouse could climb up onto and get out of the water. Mice were given

two training sessions where they could learn to identify where this platform was in relation to an Earth strength magnetic field. Then in the testing session, this platform was removed, and the amount of time they spent in one of these arms was recorded. Mice spent more time, as predicted, in the arm they were trained to associate with the magnetic field.

Newts [10] have been shown to have an extra light receptor. Newts want to align themselves on an axis where they can swim to shore. They were trained to associate the magnetic field with the direction of shore. After training sessions, newts aligned themselves bimodally on an axis perpendicular to shoreline. However, when they were tested under long-wavelength red light, they aligned bimodally parallel to shore. Under different wavelengths of light, these newts would either align with the magnetic field or 90° away from the field. Newts have a pineal gland on the top of head that can sense red light. So a red filter cap was put on top of this receptor so that under full spectrum light, only red light would get through. They found the same response as testing under red light which indicates that this pineal gland has a photoreceptor sensitive related to magnetic fields. Under the presumption that the magnetic sense is dependent on the spin of an electron, experiments were done on animals in the geostatic field with an oscillating field at precise frequencies to disrupt any magnetic ability. A weak oscillating field would disrupt the chemical process and the angle this oscillating field makes with the static field would affect the amount of this disruption. Birds were subjected to a vertical 7 MHz at a 0.47 μT magnetic field [40], and found that the birds would lose their directional sensitivity. When this field was parallel with the geomagnetic field, directional sensitivity was not lost. This would also indicate that magnetite particles are not in play because a much stronger field at the vertical angles is needed to create a comparably different direction magnetic field. More tests were done at 1.315 MHz [46], or the Larmor frequency of an electron at an Earth strength magnetic field. This Larmor frequency is the rate at which an electron precesses in a magnetic field. The strength of this oscillating field was 485 nT, roughly 100 times smaller than the Earth strength magnetic field. The magnetic sense was still disrupted, indicating that this resonance frequency that disrupts the electron

spin greatly affects the magnetic sense. Magnetite has a natural resonant frequency at 1.3 GHz, so these experiments were done in a range far away from a frequency that could affect magnetite particles [40].

1.3 Basic Physics

1.3.1 Radical Pair Mechanism Introduction

Much of the experimental biology points to a close relationship between the ability to use the magnetic field as a compass and the ability to perceive certain frequencies of light. The radical pair mechanism is the main theory of magnetoreception other than the use of magnetite particles. The radical pair mechanism utilizes the magnetic field effect on energy levels at a quantum level. These differing energy levels cause certain spin states to be more probable, and then these spin states are propagated to cause certain chemical reactions to happen more frequently which can lead to a nervous system response and the ability to perceive information about Earth's magnetic field.

A radical is an atom or molecule with an unpaired electron in its valence shell. A radical pair is created when a pair of valence electrons gets split up and one electron hops over to another molecule. In this scenario, we have two molecules that are now radicals, and because the electrons came from the same pair, the spins are correlated. This is called the radical pair.

1.3.2 Light Activation

Through the evidence that magnetic ability is linked to blue-green photoreceptors, the next logical idea is that these photoreceptors are obviously located in the eye. Because of the

evidence of sensitivity to specifically blue-green light, there are a few photoreceptors that are candidates to start the magnetic sense. Birds have rods and cones as humans do. Birds have four cone receptors for color [17]. These four correspond with a red, green, blue, and ultraviolet cone. These cones are closely related and contain different pigments made of oil droplets. They are located in the distal portion of the cone cell and contain carotenoid pigments. The rods contain rhodopsin and they also sense blue-green light. Under this model, it may be reasonable that magnetic sensitivity increases as intensity of the light increases. However, both aviary rods and cones do not contain the mechanisms needed to create a radical pair. The other photoreceptor in the required frequency range is cryptochrome, which is a blue ultraviolet-A receptor [8]. In Drosophila and mammals, cryptochromes mediate various light responses that affect different circadian rhythms such as time awake and protein generation cycles. Cryptochrome has two chromophores which are responsible for the color. When light hits the chromophore, it changes shape and then reflects and transmits light. There are two main forms of natural, un-mutated cryptochrome: Cry1 and Cry2. They are very similar, but Cry1 is slightly more potent. Cryptochrome is capable of creating a radical pair.

The cryptochrome molecule is relatively large molecule. Because we specifically want to look at the photoreception mechanism, we need to consider the specific parts of cryptochrome that react to light. Cryptochromes are a flavoprotein contains a photolyase structure. A flavoprotein contains a flavin molecule which are known to accept one or two electrons in a oxidation-reduction reaction. Photolyases are enzyme photoreceptors typically found in plants that repair DNA caused by UV light. The process is started by exposure to visible light that initiates a redox reaction. This flavin molecule is often attached with adenosine diphosphate to form FAD ($C_{27}H_{33}N_9O_{15}P_2$). Cryptochrome has two chromophores: one is FAD which is the catalytic enzyme for photolyases. The second chromophore, which is either pterin or deazaflavin, is the light harvester, whose excitation energy gets transferred to the FAD. Its high extinction coefficient means that the chromophore absorbs a lot of energy

per its mass. Deazaflavin absorbs a photon of 300-500 nm. Tryptophan is a candidate pair molecule inside cryptochrome that holds the other radical pair electron. There are three tryptophan amino acids: Trp400, Trp324, Trp377. These three molecules could transfer electrons between themselves are within the cryptochrome receptor and one of them could possibly donate its electron to the FAD molecule.

It's possible to esimate the rate constant k for electron transfer from Trp377 to Trp400 using Marcus' formula [44]

$$\log_{10} k = 15 - .434\beta \cdot R - 3.1\frac{(\Delta G + \lambda)^2}{\lambda} \tag{1.3}$$

where ΔG is the driving force of the electron transfer. λ is the protein reorganization energy, β is the electrontic coupling factor and R denotes the contact distance between donor and acceptor molecules.

1.3.3 Radical Pair Basics

At the most basic level, the only additional quantum effects we need to consider are the Zeeman effect and the hyperfine interaction. The method of extracting magnetic information in the actual radical pair mechanism is based off of those interactions and others which include dipole-dipole interactions and an exchange interaction. Within a complex molecule such as cryptochrome, there can be multiple sources for these interactions, complicating the theory and the math further which requires even further techniques such as density functional theory.

1.3.4 Zeeman Interaction

The Zeeman interaction couples the unpaired radical electron with the external magnetic field. The spin of the electron creates a magnetic field, so dependent on the angle that the spin makes with the external magnetic field, the energy of the electron changes by a miniscule amount. Electrons, with opposite spin that were once degenerate, split apart so that energy levels are different. This is the basis for how Earths magnetic field can create a magnetic compass. This energy level difference will be propagated to a chemical reaction difference that can lead to a chemical and then a nervous response that can be perceived.

The Hamiltonian for the Zeeman interaction is given by:

$$H_{Zeeman} = \frac{g\mu_b B_0 \hat{S}_z}{\hbar} = \omega \hat{S}_z \tag{1.4}$$

where g is the g-factor of the particle and μ_b is the magnetic moment

1.3.5 Hyperfine Interaction

The hyperfine interaction couples the unpaired radical electron with the internal magnetic field of the nucleus. This is similar to the Zeeman effect, except the magnetic field comes internally from the nucleus and not externally. There are two contributions to the hyperfine interaction. In isotropic liquids, the molecules are usually tumbling and rotating, so this magnetic field is averaged out to zero, and the energy levels do not split. However in our case, the media is solid and oriented, so the magnetic field is anisotropic. The second contribution comes from the electron being inside of the nucleus. This only occurs for the electron that is in the s-shell, and because the electron is defined by its wavefunction, the electron can actually be inside the nucleus. In this case, the hyperfine interaction is scalar and does not depend on the spin of the electron. While the magnitude of the Zeeman effect depends on

the strength of the external field, the magnitude of the hyperfine interaction is dependent on the magnetic field created by the nucleus. In relative terms, the fine interaction, which is the coupling of the orbital angular momentum with the spin of the electron, is on an order of α^2 smaller than the electric force. The hyperfine interaction is roughly 2000 times smaller than the fine interaction. This number comes from the difference in mass between the proton and electron.

The Hamiltonian for the Hyperfine interaction is given by:

$$H_{HFC} = \vec{S_1}\mathbf{A}\vec{I} \tag{1.5}$$

where $\vec{S_1}$ is the spin of one electron, $\mathbf{A}$ is the hyperfine tensor, and $\vec{I}$ is the spin of the nucleus.

1.3.6 Dipole-Dipole interaction and the Exchange interaction

While the previous two effects are the major contributors to the radical pair mechanism, there are smaller interactions that can have an effect. Because the radical pair mechanism relies on the pair of radical electrons, there is an interaction between the two that comes from the magnetic fields of the electrons on each other. This interaction becomes weak if the electrons are far away from each other [32]. At short distances, this interaction can affect the electrons spin and deter the magnetic field effect.

The dipole dipole interaction is given by

$$\hat{H_D} = \hat{\mathbf{S}}_1 \cdot D \cdot \hat{\mathbf{S}}_2 \tag{1.6}$$

where D is the dipolar tensor.

However, at certain short distances, the wavefunctions of the electrons overlap, and the electrons become indistinguishable. What happens in this domain is that the nuclear forces on one electron will also act on the other electron and vice versa. As their wavelengths overlap, the electrons are forced to take different states. This causes one electron to have a higher energy than the other. The lower energy electron is in a bonding orbital that is more preferential to forming a bond with another molecule. The other electron forms an antibonding orbital with a higher energy and less stability. At closer distances, this difference in energy is higher [33]. The exchange interaction and the dipole-dipole interaction can cancel each other out at certain distances.

The exchange interaction is given by

$$H_{ex} = -J\hat{\mathbf{S}}_1 \cdot \hat{\mathbf{S}}_2 \tag{1.7}$$

where J is dependent on the distance r between the electrons and is given by $J(r) = J_0 e^{\frac{-r}{r_j}}$

1.3.7 Singlet-Triplet Mixing

So now that all the interactions are introduced, the mechanism for the radical pair can be described. This model is the most basic model available, and most likely not the actual mechanism that animals use. The only interactions we describe in the most basic model are the hyperfine interaction and the Zeeman effect. The most basic radical pair is one hydrogen atom with a radical electron [48], and the other radical electron on the other nucleus but not including any interaction from that nucleus. The Hamiltonian for this basic model is

$$\hat{H} = \vec{\omega_0} \cdot (\hat{S}_1 + \hat{S}_2) + \hat{S}_1 \cdot \mathbf{A} \cdot \hat{I} \tag{1.8}$$

S_1 and S_2 are the spin angular momentum operators of the electrons, and I is the spin angular momentum operator of the nucleus, which in our simplest case is just a proton. The first term describes the Zeeman interaction on both of the electrons, and the second term describes the hyperfine interaction between one electron and one proton. There are other terms we leave out for simplicity purposes so we neglect the hyperfine interaction between the second electron and its nucleus, cross interactions between one nucleus and the other electron, multiple hyperfine interactions on one electron, and dipole-dipole and exchange interactions between the electrons.

Back to the Hamiltonian, ω_0 is the Larmor frequency in the applied magnetic field **B** that describes the electrons precession in a magnetic field that is determined by the mass and charge of the electron. **A** describes the anisotropic hyperfine tensor.

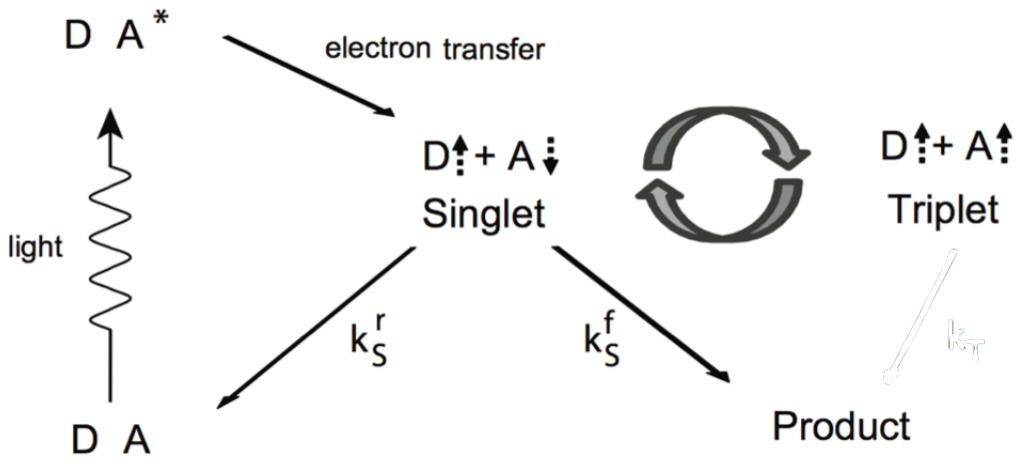

Figure 1.1: Basic Radical Pair Mechanism Diagram, [38]

1.3.8 Spin Dynamics

In the radical pair mechanism, a radical pair is formed in a singlet or triplet state. Singlet triplet pairs oscillate as a variety of frequencies given by the hyperfine and Zeeman interactions.

The typical process starts with the overall system composed of two molecules that are labeled D for donor and A for acceptor. Through the light activation process, one electron transfers from the donor to acceptor. Because it was a pair, one is spin up and the other has spin down. Whether this pair starts in the singlet or triplet state depends on the ground state of the molecule. Because of conservation of angular momentum, these electrons keep their spins as they change in energy level as long as no other forces act on them. The electron transfer doesnt change the spin states moves and electron over the from the donor molecule over to the acceptor molecule, creating the radical pair.

At this point, the pair is in a singlet state because electrons still have opposite spin and zero total angular momentum. But under the effect of the hyperfine interactions and the Zeeman interactions, the electrons have a probability of converting to a triplet state. The geomagnetic field effects the zero-field singlet triplet oscillations by adding new channel oscillations.

1.3.9 Liouville von Neumann Equation

While the Schrodinger equation describes how pure states evolve in time, the Liousville von Neumann Equation describes how a density matrix evolves with time. In its most basic form, the von Neumann equation is

$$i\hbar\frac{\partial\rho}{\partial t} = [H, \rho] \tag{1.9}$$

In the case where the Hamiltonian is time independent, the differential equation can be

solved to a simplier:

$$\hat{\sigma}(t) = e^{-\frac{iHt}{\hbar}} \hat{\sigma}(0) e^{\frac{iHt}{\hbar}} \tag{1.10}$$

where $\hat{\sigma}$ is the spin density operator. In system with singlet and triplet states, the inital spin density operator is given by the singlet projection operator divided by the number of nuclear spin configurations. This gives us:

$$\hat{\sigma}(t) = \frac{1}{M} e^{-\frac{iHt}{\hbar}} \hat{P}^S e^{\frac{iHt}{\hbar}} \tag{1.11}$$

1.3.10 Introduction to Finding the Singlet Yield

Then the fraction $\rho_s(t)$ of radical pairs in the singlet state of some time t is the trace of the singlet part of $\hat{\sigma}(t)$:

$$\rho_s(t) = Tr[\hat{P}^S \hat{\sigma}(t)] = \sum_{m=1}^{4M} \langle m| \hat{P}^S \hat{\sigma}(t) |m\rangle = \sum_{m=1}^{4M} \sum_{n=1}^{4M} \langle m| \hat{P}^S |n\rangle \langle n| \hat{\sigma}(t) |m\rangle \tag{1.12}$$

$|m\rangle$ and $|n\rangle$ are eigenstates of $\hat{H}$ with energies $\omega_m = \langle m| \hat{H} |m\rangle$ and ω_n. The last term $\langle n| \hat{\sigma}(t) |m\rangle$ are the coherent superpositions of pairs of eigenstates. Because only the coher-

ences depend on time, it can be separated out so that

$$\langle n|\,\hat{\sigma}(t)\,|m\rangle = \frac{1}{M}\,\langle n|\,e^{-i\hat{H}t}\,|n\rangle\,\langle n|\,\hat{P}^S\,|m\rangle\,\langle m|\,e^{+i\hat{H}t}\,|m\rangle = \frac{1}{M}P^S_{mn}e^{i\omega_{mn}t} \tag{1.13}$$

This turns into a final form of fraction of radical pairs in the singlet state:

$$\rho_s(t) = \frac{1}{M}\sum_{m=1}^{4M}\sum_{n=1}^{4M}|P^S_{mn}|^2\cos\omega_{mn}t \tag{1.14}$$

Because we are interested in the actual singlet yield over time and not at one point in time, we can use a first order integral rate law and find the total singlet yield.

$$\Phi_s = k\int_0^\infty \rho_s(t)e^{-kt}dt \tag{1.15}$$

after substituitions and some math, the final form of singlet yield becomes:

$$\Phi_s = \frac{1}{M}\sum_{m=1}^{4M}\sum_{n=1}^{4M}|P^S_{mn}|^2 f(\omega_{mn}) \tag{1.16}$$

where $f(x) = \frac{k^2}{k^2+x^2}$. Looking at this final form, P^S_{mn} describes the singlet character of the eigenstates. The new eigenstates are composed of a combination of singlet and triplet states, so it quantifies the amount of singlet state within the eigenstate. The second term, $f(\omega_{mn})$ describes the quantum coherences between the two eigenstates. It quantifies the rate at which the system will change from one eigenstate to the next.

1.3.11 Calculating the Singlet Yield

Under the above Hamiltonian, we can write a basis for three particles, each with two spin states. With two spin states, the 2×2 Pauli spin matrices are used to describe the particles.

$$\hat{S}_1 = \begin{bmatrix} \hat{S}_x \otimes \mathbb{1} \otimes \mathbb{1} \\ \hat{S}_y \otimes \mathbb{1} \otimes \mathbb{1} \\ \hat{S}_z \otimes \mathbb{1} \otimes \mathbb{1} \end{bmatrix} \qquad \hat{S}_2 = \begin{bmatrix} \mathbb{1} \otimes \hat{S}_x \otimes \mathbb{1} \\ \mathbb{1} \otimes \hat{S}_y \otimes \mathbb{1} \\ \mathbb{1} \otimes \hat{S}_z \otimes \mathbb{1} \end{bmatrix} \qquad \hat{I} = \begin{bmatrix} \mathbb{1} \otimes \mathbb{1} \otimes \hat{I}_x \\ \mathbb{1} \otimes \mathbb{1} \otimes \hat{I}_y \\ \mathbb{1} \otimes \mathbb{1} \otimes \hat{I}_z \end{bmatrix}$$

This basis can then be written in terms of:

$$\left| \hat{S}_1, \hat{S}_2, \hat{I} \right\rangle \tag{1.17}$$

Now further, we can explicitly write all eight of the possible states simply by their spins. The possibilities are

$$|\uparrow\uparrow\uparrow\rangle, |\uparrow\uparrow\downarrow\rangle, |\uparrow\downarrow\uparrow\rangle, |\uparrow\downarrow\downarrow\rangle, |\downarrow\uparrow\uparrow\rangle, |\downarrow\uparrow\downarrow\rangle, |\downarrow\downarrow\uparrow\rangle, |\downarrow\downarrow\downarrow\rangle \tag{1.18}$$

However, it can also be written in a singlet and triplet basis for the electrons. The arrow still represents the state of the nucleus in our system. So these would be written as

$$|S_0 \uparrow\rangle, |T_- \uparrow\rangle, |T_0 \uparrow\rangle, |T_+ \uparrow\rangle, |S_0 \downarrow\rangle, |T_- \downarrow\rangle, |T_0 \downarrow\rangle, |T_+ \downarrow\rangle \tag{1.19}$$

To convert between these two basis, we can use this 8×8 matrix.

$$
\begin{array}{c}
 \\
|T_+ \uparrow\rangle \\
|T_+ \downarrow\rangle \\
|T_0 \uparrow\rangle \\
|T_0 \downarrow\rangle \\
|S_0 \uparrow\rangle \\
|S_0 \downarrow\rangle \\
|T_- \uparrow\rangle \\
|T_- \downarrow\rangle
\end{array}
\begin{array}{c}
\begin{array}{cccccccc}
|\uparrow\uparrow\uparrow\rangle & |\uparrow\uparrow\downarrow\rangle & |\uparrow\downarrow\uparrow\rangle & |\uparrow\downarrow\downarrow\rangle & |\downarrow\uparrow\uparrow\rangle & |\downarrow\uparrow\downarrow\rangle & |\downarrow\downarrow\uparrow\rangle & |\downarrow\downarrow\downarrow\rangle
\end{array} \\
\left[\begin{array}{cccccccc}
1 & 0 & 0 & 0 & 0 & 0 & 0 & 0 \\
0 & 1 & 0 & 0 & 0 & 0 & 0 & 0 \\
0 & 0 & \frac{1}{\sqrt{2}} & 0 & \frac{1}{\sqrt{2}} & 0 & 0 & 0 \\
0 & 0 & 0 & \frac{1}{\sqrt{2}} & 0 & \frac{1}{\sqrt{2}} & 0 & 0 \\
0 & 0 & \frac{1}{\sqrt{2}} & 0 & -\frac{1}{\sqrt{2}} & 0 & 0 & 0 \\
0 & 0 & 0 & \frac{1}{\sqrt{2}} & 0 & -\frac{1}{\sqrt{2}} & 0 & 0 \\
0 & 0 & 0 & 0 & 0 & 0 & 1 & 0 \\
0 & 0 & 0 & 0 & 0 & 0 & 0 & 1
\end{array}\right]
\end{array}
\tag{1.20}
$$

The singlet projection operator for this one-proton radical pair is

$$\hat{P}^S = |S \uparrow\rangle \langle S \uparrow| + |S \downarrow\rangle \langle S \downarrow| \tag{1.21}$$

which explicity written is

$$\hat{P}^S = \begin{array}{c} \\ |\uparrow\uparrow\uparrow\rangle \\ |\uparrow\uparrow\downarrow\rangle \\ |\uparrow\downarrow\uparrow\rangle \\ |\uparrow\downarrow\downarrow\rangle \\ |\downarrow\uparrow\uparrow\rangle \\ |\downarrow\uparrow\downarrow\rangle \\ |\downarrow\downarrow\uparrow\rangle \\ |\downarrow\downarrow\downarrow\rangle \end{array} \begin{array}{c} \begin{array}{cccccccc} |\uparrow\uparrow\uparrow\rangle & |\uparrow\uparrow\downarrow\rangle & |\uparrow\downarrow\uparrow\rangle & |\uparrow\downarrow\downarrow\rangle & |\downarrow\uparrow\uparrow\rangle & |\downarrow\uparrow\downarrow\rangle & |\downarrow\downarrow\uparrow\rangle & |\downarrow\downarrow\downarrow\rangle \end{array} \\ \left[\begin{array}{cccccccc} 0 & 0 & 0 & 0 & 0 & 0 & 0 & 0 \\ 0 & 0 & 0 & 0 & 0 & 0 & 0 & 0 \\ 0 & 0 & \frac{1}{2} & 0 & -\frac{1}{2} & 0 & 0 & 0 \\ 0 & 0 & 0 & \frac{1}{2} & 0 & -\frac{1}{2} & 0 & 0 \\ 0 & 0 & -\frac{1}{2} & 0 & \frac{1}{2} & 0 & 0 & 0 \\ 0 & 0 & 0 & -\frac{1}{2} & 0 & \frac{1}{2} & 0 & 0 \\ 0 & 0 & 0 & 0 & 0 & 0 & 0 & 0 \\ 0 & 0 & 0 & 0 & 0 & 0 & 0 & 0 \end{array}\right] \end{array} \tag{1.22}$$

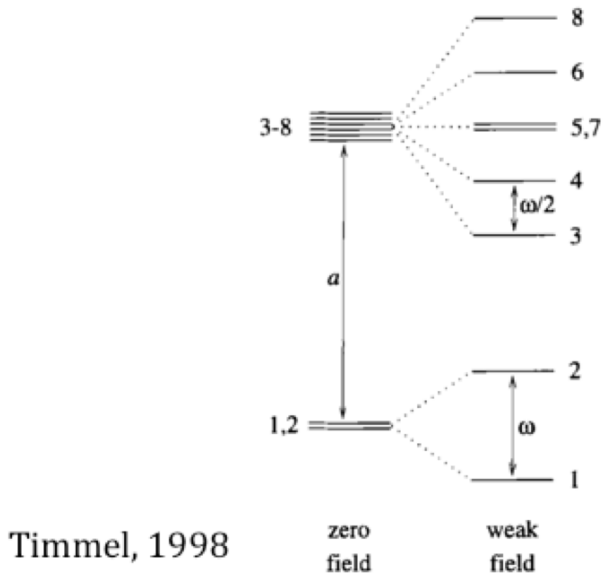

Figure 3. Energy levels of a one-proton radical pair in zero field (left) and in the presence of a weak ($\omega \ll a$) magnetic field (right). a and ω are, respectively, the hyperfine coupling and the electron Larmor frequency, $\omega = \gamma B_0$.

Figure 1.2: Energy Eigenstates with hyperfine and zeeman interactions,[48]

Under a zero field, the two singlet states are degenerate and the six triplet states are also

degenerate. Under weak field however, the states become mixed. With an isotropic hyperfine interaction a and an electron precession frequency of ω, the Hamiltonian in matrix form is:

$$\begin{bmatrix} \frac{a}{4}+\omega & 0 & 0 & 0 & 0 & 0 & 0 & 0 \\ 0 & -\frac{a}{4}+\omega & 0 & 0 & \frac{a}{2} & 0 & 0 & 0 \\ 0 & 0 & \frac{a}{4} & 0 & 0 & 0 & 0 & 0 \\ 0 & 0 & 0 & -\frac{a}{4} & 0 & 0 & \frac{a}{2} & 0 \\ 0 & 0 & 0 & 0 & -\frac{a}{4} & 0 & 0 & 0 \\ 0 & 0 & 0 & 0 & 0 & \frac{a}{4} & 0 & 0 \\ 0 & 0 & 0 & 0 & 0 & 0 & -\frac{a}{4}-\omega & 0 \\ 0 & 0 & 0 & 0 & 0 & 0 & 0 & \frac{a}{4}-\omega \end{bmatrix} \tag{1.23}$$

These are the states in terms of the spin up/down basis. Then diagonalizing this matrix

$$\begin{bmatrix} \frac{a}{4} & 0 & 0 & 0 & 0 & 0 & 0 & 0 \\ 0 & \frac{a}{4} & 0 & 0 & 0 & 0 & 0 & 0 \\ 0 & 0 & \frac{a}{4}-\omega & 0 & 0 & 0 & 0 & 0 \\ 0 & 0 & 0 & \frac{a}{4}+\omega & 0 & 0 & 0 & 0 \\ 0 & 0 & 0 & 0 & -\frac{a}{4}-\frac{\omega}{2}-\frac{\sqrt{a^2+\omega^2}}{2} & 0 & 0 & 0 \\ 0 & 0 & 0 & 0 & 0 & -\frac{a}{4}+\frac{\omega}{2}-\frac{\sqrt{a^2+\omega^2}}{2} & 0 & 0 \\ 0 & 0 & 0 & 0 & 0 & 0 & -\frac{a}{4}-\frac{\omega}{2}+\frac{\sqrt{a^2+\omega^2}}{2} & 0 \\ 0 & 0 & 0 & 0 & 0 & 0 & 0 & -\frac{a}{4}+\frac{\omega}{2}+\frac{\sqrt{a^2+\omega^2}}{2} \end{bmatrix} \tag{1.24}$$

This diagonal terms are the eigenvalues, and they are the energy values of the eigenstates.

Under the normal assumption that $a > \omega$ then these states can be written out in order of increasing energy levels. Also this entire process can be done under a singlet/triplet basis or the up/down basis results can be converted to the singlet/triplet basis which will both lead to the same result. Of course, we get the same eigenvalues, but the eigenvectors correspond to singlet/triplet states and are included in the below table. The eigenstates are not normalized for the sake of space.

$$\left[\begin{array}{cccc} \text{new state number} & \text{energy} & \text{up/down basis} & \text{singlet/triplet basis} \\ 1 & -\frac{a}{4} - \frac{\omega}{2} - \frac{\sqrt{a^2+\omega^2}}{2} & b_1 \left|\uparrow\downarrow\downarrow\right\rangle + \left|\downarrow\downarrow\uparrow\right\rangle & c_1 \left|T_0 \downarrow\right\rangle + c_2 \left|S_0 \downarrow\right\rangle + c_3 \left|T_- \uparrow\right\rangle \\ 2 & -\frac{a}{4} + \frac{\omega}{2} - \frac{\sqrt{a^2+\omega^2}}{2} & b_2 \left|\uparrow\uparrow\downarrow\right\rangle + \left|\downarrow\uparrow\uparrow\right\rangle & c_4 \left|T_+ \downarrow\right\rangle + c_5 \left|T_0 \uparrow\right\rangle + c_6 \left|S_0 \uparrow\right\rangle \\ 3 & \frac{a}{4} - \omega & \left|\downarrow\downarrow\downarrow\right\rangle & \left|T_- \downarrow\right\rangle \\ 4 & -\frac{a}{4} - \frac{\omega}{2} + \frac{\sqrt{a^2+\omega^2}}{2} & b_4 \left|\uparrow\downarrow\downarrow\right\rangle + \left|\downarrow\downarrow\uparrow\right\rangle & c_7 \left|T_0 \downarrow\right\rangle + c_8 \left|S_0 \downarrow\right\rangle + c_9 \left|T_- \uparrow\right\rangle \\ 5 & \frac{a}{4} & \left|\uparrow\downarrow\uparrow\right\rangle & \left|T_0 \uparrow\right\rangle + \left|S_0 \uparrow\right\rangle \\ 6 & \frac{a}{4} & \left|\downarrow\uparrow\downarrow\right\rangle & -\left|T_0 \downarrow\right\rangle + \left|S_0 \downarrow\right\rangle \\ 7 & -\frac{a}{4} + \frac{\omega}{2} + \frac{\sqrt{a^2+\omega^2}}{2} & b_7 \left|\uparrow\uparrow\downarrow\right\rangle + \left|\downarrow\uparrow\uparrow\right\rangle & c_{10} \left|T_+ \downarrow\right\rangle + c_{11} \left|T_0 \uparrow\right\rangle + c_{12} \left|S_0 \uparrow\right\rangle \\ 8 & \frac{a}{4} + \omega & \left|\uparrow\uparrow\uparrow\right\rangle & \left|T_+ \uparrow\right\rangle \end{array}\right] \tag{1.25}$$

$$\begin{bmatrix} b_1 = -\frac{(-\omega+\sqrt{a^2+\omega^2})}{a} \\ b_2 = -\frac{(-\omega+\sqrt{a^2+\omega^2})}{a} \\ b_4 = -\frac{(-\omega-\sqrt{a^2+\omega^2})}{a} \\ b_7 = -\frac{(-\omega-\sqrt{a^2+\omega^2})}{a} \\ c_1 = \frac{\sqrt{2}(\omega-\sqrt{a^2+\omega^2})}{a} + \frac{a-\omega+\sqrt{a^2+\omega^2}}{\sqrt{2}(a+\omega+\sqrt{a^2+\omega^2})} \\ c_2 = -\frac{a-\omega+\sqrt{a^2+\omega^2}}{\sqrt{2}(a+\omega+\sqrt{a^2+\omega^2})} \\ c_3 = 1 \\ c_4 = \frac{\sqrt{2}(-\omega+\sqrt{a^2+\omega^2})}{a} \\ c_5 = -1 \\ c_6 = 1 \\ c_7 = \frac{\sqrt{2}(\omega+\sqrt{a^2+\omega^2})}{a} - \frac{a-\omega-\sqrt{a^2+\omega^2}}{\sqrt{2}(-a+-\omega+\sqrt{a^2+\omega^2})} \\ c_8 = \frac{a-\omega-\sqrt{a^2+\omega^2}}{\sqrt{2}(-a-\omega+\sqrt{a^2+\omega^2})} \\ c_9 = 1 \\ c_{10} = -\frac{\sqrt{2}(\omega+\sqrt{a^2+\omega^2})}{a} \\ c_{11} = -1 \\ c_{12} = 1 \end{bmatrix}$$

If we take this result and plug it into equation 1.16, we can get an exact expression for singlet yield in this simple one hyperfine interaction case.

$$\begin{aligned} \Phi_S = & \frac{3}{8} + \frac{1}{8}\frac{\omega^2}{\Omega^2} + \frac{1}{8}\frac{a^2}{\Omega^2} f(\Omega) \\ & + \frac{1}{8}[1 - \frac{\omega}{\Omega}] f(\frac{1}{2}a + \frac{1}{2}\omega + \frac{1}{2}\Omega) \\ & + \frac{1}{8}[1 - \frac{\omega}{\Omega}] f(\frac{1}{2}a - \frac{1}{2}\omega - \frac{1}{2}\Omega) \\ & + \frac{1}{8}[1 + \frac{\omega}{\Omega}] f(\frac{1}{2}a - \frac{1}{2}\omega + \frac{1}{2}\Omega) \\ & + \frac{1}{8}[1 + \frac{\omega}{\Omega}] f(\frac{1}{2}a + \frac{1}{2}\omega - \frac{1}{2}\Omega) \end{aligned} \tag{1.26}$$

where $\Omega = (a^2 + \omega^2)^{\frac{1}{2}}$. If the reaction rate k is much greater than a and ω, every term lives except the second term, and $\Phi_S = 1$. This makes sense because if k is high, then as soon as the radical pair ends up in a singlet state, it will be converted into singlet yield without a chance to convert to a triplet state. In the case where the anisotropy a is much greater than k which is much greater than ω, the 2nd, 3rd, 5th, and 7th term become zero, and we are left with a limiting case of $\Phi_S = \frac{5}{8}$. This also represents the largest possible singlet yield with mixing because we have maximum anistropy compared to the magnetic field and the rate constant. In a final limiting case of a being much greater than ω which is much greater than k, all terms except the first one go to zero. This leaves us with the minimal amount of singlet yield of $\Phi_S = \frac{3}{8}$. This represents that the states will be naturally populated and those will create singlet yield, but transitions become extremely unlikely which reduce to zero any more transitions to singlet states.

1.3.12 Hyperfine Anisotropy

The magnetic sensitivity depends on the anisotropy of the nucleus of the radical pair. If the hyperfine interaction were isotropic, the angle that the molecule makes with the external field would result in the same amount of singlet/triplet mixing no matter the direction. With an anisotropic hyperfine interaction under certain angles, the external field will add to the magnetic field of the nucleus, increasing the energy difference between singlet and triplet states, and typically increasing the amount of singlet yield. Hyperfine anisotropy comes from the geometry of the molecule. The ideal molecule is one that is symmetric on the x-axis and y-axis but long on the z-axis, such as a cylinder. In this configuration, the hyperfine interaction is most different on the z-axis in which case the amount of singlet/triplet product created depends on the direction of the magnetic field.

A is isotropic

$$\begin{bmatrix} a & 0 & 0 \\ 0 & a & 0 \\ 0 & 0 & a \end{bmatrix}$$

A is completely anisotropic

$$\begin{bmatrix} a_{1,1} & a_{1,2} & a_{1,3} \\ a_{2,1} & a_{2,2} & a_{2,3} \\ a_{3,1} & a_{3,2} & a_{3,3} \end{bmatrix}$$

A is anisotropic only along the z-axis

$$\begin{bmatrix} a & 0 & 0 \\ 0 & a & 0 \\ 0 & 0 & b \end{bmatrix}$$

1.3.13 Energy Eigenstates

Once the electron transfer occurs, singlet states and triplet states are no longer eigenstates of the Hamiltonian. This is why the singlet/triplet mixing happens. In more correct terms, the orbitals that were once distinct s and p orbitals become hybrid orbitals. The former orbitals that were three p orbitals and one s orbital, each capable of holding two electrons become eight orbitals that are a linear combination of singlet and triplet states.

The limiting singlet yield under zero field and an axiality of one is $\frac{1}{4}$ of total product created because there are four possible states that the radical pair can be in, and the singlet state is just one of those four. Under a high magnetic field, the limiting value is $\frac{1}{2}$ because triplet states T_+ and T_- become energetically far away from the singlet state. However T_0 does not change, and that conversion is still possible, resulting in a one in two change that the pair is in the singlet state.

Under even a weak field, the eight energy eigenstates are linear combinations of singlet and triplet states. The limiting singlet yields in this case is $\frac{3}{8}$ when the weak field effect is greater than the time to cause mixing. In the case where the weak field does not have time to mix states before recombination, the upper limit on singlet yield is $\frac{5}{8}$.

1.4 Methods and Current Model

1.4.1 Optimal Nuclear Spin Environment

Under the most basic model, there is only one hyperfine interaction between the nucleus and the electron. However in the real molecule, there are most likely many hyperfine interactions between the surrounding nuclei and the electron. In this situation, magnetic sensitivity is most likely lessened unless the hyperfine interactions act in such a way that they increase the total anisotropy. Doing analytical calculations are very difficult as the spin Hamiltonian is mostly likely not possible to diagonalize analytically [48]. Most radical pair spin dynamics are only numerically possible with the appropriate quantum equations of motion.

In the case in which both radical electrons experience a separate hyperfine interaction, magnetic sensitivity becomes very difficult and decreases as the system becomes disordered and any extra anisotropic hyperfine interaction does not increase the magnetically sensitive yield.

1.4.2 Calculation Methods

These electrons can be described under a full wavefunction $\Psi(r_i, s_i, t)$ where we describe its position in coordinates, its spin, and time [42]. However, this requires that we take into account interactions with the nucleus and every other electron in the molecule. This means that electron correlation effects arise and solving the Schrodinger equation with many terms is difficult. Even after making an approximation by breaking the Hamiltonian down into its rotational and vibrational components, it is still very difficult to solve. Under the assumption that the spin evolution and time evolution are independent of each other, we can convert our Hamiltonian into a spin Hamiltonian and reduce the number of variables greatly.

1.4.3 Constraints of Radical Pair Mechanism

Kinetics & Spin Selective Radical Reactions

The singlet yield comes from the radical pair being in the singlet state. Some conversion process must happen between these two states. A rate k is used to calculate the amount of singlet yield product as a result of the singlet state [41]. The lifetime of a radical pair is approximately $1\mu s$. The rates of the singlet states and the rate of the triplet product must be around $106s^{-1}$ to allow sufficient mixing of states but not so long that the spins relax. At this rate, the radical electrons must be around $1.5nm$ in separation. This distance comes from optimum electron transfer rate which occurs when the reaction Gibbs energy matches the reorganization energy. Under a basic model, the rate k is constant, and the amount of product created is based on the amount of radical pair in the singlet or triplet state.

Thermal Equilibrium

The energy difference in the singlet triplet conversions is approximately a million times smaller than the surrounding thermal energy [26]. Normally, this means that the singlet triplet conversion energy effect is negligible. However, the activation energy that excites the electron is much greater than room temperature energies. The singlet triplet conversion does not require an activation energy itself, so the whole conversion process takes place far away from thermal equilibrium. This can be found in various ways. If the mechanism requires the absorption of blue light, then $E = h\nu$ where $\nu \approx 450nm$ so $E = 2.76eV$. Room temperature energies can be found with $E = k_b \cdot T$ where $T = 293K$ gives us $E = 0.0252eV$. This shows that the system takes place at an energy that is over $100\times$ greater than thermal equilibrium.

1.4.4 Low Field Effect

At very high fields, the triplet energy levels split very far apart from the singlet levels except for the T_0 energy level. This means that the conversions between the singlet and triplet states are much fewer. When the radical pair starts in the singlet state, it has a lower probability of transitioning to the triplet state which means that the singlet yield goes up as a function of the magnetic field strength. At a zero field, there is some order as the electron and the nucleus precess around each other [47]. This means there is a tiny amount of splitting and the energy levels are not truly degenerate. Once there is a tiny magnetic field, the singlet yield actually goes down because the electrons are affected on similar magnitudes by the nucleus and by the magnetic field, and the electrons precess around the combination of the external and internal fields. As the external magnetic field gets stronger, the electrons start to precess more around the external field, and the energy levels split which leads to greater singlet yield.

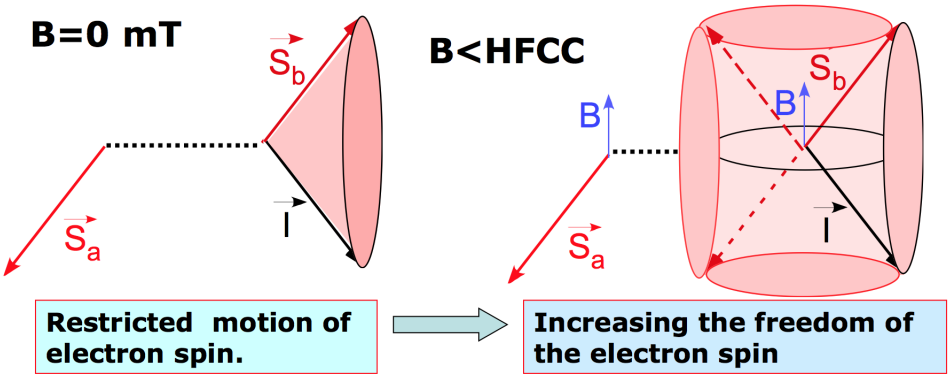

Figure 1.3: Low Field Effect

1.4.5 Experimental Techniques to Probe the Radical Pair

Electron paramagnetic resonance is a technique to study the hyperfine g-tensor of unpaired electrons of the radical pair [26]. To find the electron splitting energy, the radical pair is

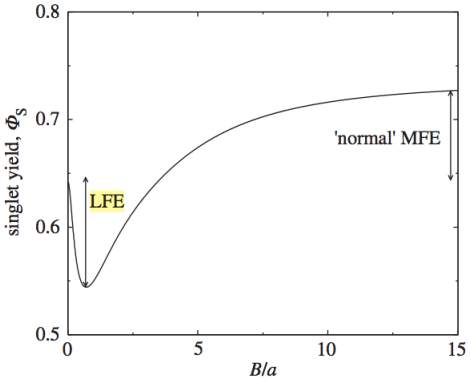

Figure 1. Typical curve for the magnetic field dependence of the singlet yield of a singlet–born radical pair. Magnetic field strength, B, is given in units of the average hyperfine interaction, a, in the system.

Figure 1.4: Singlet Yield at Low Fields,[47]

hit with a specific wavelength of light. The electron will not jump to the other energy level unless the difference in energy levels is equivalent to the energy of the incident light. The external magnetic field is then changed until the energy splitting equals the energy of the incident light. At this point the radical pair will emit a photon as the molecule and the light hit resonance. Transient Absorption Spectroscopy is a technique to measure the lifetime of the radical pair. The absorption of spectra is measured as a function of time after the initial excitation energy. The timescale of the radical pair lifetime can be measured from the very start of the reaction.

1.4.6 Density Function Calculations

In order to calculate the effect of many hyperfine interactions and their couplings on a single electron, density functional theory (DFT) is needed to calculate the g-tensor of the molecule [42]. DFT reduces a many electron system into a density cloud that only depends on three spatial coordinates instead of 3N for the number of electrons. Further methods and theory for DFT are centered in spin chemistry and are beyond my scope of expertise.

1.4.7 Current Model

Most models currently have FAD as the acceptor molecule. There is still ongoing research in what the donor molecule is though the triad of tryptophans has been a leading candidate as well as superoxide. Under the basic model that the donor molecule is a single proton, the magnitude of anisotropic hyperfine interaction is on the left. However, under the case of tryptophan as the donor molecule, that system requires a complex density functional theory to calculate the hyperfine parameters, and those hyperfine parameters produce the plot on the right [24].

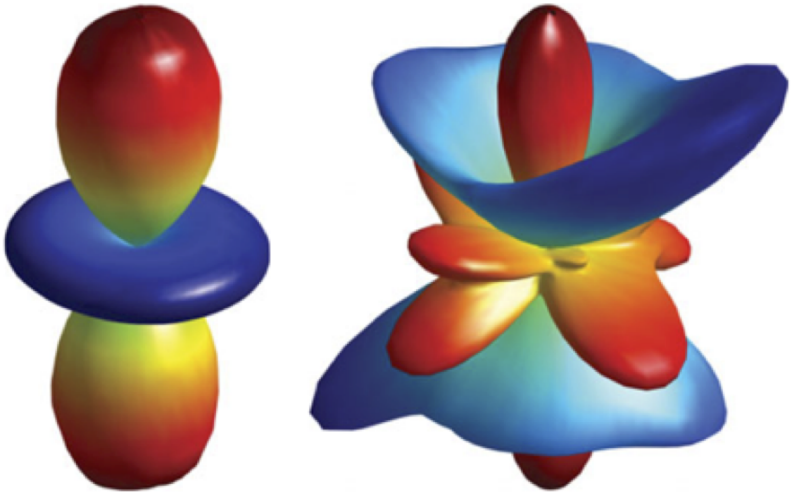

Figure 1.5: Theoretical Anisotropic Singlet Yields for basic and complex cases. [24]

1.4.8 Experimental Radical Pair

The exact process for the radical pair mechanism that causes a chemical reaction has not been and is very difficult to be seen in biology. In a paper [26], they use a carotenoid-porphyrin-fullerene molecule. After being irradiated by green light, it produces the singlet state ${}^{S}[C^{\cdot+} - P - F^{\cdot-}]$. Here is can either revert back to the ground state $[C - P - F]$ or it

can convert into the triplet state ${}^{T}[C^{\cdot+} - P - F^{\cdot-}]$and later revert back to the ground state $[C - P - F]$. The conversion step is magnetically sensitive which means that the lifetime of the radical pair changes depending on the magnetic field strength and direction. In solution, this molecule was frozen to 133K so that its orientation was stable. Radical lifetimes were determined by the absorption signal on the carotenoid molecule. They were able to double the lifetime of the radical pair from 190 ns to 380 ns in an 8mT field, which is roughly 100 times stronger than an Earth strength field. At Earth strength magnetic fields, the lifetime of the radical pair changed by 1.5%, which is the first observation of a chemical reaction affected by an Earth strength magnetic field. This group was even able to see the low field effect as the lifetime of the radical pair went down under very small fields and then was longer as the field went up.

1.4.9 Spin Selective Reactions

The radical pair mechanism requires a spin selective reaction in that the singlet state produces a different chemical product from the triplet state. This means that a molecule that has two electrons with spin down and spin up will produce a different product from a molecule with two spin up electrons. With the same molecule that saw Earth strength magnetic field effects [C-P-F] [27], they found that the k constant for singlet lifetime of this molecule was $k_s = 1.8 \cdot 10^7 s^{-1}$ at 110 K. They also found that the lifetime for the triplet state was roughly 250 times longer. This means that when the molecule $[C^{\cdot+} - P - F^{\cdot-}]$ reverts back to the ground state [C-P-F] much quicker in the singlet state than the triplet state.

Chapter 2

Magnetic Orientation Simulation

2.1 Introduction

Experimentation on migratory birds has been performed since the 1960's. A theoretical model of magnetic orientation should expect to demonstrate these behaviors outlined in Ritz et al. [39]. The major results from studies on long distance and short distance migratory birds are as follows:

1. The magnetic compass they contain is an inclination compass which means that these birds are sensitive to the axis of the magnetic field and not the polarity. Flipping the polarity of the magnetic field had no affect on the ability to orient itself north.

2. Both northern and southern hemisphere birds showed good orientation under blue light (peak at 443 nm) and green light (peak at 565 nm), but they were disoriented under red light (peak at 630 nm) [53] despite being tested and shown to be able to perceive all of the visible spectrum [28]. It's likely that light of a high enough energy is needed to start any sort of magnetic compass process.

3. The range of magnetic field strengths at which the birds are oriented is quite narrow from between 0.43 Gauss and 0.54 Gauss while be disoriented at field strengths of 0.16G, 0.34G, 0.6G, 0.81G, and 1.5G. Earths magnetic field strength is approximately 0.5 Gauss which may indicate that their magnetic sensitivity may be tuned to the Earth.

2.1.1 Motivation

The current biological model for the eye and magnetic field system under the radical pair mechanism must have the key property of the radical pair ordered in some fashion along the retina of the eye [39]. This ordering means that the radical pairs at different locations on the retina will respond based on its orientation with the magnetic field. This theoretical structure is modeled after our understanding of vision where rod and cones cells hold visual pigments parallel to the surface of the retina. The information from these visual cells does not change depending on its angular orientation on the retina. The radical pair mechanism could send signals along the same channel as the visual pathway and allow an animal to see an image created by the magnetic field.

The model for the magnetic image should be as flexible as possible since the ability of the perception of the magnetic image is unknown. There are many variables in the reception of magnetic information and many variables in the processing of that information to result in the ability to orient oneself. There may be an ideal size or minimum resolution of the magnetic image necessary to orient, as well as noise that could arise from the radical pair not being completely ordered in the retina, objects that alter the magnetic field, and a multitude of areas in between the radical pair model to the ability of a brain to process this magnetic image signal. The model should be robust enough to test these variables against each other to find some method of orientation and be able to quantify how well the method works.

In order to get information out of any visual image, contrast is the essential quality to

enhance differences. The radical pair reaction scheme is initialized by light energy, and under the reaction scheme some minimum of singlet yield will be produced even under no magnetic field. This is known as the isotropic contribution to the singlet yield of the radical pair because no matter what direction the radical pair is oriented, within the magnetic field, some singlet yield will be created. What creates contrast between receptors is the anisotropic contribution to the singlet yield. Following the work of Ritz et al. [39] which formulated triplet yield products as a result of the radical pair mechanism, images were created to show what the anisotropic magnetic information would look like on the entirety of a hemispherical retina. Lau et al. [24] further expanded on this work to create analytical results for the anisotropic singlet yield signal of a receptor located on the retina. The expansion also included extra conditions such as the axes that the receptor molecules are aligned with, and also includes photoselection effects from polarized and unpolarized light. The simplest case of this analysis is unpolarized excitation and without photoselection effects, which means that every point on the retina is equally capable of reacting to the magnetic field. An ideal method of orientation will be formulated around these two basic conditions with the radical pairs oriented along the z axis of the molecule as shown in Table S3 of Lau et al, 2012.

2.1.2 From Radical Pair to Magnetic Vision

To model the mechanics of an eye, the eye and its receptors are modeled as a pin-hole camera with light entering the eye at a spherical pole opposite the other spherical pole which is the center of the retina. The retina of the eye is a spherical shell which is most commonly thought to be a hemisphere, though it is possible to be larger than a hemisphere when the field of view for an eye is larger than 180°. Although light must enter through the pupil, the magnetic field does not have such a restriction so that the entirely of the retina is under the magnetic field. The effect to which the magnetic receptor reacts to the field could be dependent on that receptors exposure to light, its angle with the magnetic field vector at

that point, or other reason.

The equation in [24] in table S3 along the z-axis, we can find the anisotropic singlet yield at any point on a sphere. The magnetic image can then start to be formulated by using receptors as if they were pixels on an image. We can choose the dimensions of the magnetic image to accept which is analogous to the size of a photo, as well as attempt different receptor densities which is analogous to changing the resolution of a photo.

In order for the magnetic image to produce a quantifiable value, we can take an average value of the anisotropic singlet contribution of the magnetic image. This value would depend on the direction the eye is facing, the angle of the magnetic field, and the choices made on the dimensions, density, and layout of the receptor field as well as possible noise effects. While it may be possible to retrieve more orientation information by comparing different parts of a single magnetic image, the most basic analysis is to get one average value of a magnetic image with the assumption that all of the receptors contribute equally to the signal.

2.1.3 From Magnetic Vision to Orientation

Once a method of retrieving a quantifiable value from the magnetic image is achieved, then there needs to be a method of orienting oneself using this value. An iterative process where the eye can start in any direction along the horizon and take steps to orient oneself using purely the values from the magnetic image can be formulated to see how feasible the radical pair mechanism may allow an organism to orient in ways that the biological experiments have shown are possible.

This orientation process needs to be examined and rated over many trials as both accuracy of orientation and precision around such axis are important features. Certain recipe of conditions may lead to high quality orientation or consistently the wrong direction or create

disoriented directions.

Defining Coordinate Systems

A potential magnetic image process contains many components each with their own coordinate system. Combining all of them into one system means that many rotational transformations need to be accounted for. The components that require spherical coordinates are as follows:

1. The geomagnetic field vector of the Earth varies from perpendicular to the ground at the poles to nearly parallel at the equator. The magnetic field vector in Frankfurt, Germany has an inclination angle of 66°, which is where many of the biological experiments on migratory birds were performed.

2. The head has its three principle axes that must be accounted for. In aeronautical terms, the eye has degrees of freedom around its x, y, and z, axis which are its pitch, yaw, and roll, respectively.

3. If the organism is not cyclopean and its eye is located off center or on the side of a head like many preyed upon species, then its offset from the front of the head and its other eye would need to be accounted for.

4. The choice in what portion of the spherical shell of the retina is sensitive to magnetic fields with additional variables in how many receptors lie within that shell how are they distributed.

Layout of Receptors

In this model of radical pair ordering on the retina of the eye, magnetic receptors try to replicate visual receptors as much as possible. We use the assumption that the receptors are spread as equally as possible and at various densities but maxed out at the density of visual receptors.

Evenly distributed points on a sphere has a long mathematical history. There are many methods to try to create evenly distributed points, and the quality of the method varies based on the metric used to measure its evenness. This model and simulation uses a lattice method where center z-axis of the eye intersects the middle receptor of the receptor patch. Then the rest of the receptors are ordered around that middle receptor. The lattice is created in rings, where every surrounding ring contains four more receptors than the one directly inside of it. The density of the receptor patch can be modified by changing the radius of the rings, and the size of the patch can be modified by adding more rings. To show that this particular lattice method works as an approximation of an evenly distributed receptor patch, the results of a full integration within a patch area of magnetic information vs. X number of random receptors located within the patch area vs. X number of latticed receptors is shown to be equal within a small amount.

Model Definitions

The cardinal directions of north, south, east, and west lie on the plane created by the horizon. The middle of the head sits at the origin. The head direction has three degrees of freedom which are rotations around the x, y, and z axis. For ease to imagine with many organisms, the direction of the head is dictated by the nose of either a bird or human. An eye is a sphere with its center resting on the surface of the head. In a cyclopean case, the eye points forward along the same axis as the nose. In the case of a bird, there is an angle between

each eye and the nose horizontally.

An eye operates as a pinhole camera, where the side of the sphere facing outward contains the pupil where light would enter, and the other side of the sphere contains the retina which contains the magnetic receptors.

Every magnetic receptor contains a radical pair which is capable of reacting to magnetic fields. The magnetic receptors are ordered on the retina around the base receptor. The area of working receptors or area of receptors creating a signal is the receptor patch. Receptor patches are spherical caps made by intersecting a plane with a normal vector along the same line as one that connects the center of the eye to the base receptor of the patch, and extends to the direct line of sight of the eye. Each receptor is ordered such that its z-axis is perpendicular with the surface of the retina and extends through the center of the eye.

Variable Definitions

Receptor patch size The receptors which create the magnetic image and submit the magnetic signal is the receptor patch. This rotationally symmetric patch from which to accept information can be any non-zero angle below 180°. This is the typical limit for the field of view of most eyes, and stretching further means that the retina and its receptors would extend into the area where the iris, pupil, and lens would normally be. Also, in the lattice structure composed of rings, going past 180° should result in rings with fewer receptors instead of more.

Patch Locations The default location of the patch is centered at the center of the retina opposite of the pinhole pupil, and along the direction that the eye is pointed. However, the center location can be translated to another spot on the retina to possibly model cases where only certain areas on the retina would process magnetic information i.e. if exposure to light

on an area of the retina begins the radical pair mechanism. A limitation of this translation is that the patch size should be small enough to remain on the retina and not extend out past the hemisphere to the iris.

Noise Range There are no assumptions on where noise to this system may arise whether it exists in random fluctuations of the radical pair mechanism to the process by which its converted into a nervous signal. There are many ways to distort the signal coming out of a receptor or distort the signal resulting from the entirety of the receptor patch. Additive noise is a random value within a range that is added to the anisotropic singlet yield. There is also an option to create a multiplicative noise that is a random value within a range that is multiplied by the anisotropic singlet yield. Every receptor experiences an independent random noise value, and theres an option to hold those noise values when the head changes direction (static noise) or to create new noise values for every receptor when the head moves (dynamic noise). Static noise indicates some structural affect that remains constant and attached to the eye as it moves. Noise in which a single value of noise that affects the entirety of the receptor patch is not performed here, but would indicate some amplification process of the final signal. The results of this study focus on dynamic, additive noise at the receptor level and examines the robustness of a process of orientation under varying levels of noise.

Density of Receptors The density of the receptors is initially based on an assumption that every color photoreceptor contains a magnetic receptor. The color receptor is the cone, and makes up approximately 5% of the total photoreceptors in the human eye. In birds, however, cones make up between 80%-90% of the total photoreceptors. [28] found the total number of photoreceptors in a sparrow. If the robin's eye contains roughly 200,000 total photoreceptors, the density of photoreceptors is roughly 25,000 cone cells per steradian or 8 cone cells per square degree. Using these values as a ceiling, we can test the ability to orient

while considering some fraction of cone cells as actual magnetic receptors.

Magnetic Field Vector The geomagnetic field is assumed to be uniform and static. Although as a migratory bird traverses the world, the strength and direction of the field will change, we assume that orientation is a local process so that inclination, angle, and strength remain constant throughout a single orientation process. The work of [24] uses a magnetic field magnitude of 50 μT to compose the anisotropic singlet yields.

Basic Orientation Process

Alignment vs Orientation The goal of an orientation process is to be able to receive and use the magnetic information to put oneself in direction to be able to navigate. There are different metrics to define good orientation. Although it may be ideal to be able to orient oneself north, it may be equally useful to be able to align oneself along the north south axis and use the inclination feature of the magnetic field to tell if one is facing north or south. The ability to align oneself in one direction such as north would be unimodal orientation, and the ability to align oneself in two directions, not necessarily opposite of each other is called bimodal orientation.

Steps towards Orientation This simulation uses all of the information from a single snapshot to give one average value of the magnetic image. When the head changes direction, then a new average value of the new magnetic image is calculated. These two values are compared and will dictate the next direction that the head should be pointed in. This algorithm should allow the head to eventually point in some direction. We can design and tweak an algorithm that would allow a head to orient itself accurately and consistently.

Variables of the Orientation Process This iteration process has some variables that can be optimized to gradually orient oneself. A step is an angular change of direction. The initial step size is an important feature where a step too large might cause the head to turn erratically, and a step that is too small may cause the head to never eventually turn towards north. The gain is a multiplicative factor that is multiplied by the difference between the signal at one step and the one before it to determine the next step. Finally, there should be some way to end the iteration process which might be after a certain number of steps or if enough steps are under a certain threshold.

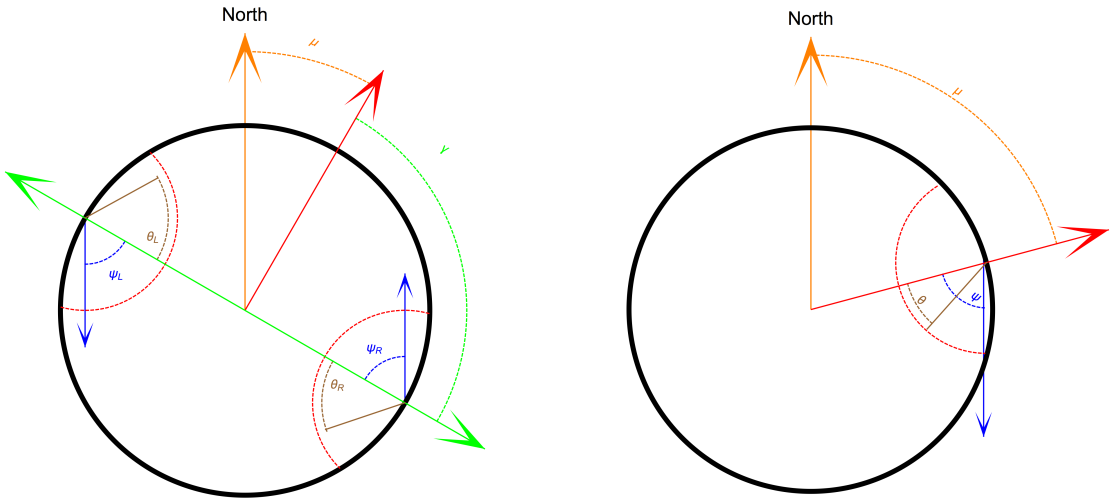

(a) Two Eye Model

(b) Single Eye Model

Figure 2.1: This two dimensional top view representation of the head displays the orientation of the magnetic field, head, eye, and receptor. Orange μ is the horizontal angle that the head makes with the magnetic field. Green γ is the horizontal angle that the view direction of the eye makes with the front of the head in the two eye model. Brown θ shows the horizontal angle that the receptor makes with the view direction of the eye. θ is typically the vertical angle, but in the top view, $\phi = \pi/2$, so theta is preserved as it rotates around the eye direction vector.

Basic Anisotropic Singlet Yield In the formulation of amount of anisotropic singlet yield for a given receptor location and magnetic field, Lau et al. [24] also considered two more effects of photoselection and polarization of light. Photoselection is the idea that only areas of the retina which are hit with light can have an activated radical pair mechanism. While

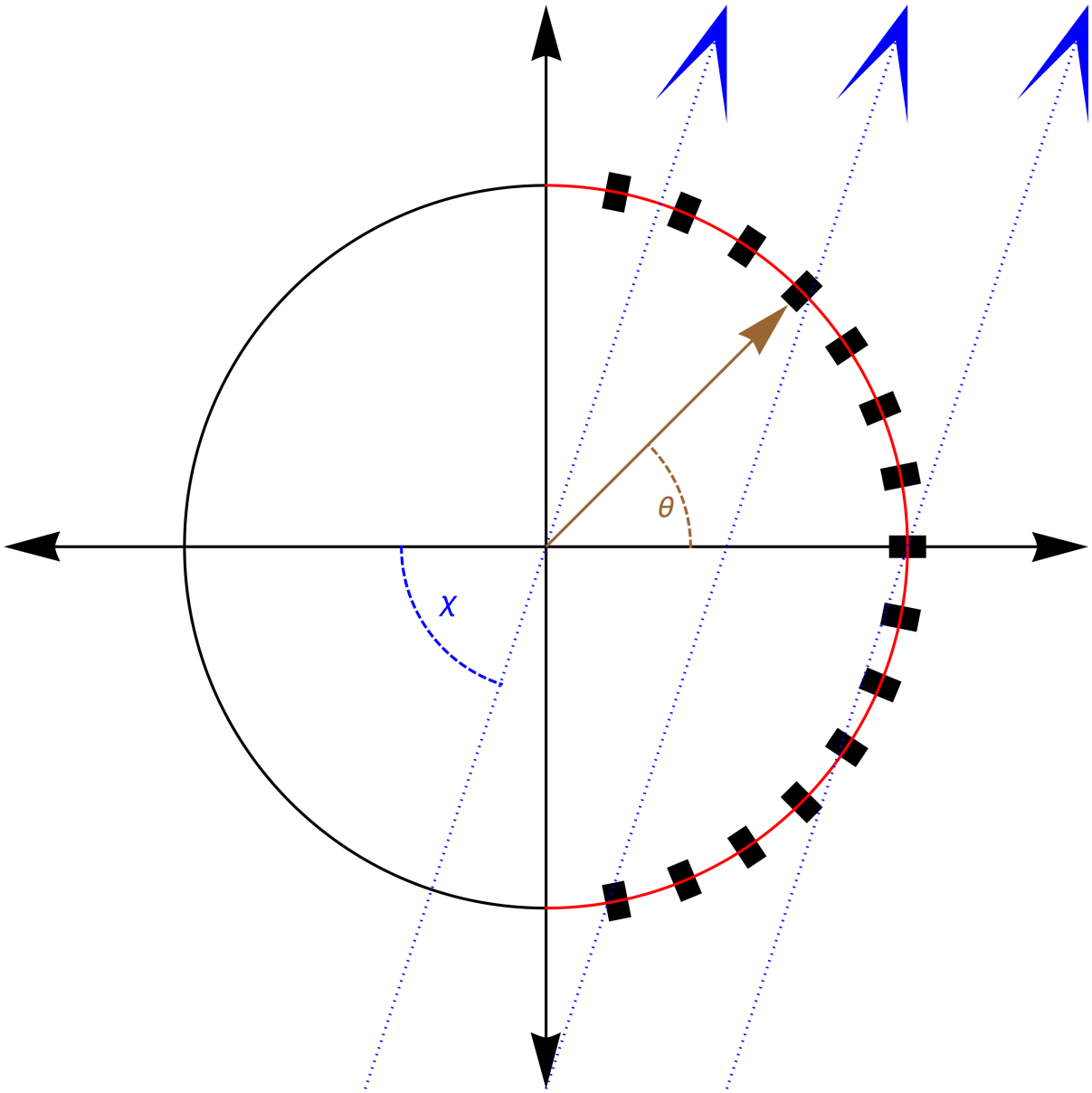

Figure 2.2: In this side view, the receptors are ordered with their normal vector pointed towards the center of the eye. θ is the vertical location of the receptor in the middle slice of the eye. Blue χ is the angle that the magnetic field makes with the view direction of the eye.

the magnetic field permeates the entirety of the eyeball, light can only enter through the iris which is theoretically characterized as a pinhole. The angle of incoming light then affects the sensitivity of receptor cells, so some parts of the image may be stronger than others. The receptors may also only be sensitive to a certain polarization of light to add another

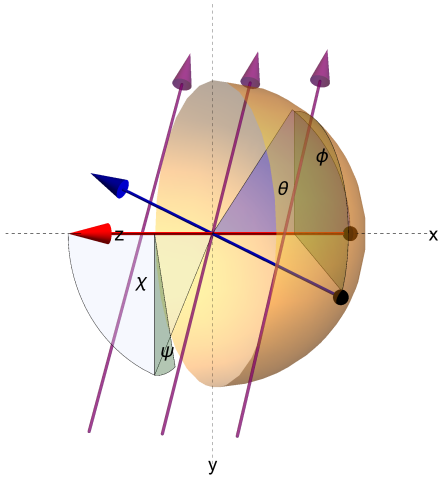

(a) Side View

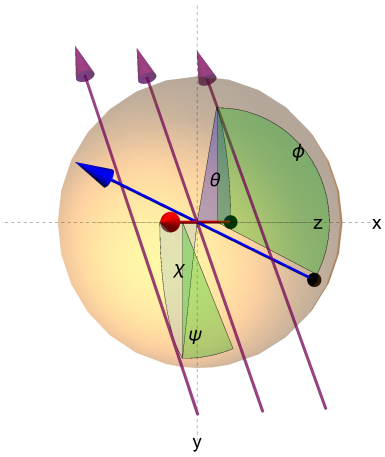

(b) FrontView

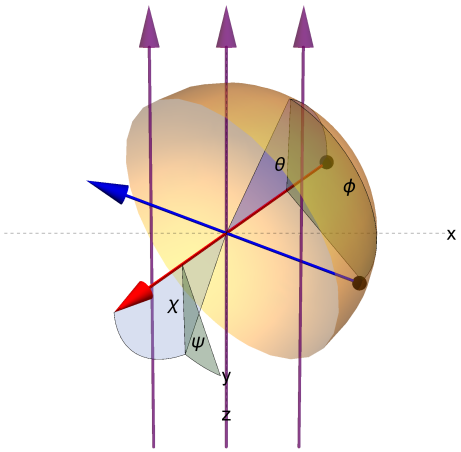

(c) Above and Side View

Figure 2.3: In this three dimensional representation of the orientation of receptors, the magnetic field vectors are parallel with the y-z plane and makes $\chi = 66°$ angle with the z axis. The hemisphere represents the retina. The view direction, in this case is 30°, which is the angle between the red view direction of the retina with the z axis. The purple magnetic field is defined by angles $0 < \chi < \pi/2$, and $0 < \psi < 2\pi$ in relation to the view direction of the retina. The receptors on the retina are defined by two angles, $0 < \theta < \pi/2$ and $0 < \phi < 2\pi$. The normal vector of a receptor on the retina is shown by the blue vector that extends from the surface of the retina and goes through the center of the sphere of the eye.

variable to the amount of radical pair reactions occurring on the retina. My simulation calls for the simplest possible case which is unpolarized light and without photoselection effects. Also, the z-axis of the receptor molecule is parallel with the z-axis of the cell. The singlet yield in this basic case is given by [24] table s3 for z-axis:

$$\begin{aligned}\widetilde{S}(\theta,\phi,\chi,\psi) = \frac{1}{8}\{&(1+3\cos 2\theta)(1+3\cos 2\chi)\\ &+12\cos 2(\phi-\psi)\sin^2\theta\sin^2\chi\\ &+12\cos(\phi-\psi)\sin^2 2\theta\sin^2 2\chi\}\end{aligned} \tag{2.1}$$

where θ and ϕ are the location of the receptor on the eye, and χ and ψ describe the angle of the magnetic field.

Quality of Orientation The ability to point oneself magnetically north is not a requirement of orientation. A compass needle that consistently points west serves just as good a purpose as one that points north. Because the radical pair model does not react to the polarity of the magnetic field but only to strength and direction, the eye may find the magnetic image of north and south indistinguishable, particularly if the magnetic field is horizontal. However, because the geomagnetic magnetic field contains an inclination, the ability to orient oneself south will give the same information as the ability to orient north because if an animal is able to perceive the inclination, the knowledge of the north-south axis in combination with the inclination is enough information to orient oneself.

In order to quantify the quality of an orientation, two resulting values must be accounted for. When orienting oneself, the head attempts to align itself with the north-south axis. The final direction must be accurate in that the axis that it orients to is actually the north-south axis. Then, the consistency needs to be quantified so that repeated attempts at orientation

will yield the same result. These two qualities should be combined into one statistical value that rates how well the head has oriented.

Under the hypothesis that the orientation will be bimodal and centered on the axis that runs from 0° north to 180° south, there needs to be a method to convert the final orientations that spans 0° to 360° into a mean vector and spread and then compared to 0° in order to form the statistic. This is accomplished by slightly modifying the V test formulated by Batschelet [2]. The V test leads to significance if there is clustering around a predicted direction. To see if our data set follows a bimodal distribution centered on the 0°-180° axis, we modify an existing statistic by multiplying every angle by 2, and reducing the angle to be within 0° to 360°. Then we perform a modified Rayleigh test (V-test) on the resulting directions to determine if there is significant clustering around the predicted direction. To determine significance using the V-test, a test statistic $u = (2/n)^{\frac{1}{2}}V'$, where $V' = R\cos[\mu - \theta_0]$ where R is the length of the resultant mean vector, μ is the angle of the resultant vector, and θ_0 is the predicted direction. The u-statistic is then compared to a table to determine significance.

2.2 Results

2.2.1 Basic Values

2.2.2 Receptor Layouts and their Differences

The position of the receptors along the retina is defined by a lattice that is created by defining a center receptor, then building rings of receptors around it. The structure of the lattice modified by adjusting the number of rings, ring density, and radius of the rings. These factors allow the receptor patch to be modified by area of the retina covered, and density of receptors while controlling the distribution such that the distance between points on a ring

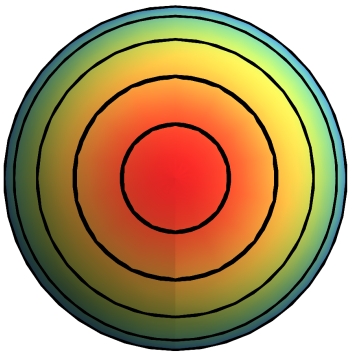

(a) Entire Retina

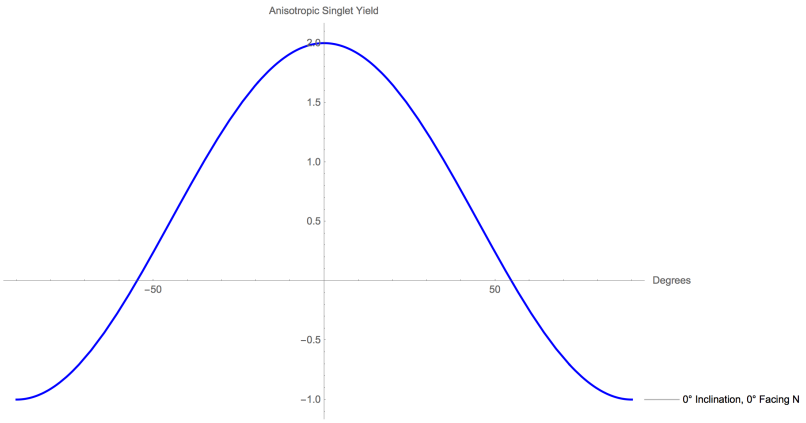

(b) Center Horizontal Slice of Retina

Figure 2.4: The retina hemisphere as seen from behind the eye. The magnetic field is parallel with the view direction of the eye. The colors range from red to purple, with red =2 and purple =-1 anisotropic singlet yield. The black rings indicate different areas of the retina starting in the middle at 30° diameter to 60°, 90°, 120°, 150°.

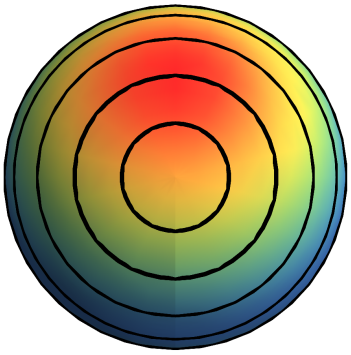

(a) Entire Retina

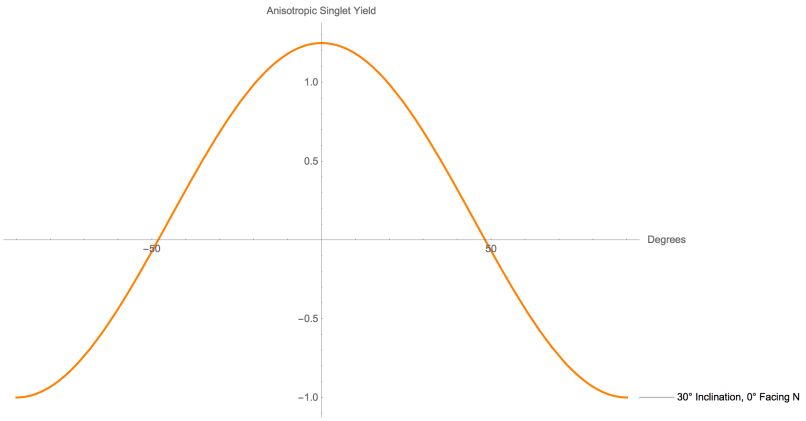

(b) Center Horizontal Slice of Retina

Figure 2.5: In this case, the magnetic field has an inclination angle of 30°. The eye is still facing north, so that the view direction angle is parallel with the ground.

are similar to that of receptors between different rings.

To test the quality of these layouts and their robustness as they cover larger patch sizes, the average anisotropic singlet yield of all the receptors is compared to the integrated average over the same patch size. This integrated average assumes an infinite number of receptors within the patch and models an eye with perfect resolution. The formula for the integrated

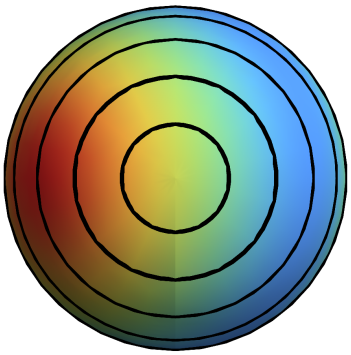

(a) Entire Retina

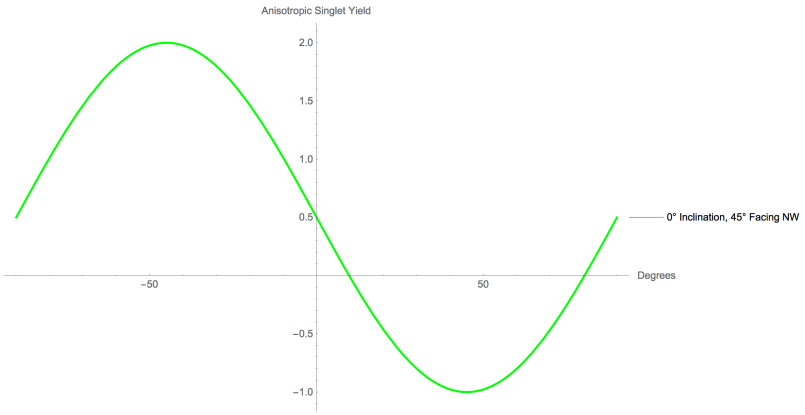

(b) Center Horizontal Slice of Retina

Figure 2.6: The magnetic field is parallel with the horizontal view direction. However the eye is pointed 45° west of north so that the area of most singlet yield occurs on the left portion of the retina.

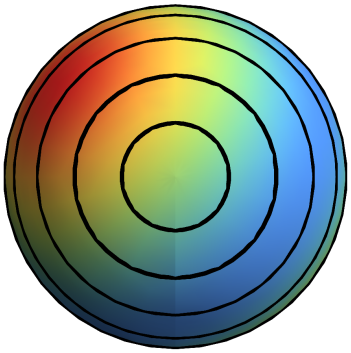

(a) Entire Retina

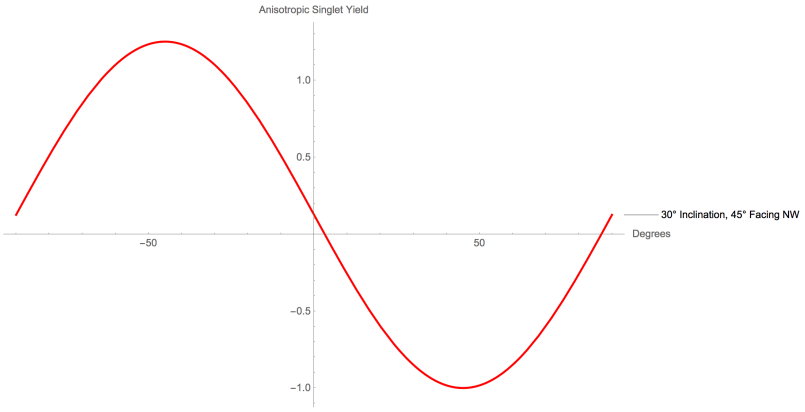

(b) Center Horizontal Slice of Retina

Figure 2.7: In this case, the above two conditions are combined so that the eye is facing 45° west of north, and the magnetic field has an inclination angle of 30°.

average for a given magnetic field direction χ, ψ, and patch size $m < \pi/2$ is as follows

$$\bar{S} = \int_0^{2\pi} \int_0^m \widetilde{S}(\theta, \phi, \chi, \psi) d\theta d\phi \tag{2.2}$$

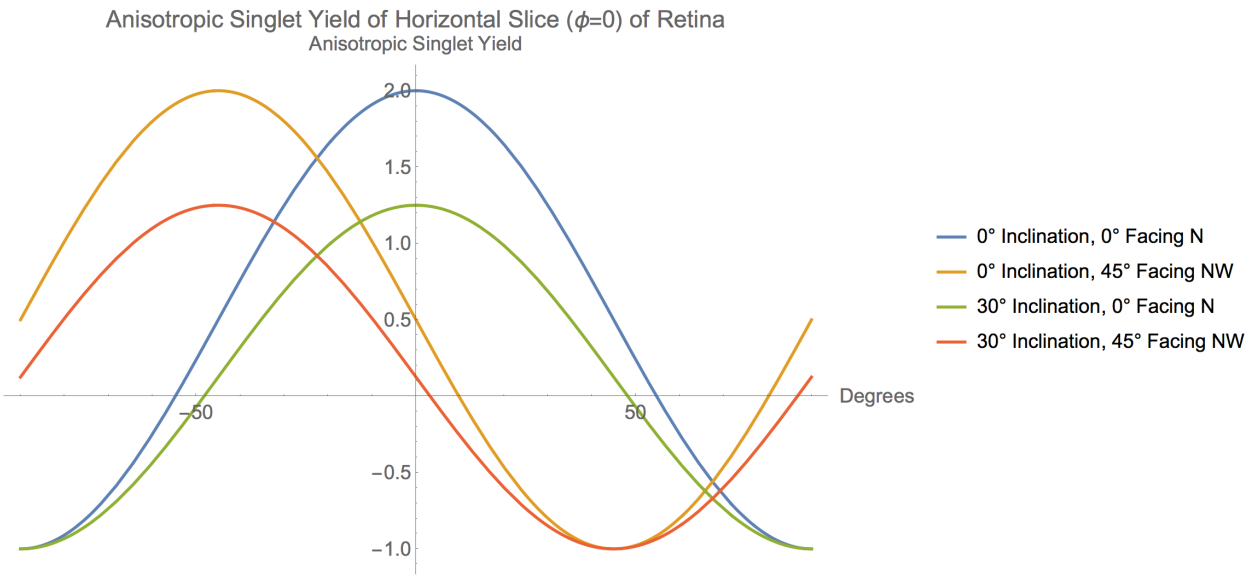

Figure 2.8: Along the horizontal slice of $\phi = 0$, for various view directions of the eye and magnetic field vector. Turning the eye horizontally shifts the anisotropic singlet yield around theta, and changing the angle of the magnetic field vector affects the maximum value and range of the singlet yield.

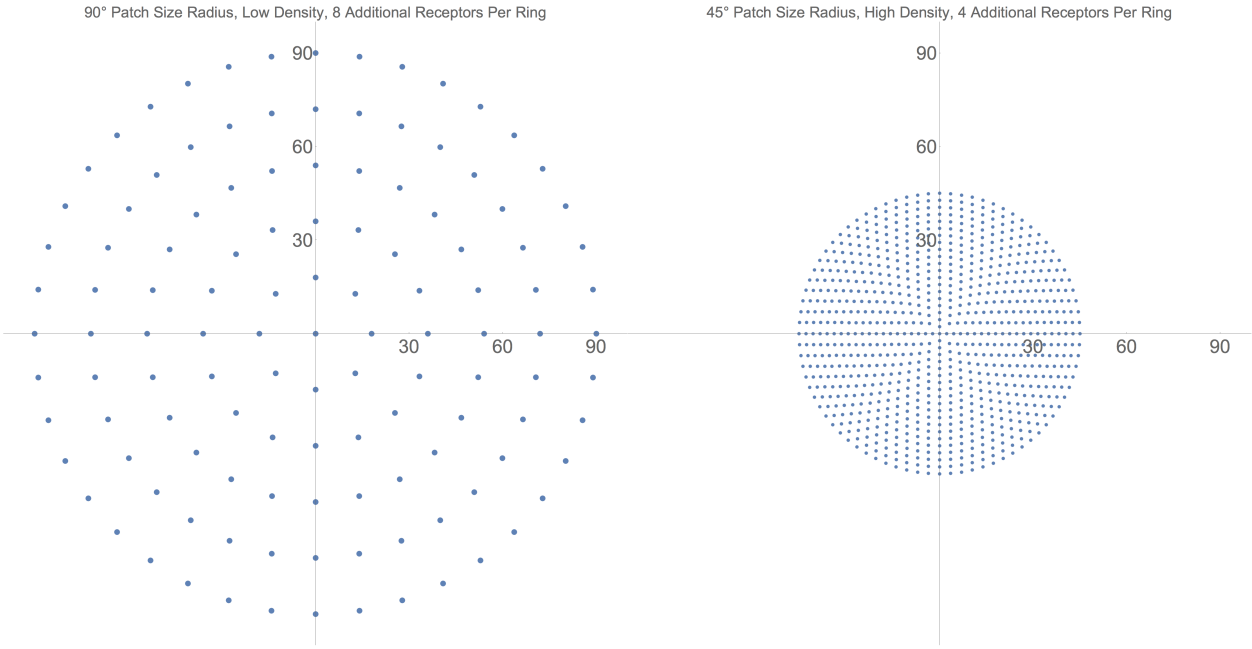

(a) 5 rings of 8 additional receptors per ring covering a full hemisphere

(b) 10 rings of 4 additional receptors per ring over a 45° radius patch

Figure 2.9: Two example layouts of receptors on the retina

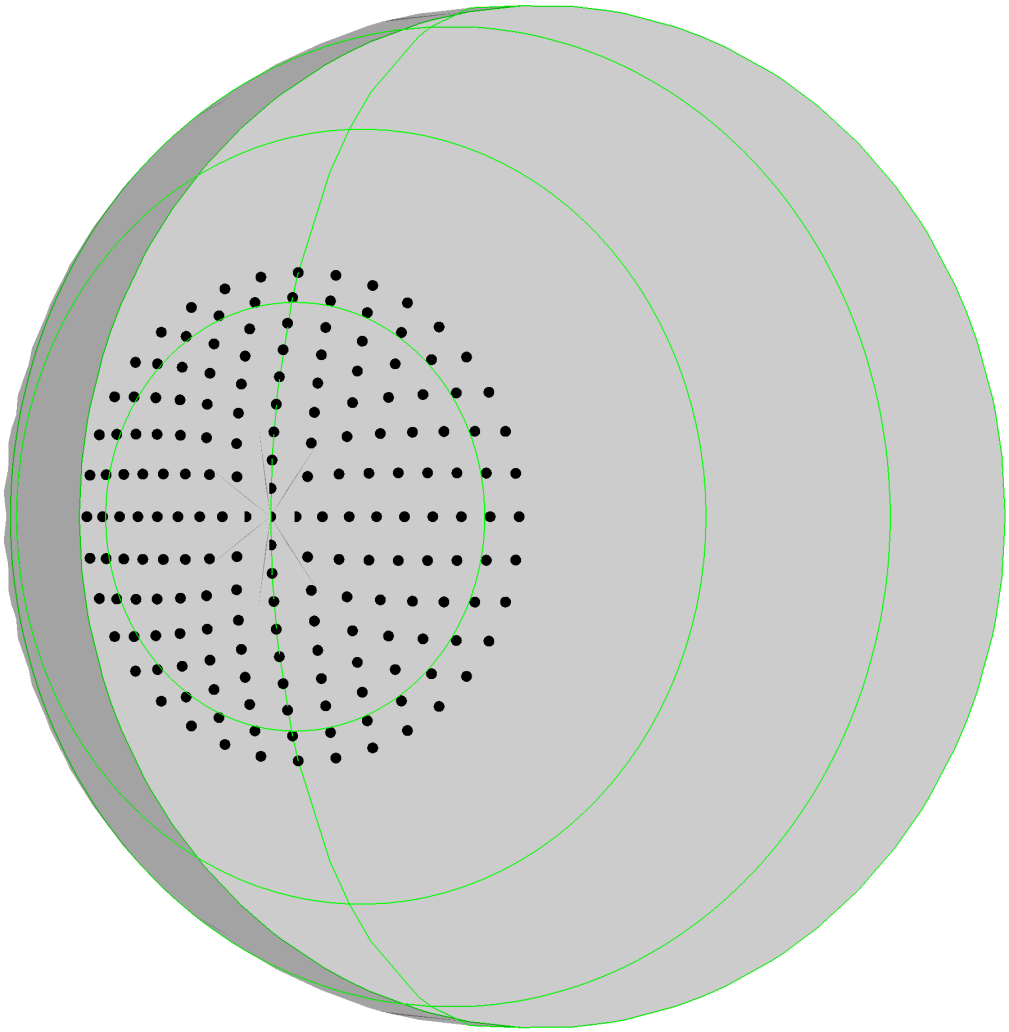

Figure 2.10: Example layout of receptors on spherical retina. 10 rings of 4 additional receptors per ring over a 30° radius patch size

2.2.3 Iteration Process

Our attempt at an algorithm by which an animal will find north takes into account some behavioral observations of birds but tries to remain simple and flexible. For a given patch size and direction the head is facing, the anisotropic singlet yield of all of the receptors

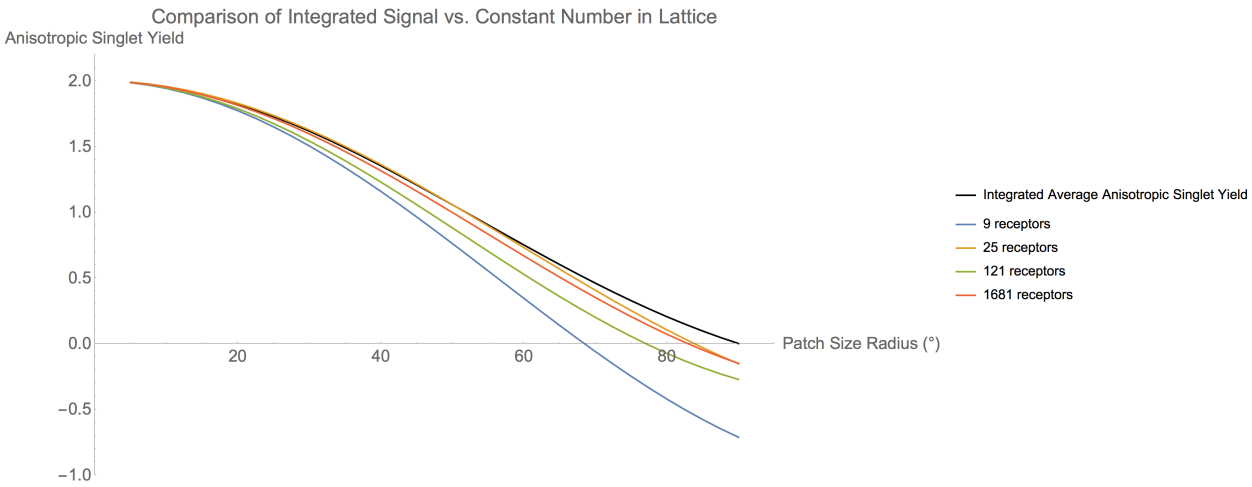

Figure 2.11: The Integrated Average Anisotropic Singlet Yield is the resulting signal from the average of the entire patch region of the retina with the magnetic field vector in line with the view direction of the eye at $\{\phi = 0, \theta = 0\}$ In the case of a constant number in the lattice, the number of receptors in the patch stays constant as the patch gets larger. More receptors means that the signal more closely resembles that of the overall integrated signal.

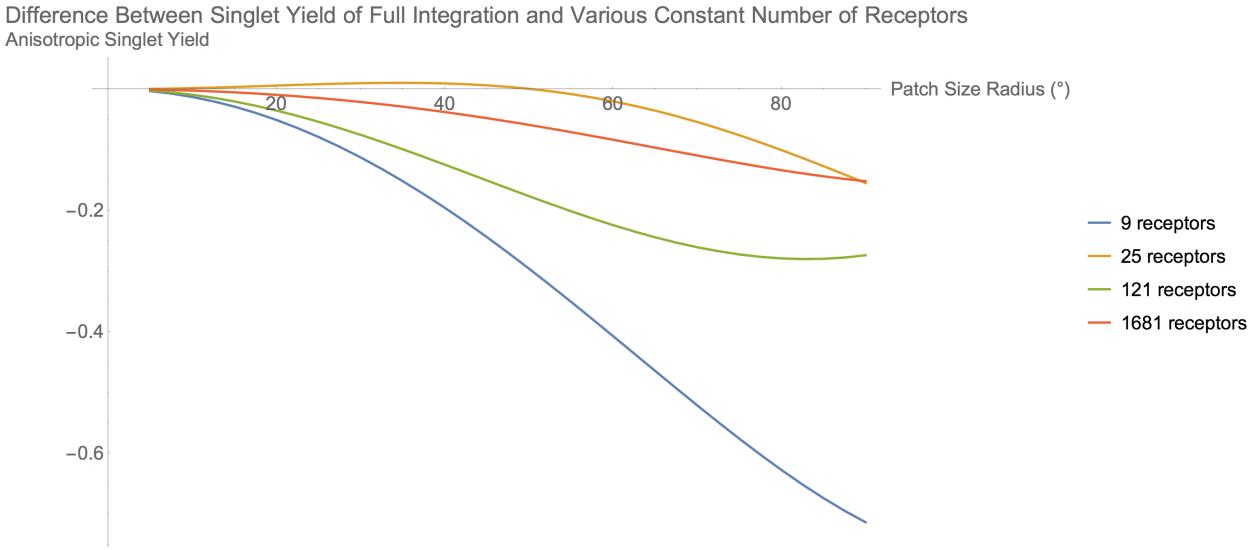

Figure 2.12: The difference in singlet yield signal between the discrete receptors and the overall average increases as the patch size gets larger. This is an artifact of choosing any lattice structure.

within the patch is averaged to compose a single value. The head then turns left or right by some initial angle, keeping the direction of the eye pointed along the horizon. The singlet yield of all the receptors is again averaged and results in a single value. These two values are compared and the difference in yield is multiplied by a gain value that will tell the head

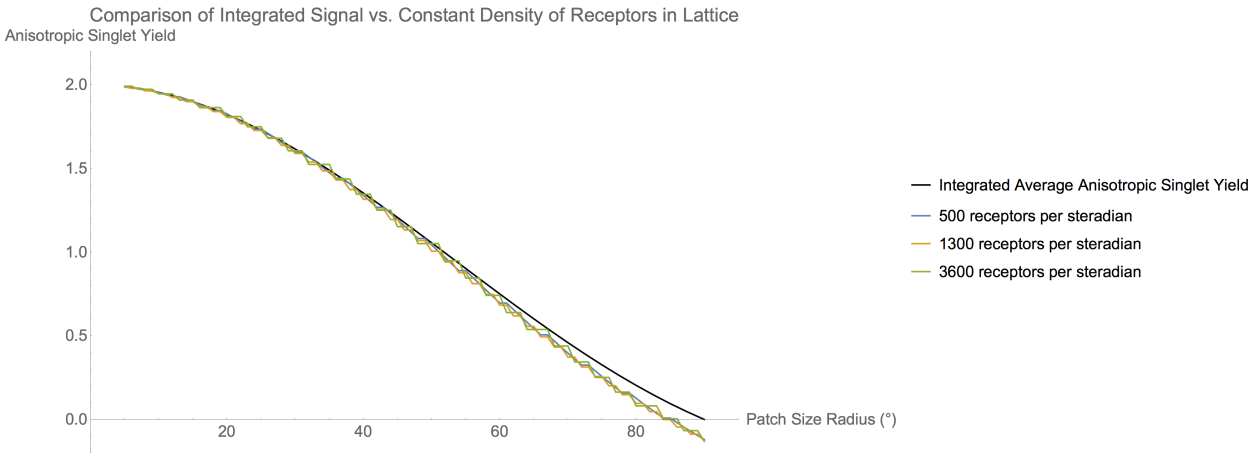

Figure 2.13: In this structure form as patch sizes get larger, the density of receptors stays constant so that the larger patch sizes have proportionally more receptors. The structure is made by creating a lattice structure that encompasses the entire retina, and patch sizes are created by cutting the lattice structure off at certain radii. Because of this, the receptors do not stretch all the way to the edge of the patch, and it results in a slightly higher signal than the integrated anisotropic yield.

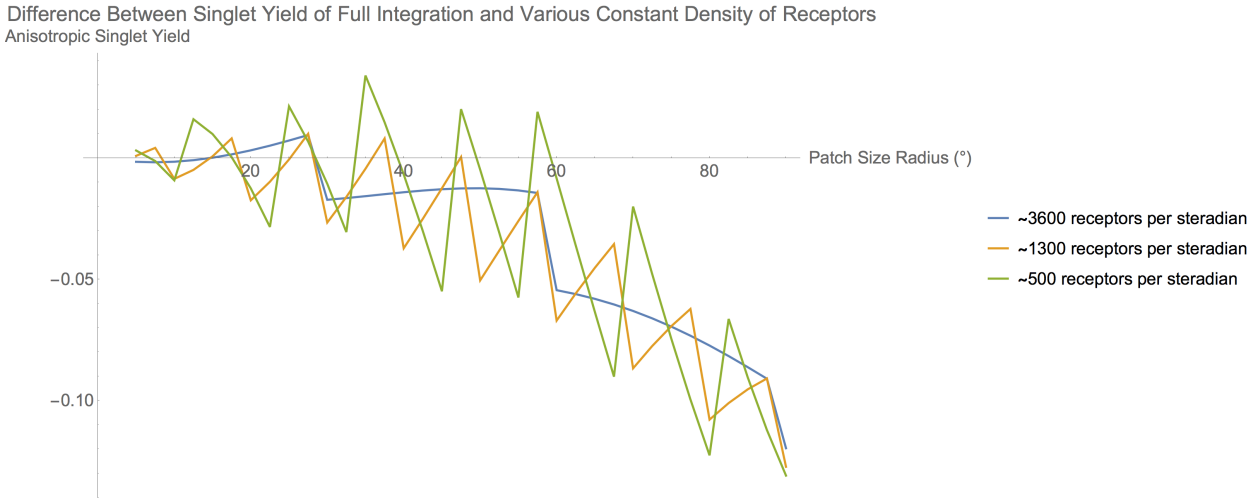

Figure 2.14: Difference Between Receptor Average for Constant Density of Receptors and Integrated Average

to continue to turn in the same direction or reverse itself, and by what angular value. This process repeats itself for many steps. This process ideally ends with the head reaching some steady state in a direction correlated with the magnetic field. This steady state is either some asymptote that is never crossed, or a direction that the oscillating head behaves as an overdamped oscillator. The algorithm concludes by either a cutting off at a certain number

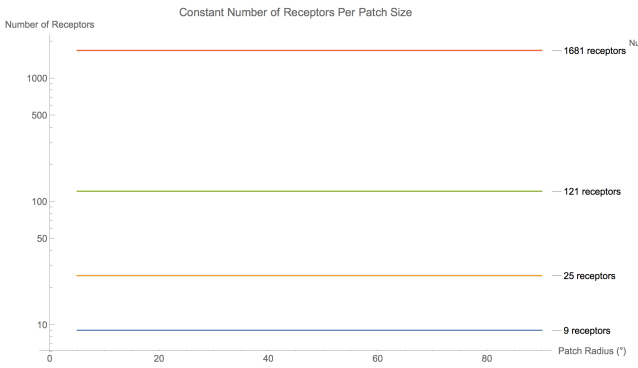

(a) constant number of receptors

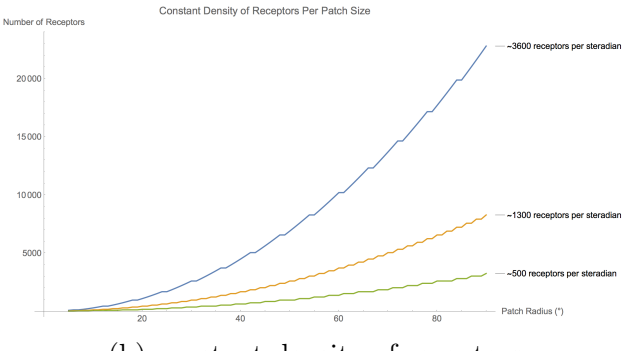

(b) constant density of receptors

Figure 2.15: The number of receptors under constant density increases parabolically as expected because the patch area increases parabolically with an increase of patch radius up until 90° at which point it reverses. The jagged nature of these plots is an artifact of having incrementally larger radii covered by the same points because the radii does not cross into a larger ring.

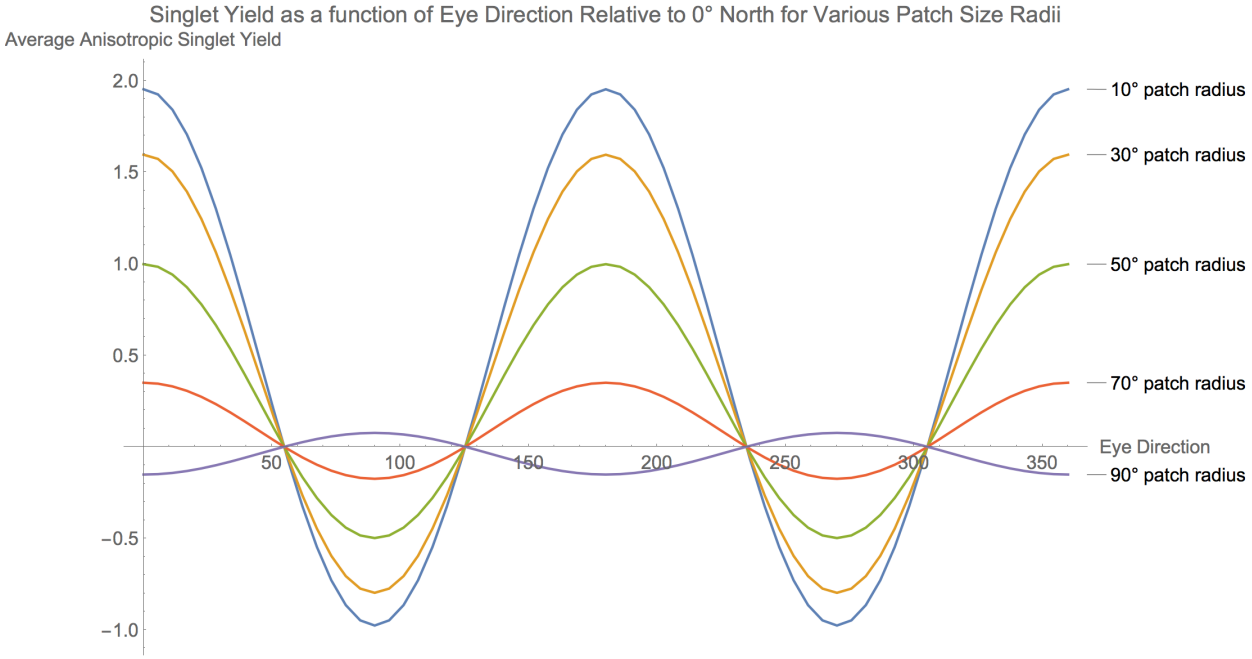

Figure 2.16: With the magnetic field pointed at $\{\phi = 0, \theta = 0\}$, the amplitude of the anisotropic singlet yield lowers as the patch size gets larger. At the patch size of using the entire hemisphere as a retina patch, an artifact of the lattice structure arises which overemphasizes the areas of low singlet yield.

of steps or until the angular change crosses some low threshold.

Under a case where the patch on the retina is centered on the middle of the retina, along

the view direction of the eye, the anisotropic singlet yield for a receptor resembles a curve of nearly $\widetilde{S} = \frac{3}{2}\cos 2\theta + \frac{1}{2}$. The maximum value of this curve is 2 and the minimum is -1. The maximum slope of this curve is 3. Under such conditions, the algorithm is configured such that under beginning at some arbitrary direction with a level eye pointed along the horizon, an animal may be able to orient.

The iteration process under these conditions is detailed as such:

1. At some direction, the average anisotropic singlet yield is calculated.
2. The head is turned 0.6 radians (17°) to the left and the yield is calculated again. And the difference of old value subtracted from the new value is computed.
3. If this difference is positive, then the head will continue to turn left by an angular value of the previous step size (in the first step, 0.6 radians) multiplied by a gain value of 1.2.
4. If the difference is negative, then the head turns the opposite direction (right) by an angular value of the previous step size (in the first step, 0.6 radians) multiplied by a gain value of 1.2.
5. This process is continued until a certain number of steps is completed.

These values of the algorithm are carefully chosen to achieve some ideal goals. The initital step size must be large enough so that there is a decent yield difference between the first two steps. If the yield difference is too small, the next steps become too small, and the head ends up changing its direction by incrementally insignificant smaller angles so that it takes an exorbitant number of steps to potentially reach some steady state. If the initial step size is too large, the head changes by a large angular value such that the yield difference is large, and the following steps will be large, meaning that the head keeps spinning out of control,

or the head jumps over orientation axis and perceives a small singlet yield, again resulting in greatly decreased step sizes and never reaching orientation.

The gain is chosen is chosen to be a factor that is two times the initial step size. A low gain means that the head almost never crosses the orientation axis while an extremely low gain means that the following steps become tiny at a faster rate and the head ends up standing still. A large gain means that there is a possibility where the head as it takes discrete angular turns may pass the orientation axis, but it can respond by turning back and eventually oscillate around the orientation axis, ideally as a critically damped or overdamped oscillator.

2.2.4 The Effect of Various Magnetic Vision Variables During the Orientation Process

Effect of Starting Direction

A method of orientation should be robust to the direction that an animal chooses to receive its first signal. The method of orientation can be tested for many directions between 0° and 360°.

In most starting directions the head is able to orient itself to the north-south axis after 20 iterations. If the starting direction is between northwest to northeast, the head is able to orient itself to north with high precision. If the starting direction is between southwest and southeast, the head orients itself south with high precision. At the starting direction near east and west, the head requires 100 iterations to orient itself.

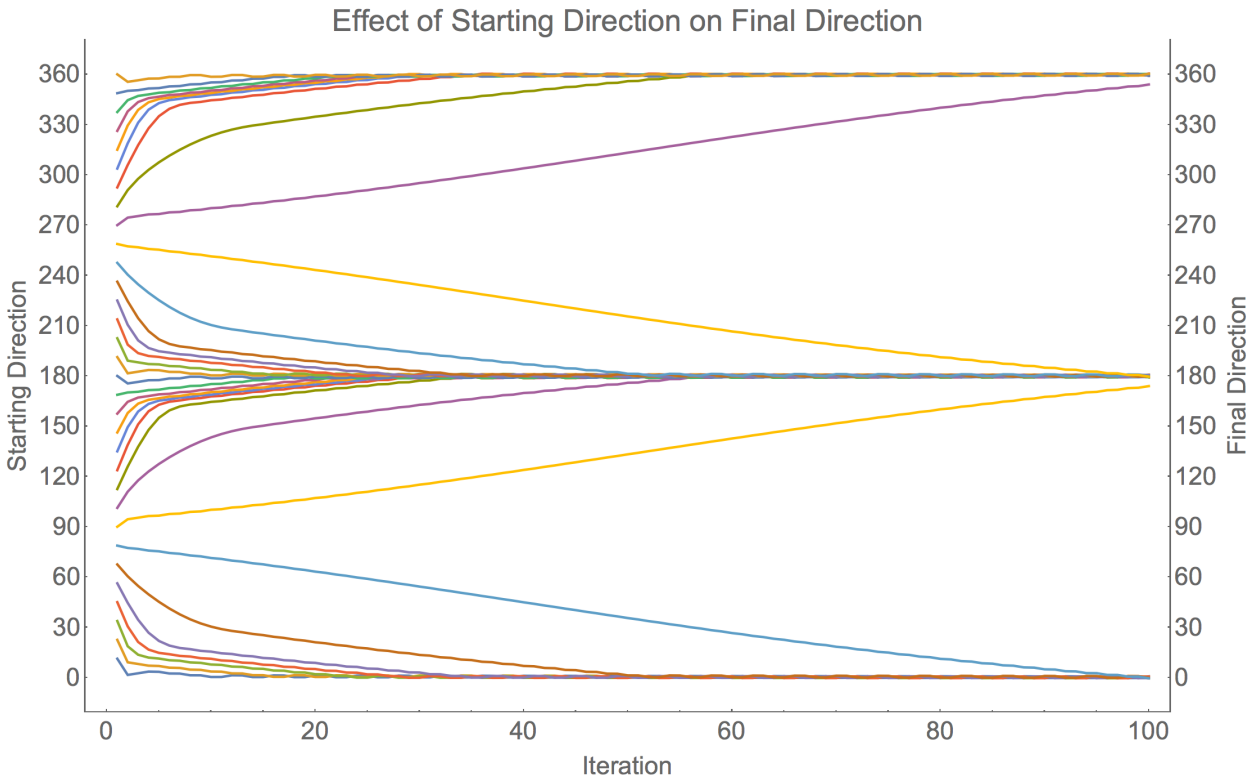

Figure 2.17: The head is allowed to iterate to a final direction after 100 iterations. The head and eye are always aimed at the horizon with an initial direction of 45° northeast. The magnetic field is also horizontal. The gain value is set to the critical value with an initial step size of 17°. The receptor patch area is 15° in radius and contains 343 receptors.

Effect of Patch Size

The size of the retina which receives and processes a magnetic signal is an interesting variable. Under the condition of no noise, all of the receptors within a small patch will produce a similar signal, so the average signal has little spread. Under a large patch size, the receptors have a large spread of signal, which always brings the average signal closer to zero. However, once noise will later be included, a large patch size with more receptors should be able to average out the noise and be more robust. There may be some middle ground in patch size where a moderate patch size will be best at averaging a signal while tolerating noise.

Keeping the starting direction constant, at 45°, corresponding to northeast, we can see how the head progresses to a final orientation. All of the patch sizes up until the full retina

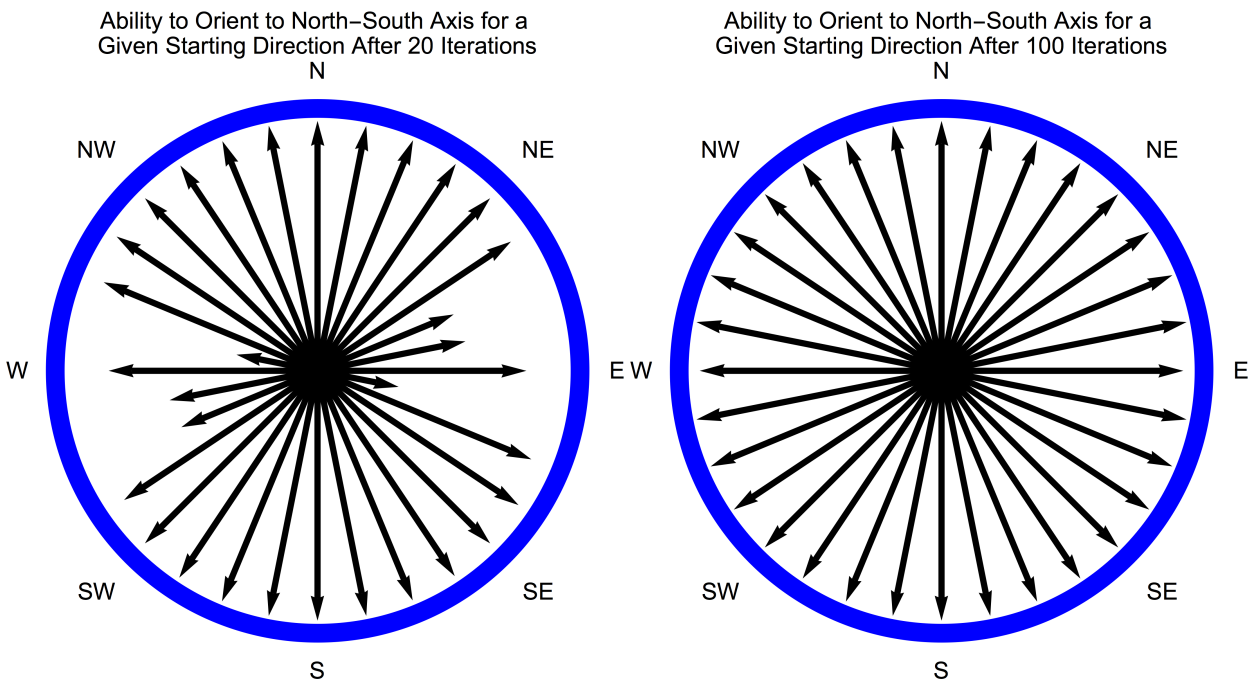

(a) Orientation After 20 Iterations

(b) Orientation after 100 Iterations

Figure 2.18: Under conditions of a 15° radius patch size with 343 receptors, the eye is initially directed horizontally pointed at the horizon. The magnetic field is also horizontal with no inclination angle. The gain is set to the critical value, and the initial step size is 17°.Each arrow indicates the initial direction that the head is pointed. The length of the arrow indicates the quality at which the head is able to navigate to the north-south axis. Because there is no noise and therefore no need for repeated trials, the length of the arrow corresponds to the angle of the head at the given iteration with the north-south axis. An arrow of 0 length means that the head is pointed either east or west, and an arrow of length 1 means that the head is pointed north or south. A single arrow is defined by a center at (0,0), and its tip is located at $\{\cos(2f)\sin(s), \cos(2f)\cos(s)\}$ where f is the final direction and s is the starting direction.

hemisphere are able to orient north, with the 90° radius full hemisphere orienting towards east. This action becomes reasonable when we can see the progression of the average signal.

Under a small patch size, the singlet yield is able to maximize itself at a larger value. The larger the patch size, the starting anisotropic singlet yield and the next step singlet yield are lower, which means that its orientation towards north takes more steps. At the large patch size of 90° radius, the average singlet yield is actually slightly below zero. Performing an initial 15° head orientation rotation produces almost no difference in singlet yield, and

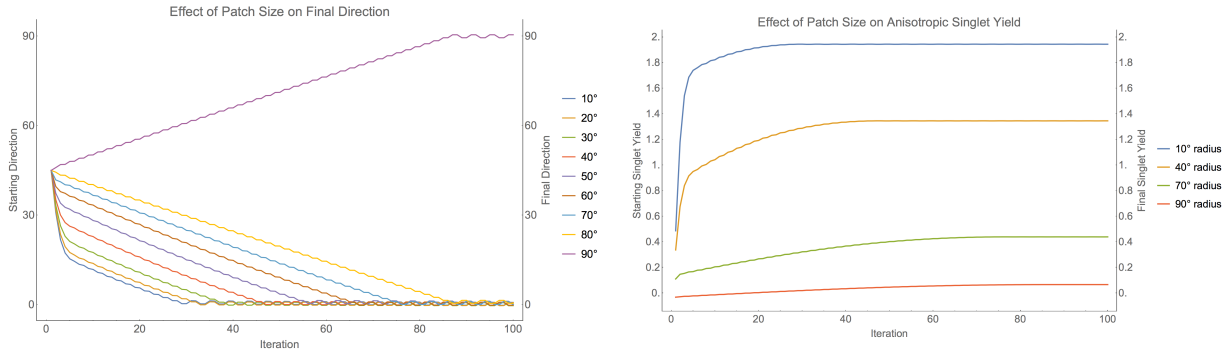

(a) Progression of Orientation

(b) Progression of Singlet Yield

Figure 2.19: Effect of Patch Size on Orientation

therefore the head does not proceed to orient itself.

Effect of Patch Density

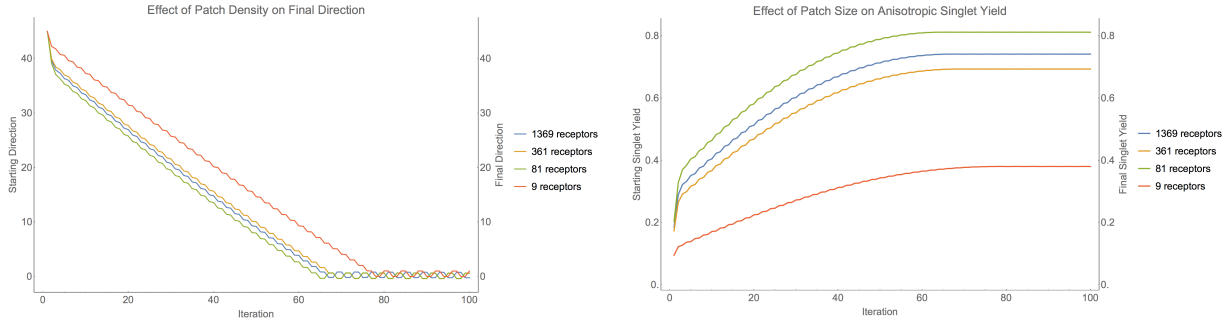

(a) Progression of Orientation

(b) Progression of Singlet Yield

Figure 2.20: The head is allowed to iterate to a final direction after 100 iterations. The head and eye are always aimed at the horizon with an initial direction of 45° northeast. The magnetic field is also horizontal. The gain value is set to the critical value with an initial step size of 17°. The receptor patch area is 30° in radius. The receptor density ranges from 1626 receptors per steradian to 10.7 receptors per steradian which corresponds respectively to the 1369 receptors to 9 receptors within the 30° radius patch.

Under no noise, the density of receptors within the patch does not have a large effect on the ability to orient. Under a 60° radius patch size and again starting from 45° northeast, multiple densities of receptors, which directly correlates with different number of receptors, the head is able to orient under all densities. Its not until an extremely low density of receptors (nine receptors total) that the head exhibits slightly different behavior from those

of higher density. With only nine receptors, there is a lot of space on the retina that is not accounted for. Above this low density, the anisotropic singlet yield is very similar. The differences that occur are mostly an artifact of the lattice structure of the receptors.

Effect of Patch Location

All of the above simulations have been performed with the assumption that the patch of receptors has been located directly behind the iris, centered on the axis of the view direction. Because the geomagnetic field has an inclination angle, the receptor patch may not ideally be located in the center of the retina but be centered along the axis of the magnetic field. To examine this feature, we need to modulate both the location of the receptor patch and also the angle of the magnetic field.

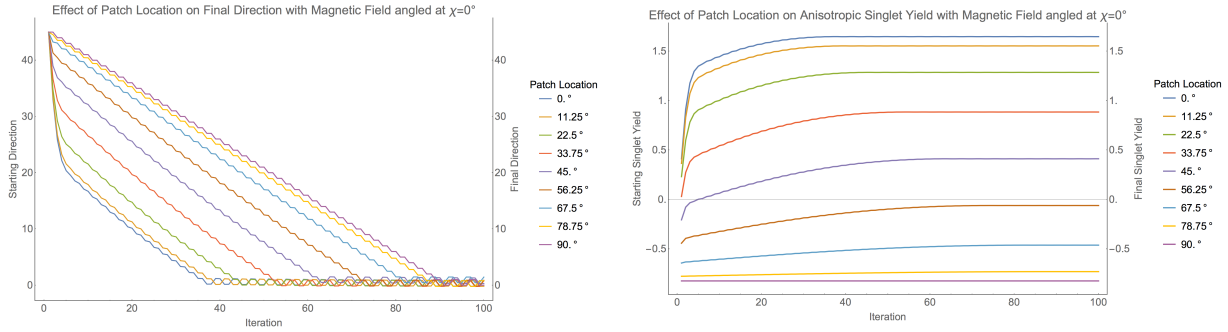

(a) Progression of Orientation

(b) Progression of Singlet Yield

Figure 2.21: The head is allowed to iterate to a final direction after 100 iterations. The head is pointed 45° northeast, and the head will remain level, but the location of the receptor patch is allowed to vary from the center of the retina to the top of the retina. The magnetic field is still horizontal. The gain value is set to the critical value with an initial step size of 17°. The receptor patch size is 15° in radius, and contains 361 receptors for a density of 1600 receptors per steradian.

Under a horizontal magnetic field, the head requires more steps to orient itself when the patch is located off center on the retina. The further the patch is, the less anisotropic singlet yield is produced as expected. The number of steps and the maximum singlet yield changes almost linearly until the maximum patch location of 90°, where the normal of the receptors

is almost perpendicular with the magnetic field.

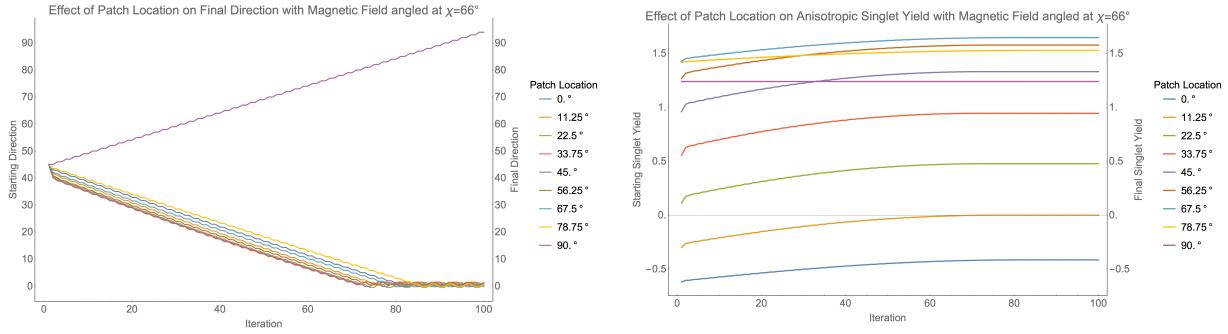

(a) Progression of Orientation

(b) Progression of Singlet Yield

Figure 2.22: The head is allowed to iterate to a final direction after 100 iterations. The head is pointed 45° northeast, and the head will remain level, but the location of the receptor patch is allowed to vary from the center of the retina to the top of the retina. The magnetic field now has an inclination angle of 66°. The gain value is set to the critical value with an initial step size of 17°. The receptor patch size is 15° in radius, and contains 361 receptors for a density of 1600 receptors per steradian.

When the magnetic field changes to a direction that replicates the geomagnetic field of 66°, the patch of receptors located at the center of the retina directly behind the iris no longer requires the fewest steps to orient itself. For all of the locations, the maximum and minimum singlet yield are different, but the difference between the two is quite similar. This feature occurs because the head turns along the horizontal, and because 66° is a high inclination angle, many of the patch locations remain closer to perpendicular than parallel with the magnetic field.

2.2.5 The Effect of Various Iteration Variables During the Orientation Process

Iteration Gain Value

The gain is the multiplier value that dictates how much the head should turn based off of the difference in singlet yield from its current direction and the previous step. The gain has a

default value that is based off of the known anisotropic singlet yield plot. The default value is initially set at a critical value so that no step can exceed the initial step size.

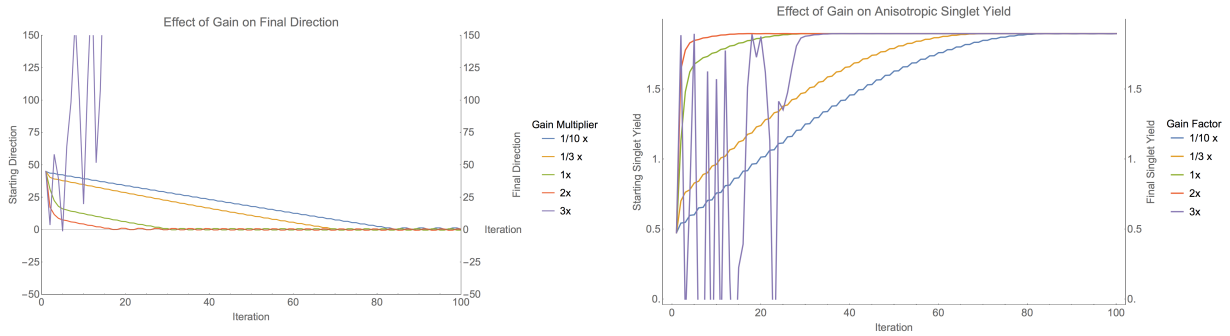

(a) Progression of Orientation

(b) Progression of Singlet Yield

Figure 2.23: The head is allowed to iterate to a final direction after 100 iterations. The head is pointed 45° northeast, and the head will remain level, but the location of the receptor patch is allowed to vary from the center of the retina to the top of the retina. The magnetic field is horizontal. The gain value is set to various values between 1/10th to 3 times the critical gain with an initial step size of 17°. The receptor patch size is 15° in radius, and contains 361 receptors for a density of 1600 receptors per steradian.

Under the condition of a horizontal magnetic field, with an initial heading direction of 45° northeast, low gain values have a predictable behavior. The head will find north, albeit slowly. At the starting direction of 45° northeast, 2x the critical gain will still yield the proper orientation, though if the starting point were very close north or south, the head may pass over north or south on its first step and have difficulty as the difference in anisotropic singlet yield may not lead the head to align itself in the direction it is nearest to. Under a 3x gain, this positive feedback loop goes out of control as the steps it takes can mean that the head spins wildly.

Because the gain is determined by the plot above (inclination and patch location plot), the gain is a variable that may need to be adjusted accordingly in order to achieve stable paths towards orientation. The gain will typically need to be higher as changes to patch location, patch size, and noise will lower the signal and require the gain variable to aid in orienting.

Total Number of Steps & Averaging

In the process of orienting, there must be some cut off that determines when the head stops turning and decides on a final orientation. The variables can be tweaked so that the head achieves orientation faster. Increasing the gain, lowering the patch size, keeping the magnetic field perpendicular with the patch location all allow fewer steps to be taken to achieve orientation. An additional method that is logical and simple is to average the final few steps. Its unlikely that the head performs its orientation process and simply uses its final direction and takes a single snapshot of both its direction and singlet yield. A more robust process would be to average the head direction of the last few steps, particularly if there is dynamic noise that may upset the final head direction.

Initial Step Size

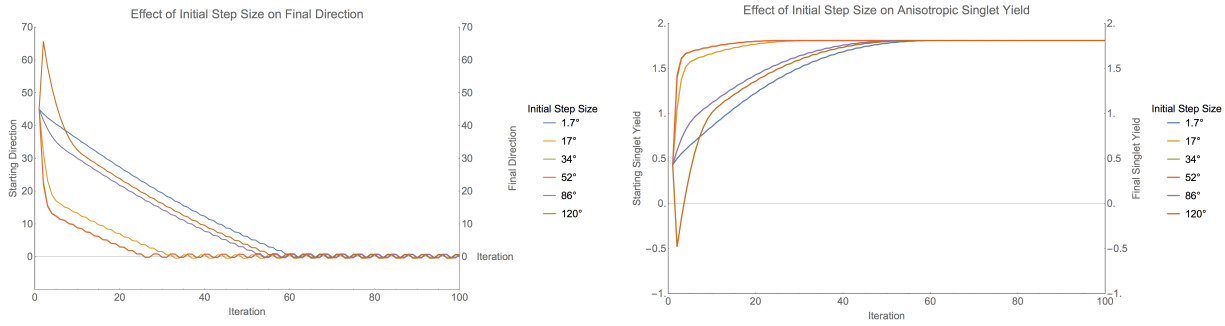

(a) Progression of Orientation

(b) Progression of Singlet Yield

Figure 2.24: The head is allowed to iterate to a final direction after 100 iterations. The head is pointed 45° northeast, and the head will remain level, but the location of the receptor patch is allowed to vary from the center of the retina to the top of the retina. The magnetic field is horizontal. The gain value is set to the critical value with various initial step sizes from very low 1.7° to wild 120°. The receptor patch size is 15° in radius, and contains 361 receptors for a density of 1600 receptors per steradian.

There is again a sweet spot in choosing the initial step size. If the first step is too small, the head proceeds to take small angular steps so that it takes a large number of steps to achieve orientation. In this scenario of starting at 45° northeast, the head makes and initial

turn towards south, and in all of the cases except for 120°, realizes that the singlet yield goes down, and therefore reverses direction and turns towards north. Then the steps get progressively smaller until it iterates around 0° north. However, under 120° initial step size, the singlet yield at 165° is larger than at 45°, so the head proceeds in the incorrect direction before more iterations at a smaller step size show that the head was turning in the wrong direction and then corrects itself.

2.2.6 Effect of Noise

Noise Entangles Everything

Noise is the most complicated factor of all of the variables. Most of the previous variables are independent of each other and predictable affect the anisotropic singlet yield and final orientation. If one of the variables during the signal collection process lowers the range of the singlet yield, the head will require more steps to orient. During the iteration process, the head requires a moderate gain and moderate initial step size. They must be high enough to proceed to orientation in a reasonable number of steps but also low enough so that the head does not turn a massive amount and compare two wildly different directions.

Noise can be introduced into the system in certain manners that would indicate where the noise would originate. A uniform noise that affects all of the receptors the same indicates a local variation in the magnetic field. A static noise that varies by receptors but stays constant as the head rotates would indicate that the noise is a characteristic of the biology of the head. A dynamic noise that is constantly changing suggests a receptor with a mechanism that doesnt produce a consistent singlet yield. Noise can be multiplicative or additive. Additive noise is overlaid on top of the singlet yield signal and indicates something affecting the receptor at the source. A multiplicative noise would lower or raise the signal by some factor. This indicates a noise within the nervous system since a large signal would be impacted by

this noise more than a small signal. If the anisotropic singlet yield is zero, then multiplicative noise does not change the signal at all. This explains why multiplicative noise indicates that an applied noise would occur after the signal reception. Additive noise is a value that is added or subtracted from the singlet yield of a single receptor. The actual value is independent of the value of the signal, and it can be given as a random number within a range.

Focusing on noise that occurs at the receptor level would tell us the most about the radical pair mechanism. Considering the current theory that radical pairs have short lifetimes in the range of microseconds, the noise that might be associated with a radical pair would be constantly changing as the radical pairs are quickly changing states. The impact of noise in concert with the other variables is less clear on the overall impact of orientation because those variables are robust to noise in various amounts.

The noise should have little to no effect on starting direction. The amount of noise does not depend on the direction the eye is pointed, so the starting direction should be independent of the noise. Increasing the density of receptors has the most obvious impact that more receptors in a given patch size allow the noise to be averaged out to achieve a more consistent anisotropic singlet signal. Adding noise to changing the patch location should further decrease the range on the singlet yield and make orientation more difficult. The interesting effect may be changing the patch size. As previously discussed, increasing the patch size brings the average singlet value of the patch closer to zero. However, at a constant density of receptors, a larger patch size means that there are more receptors to average out the noise. Similarly, a tiny patch size with few receptors will be greatly affected by noise. There should be a middle ground that balances out the low average anisotropic singlet signal of the large patch size with the high sensitivity to noise from fewer receptors of a small patch size.

Because its possible for the noise to create a random high fluctuation where a very high anisotropic singlet yield is falsely perceived to be true, the gain and initial step size may need to be conservative in order to orient oneself. The gain could potentially exaggerate the

false value and cause the head to turn farther than it should to orient itself in more steps or wildly spin so it does not reach a steady state.

Ultimately, this simulation must decide on a single direction to be oriented. With the previous variables, the simulation only needed to be run a single time with absolute certainty because the final singlet yield and final direction are predetermined by the set conditions. With the volatility of noise, every simulation will generate different singlet yields and different step sizes. Similar to bird experiments, many trials need to be done to get an average direction and determine what kind of behavior is expected under certain conditions.

2.2.7 Noise Results

As the noise is added, many of the previous variables need to be reevaluated for their effect. Also, because the randomness of noise causes every iteration to be different which makes every trial of orientation different, the result no longer is deterministic by the preset conditions but it probabalistic in nature. Many trials need to be performed per set of conditions including noise level, patch size, patch location, patch density, gain, initial step size, and magnetic field vector. The variable of initial starting direction can be eliminated by testing many evenly distributed directions every time. Below are some example trials.

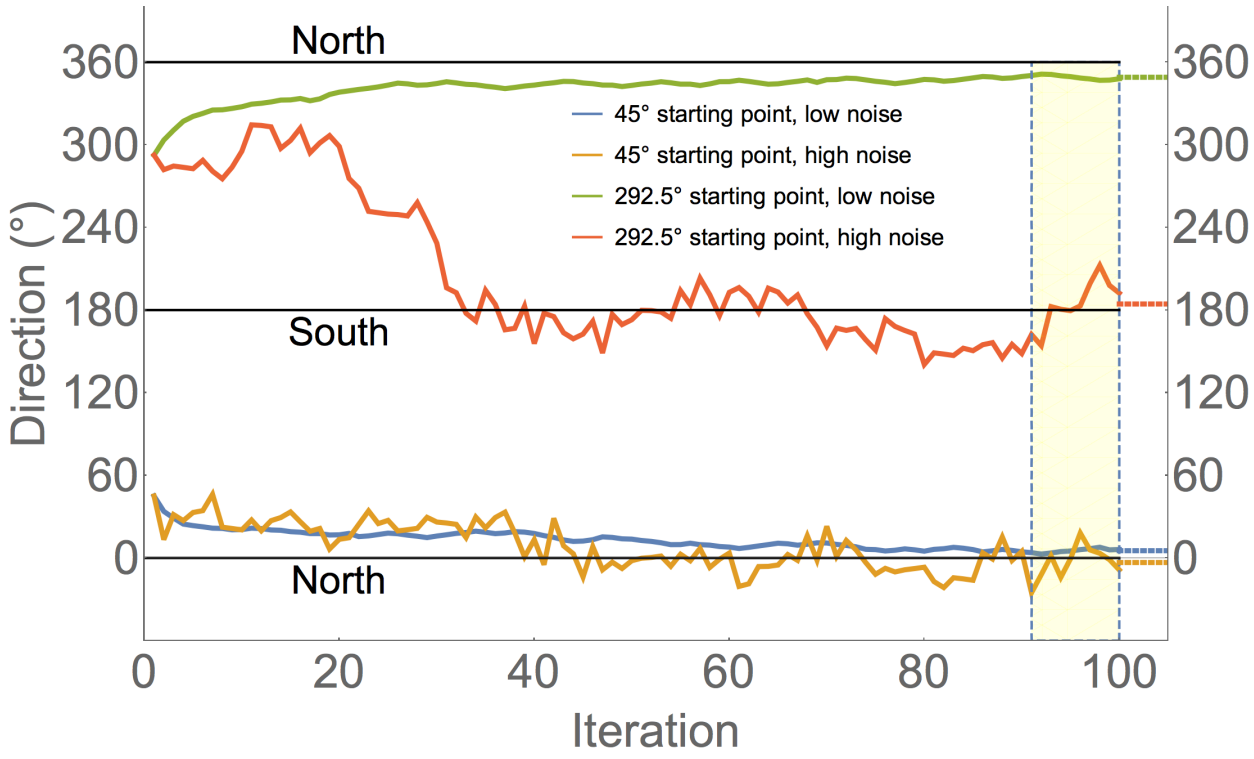

Figure 2.26: Example Trials at different starting points

Ideal Patch Size

This simulation that includes noise can be performed similar to bird experiments where given a certain set of initial conditions, the bird can attempt to orient itself. But because this is a simulation, its possible to test certain conditions repeatedly until significance is found. The measure then becomes finding conditions that create the highest significance. The first simulation to perform is one with ideal conditions such that as the head turns, the eye will perceive maximal contrast, which gives the most magnetic information. With the magnetic field at horizontal 0° and the patch located directly center on the retina at 0°, we expect to receive the full range of maximal and minimal anisotropic singlet yield possible which should be the most robust to noise. Within the 360° of possible starting directions, we choose to test a starting direction at every 22.5° so that there are 16 directions that uniformly encompasses the horizon. The density of receptors is set to an extremely low 133 receptors per steradian.

The size of the patch ranges from 10° radius to 90° full hemisphere. The noise levels extend from 5% to 500% of the range of the anisotropic singlet yield, and the noise is applied to each receptor and is randomized within the given noise level with every change of direction. The gain is set to the critical level such that every step will not exceed the size of the first step, and the first step is a head turn of 17° The head is allowed to propagate through 100 iterations, and the average of the last 10 iterations is the final direction for that test. 20 tests are performed for every starting direction, which means that every patch size and noise level is tested 320 times.

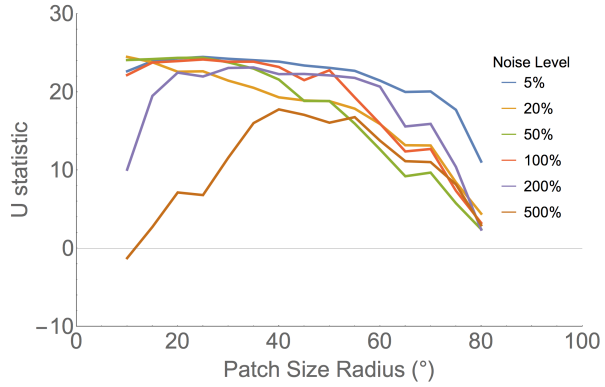

(a) Bimodal Quality of Orientation for many patch sizes and noise levels

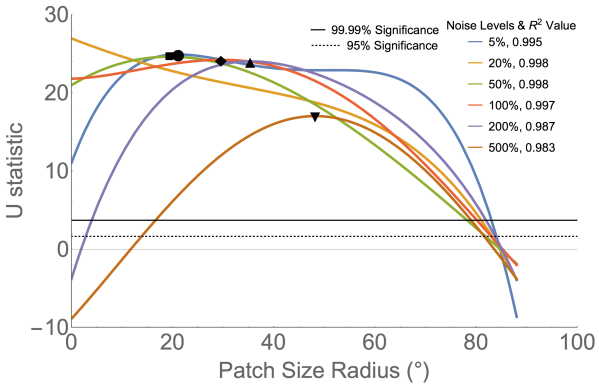

(b) 4th order best fit curves of (a)

Figure 2.27: Quality of Orientation for various noise levels

The lines are fit with a 4th degree polynomial to best characterize the peak. A quadratic equation goes not fit as well since the peak is skewed to be flatter on the left side, and a higher order polynomial may have a higher RSquared value but loses resolution on the peak. All of the best fit lines of 4th order polynomial have an extremely high RSquared value. The black line signifies the minimum U-statistic required at 320 tests to be 99.99% confident that behavior is bimodally clustered around the 0° to 180° axis line. These best fit lines can be evaluated by some key characteristics: patch size at which the line first crosses above the critical significance threshold, patch size at which the line crosses below, and patch size at which peak orientation is achieved. The statistics for the lines are in the below table.

Noise	Patch Radius Range	Patch Radius Range Difference	Patch Radius of Peak Significance	U-statistic at Peak
5%	(0, 83.047)	83.047	21.147	22.899
20%	(0, 81.004)	81.004	0	26.961
50%	(0, 78.202)	78.202	19.41	24.625
100%	(0, 80.141)	80.141	29.602	24.226
200%	(3.972, 81.954)	77.982	35.363	24.024
500%	(16.599, 79.014)	62.415	48.191	17.028

Table 2.1: Characteristics of Best Fit Curves

The patch size range becomes predictably smaller as the noise level increases. At low noise levels, the quality of orientation remains fairly level at small patch sizes and only gets worse at large patch sizes. The patch size radius at which the critical significance passes below 0.0001 becomes smaller as the noise level increases. We can estimate the patch size radius of peak orientation with the best fit polynomial. The U-statistic of the peak decreases as the noise increases, but the peak also shifts to a larger patch size radius. This data can be used to interpolate or extrapolate the relationship between the noise level and the ideal patch size.

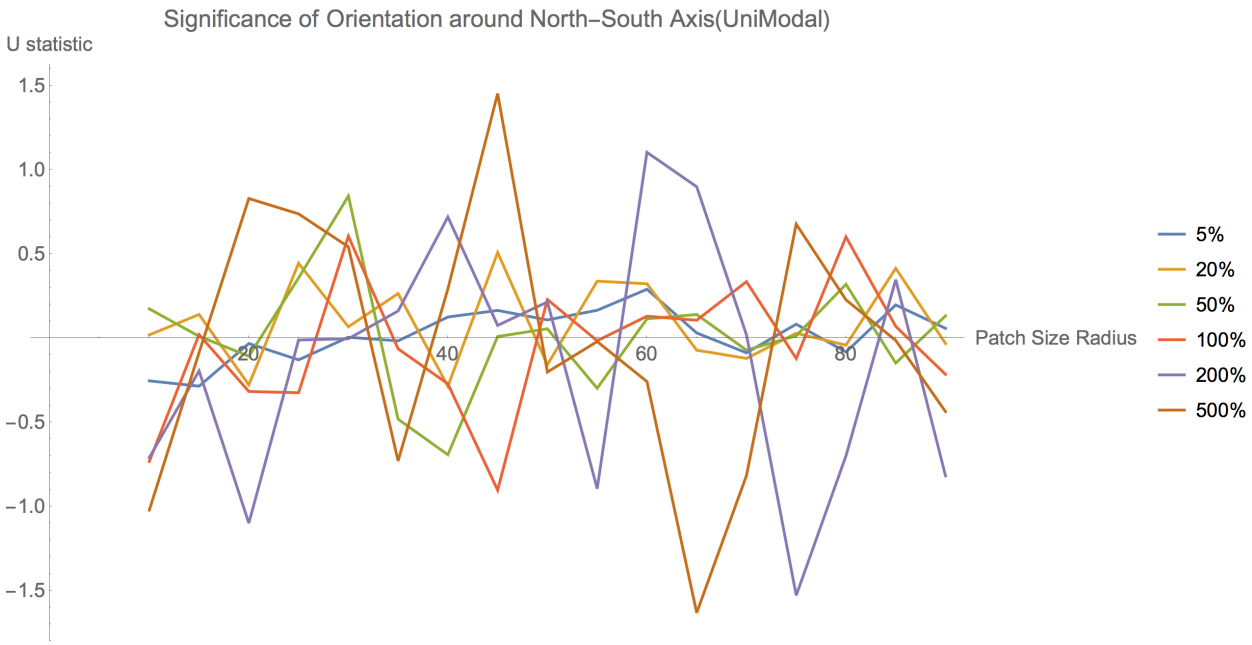

Figure 2.28: Unimodal Quality of Orientation

When applying unimodal statistics to the same set of data, the quality of orientation is poor. This is because with the magnetic field horizontal, the head finds north and south identical, which results in an insignificant mean vector.

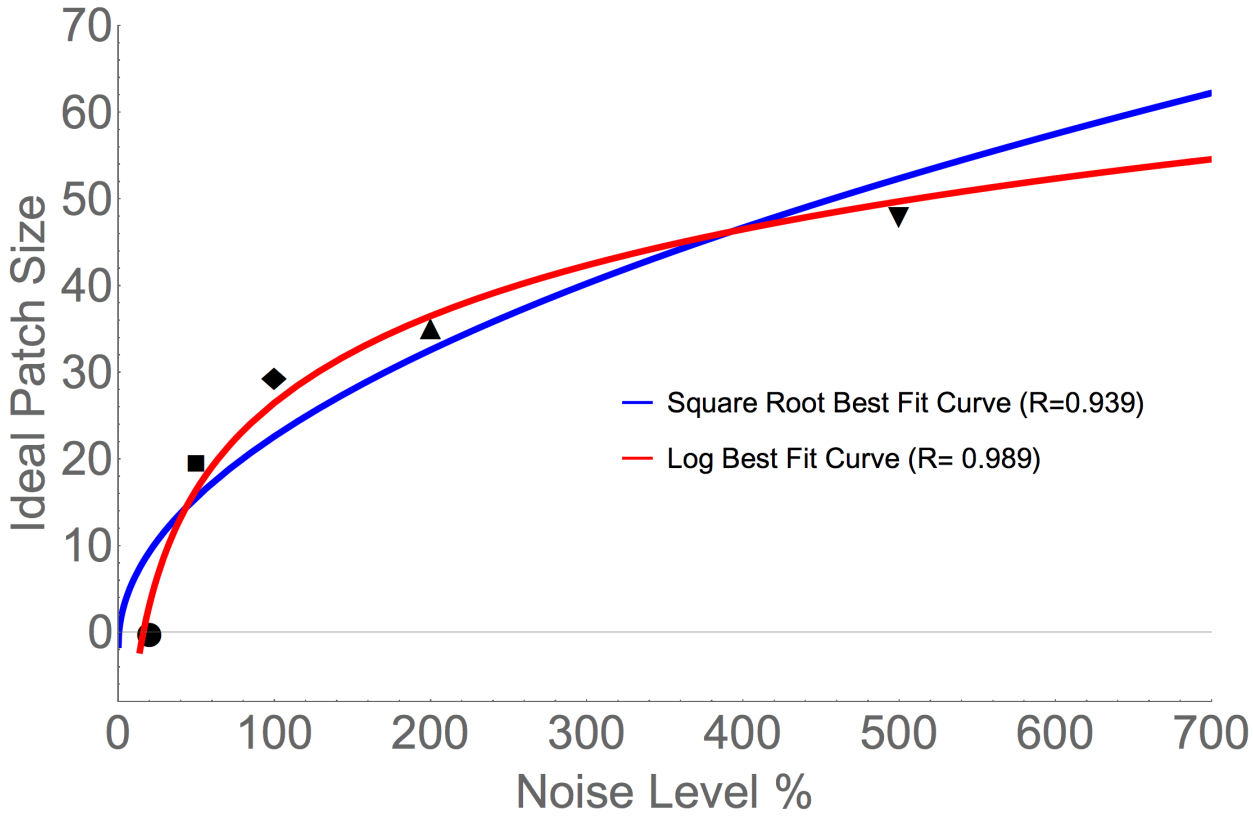

Figure 2.29: Trendline of Best Fit Line

The relationship between the noise level and the ideal patch size appears to be logarithmic in nature. Although its possible to improve on this best fit by also combining a linear component, theres no reason why a linear component would exist in this scenario. The best fit line of the log plot is $-41.6267 + 14.9224 \log[\theta]$, which extrapolates the scenario that a full hemisphere of receptors is robust up to 6000% noise.

Effect of Noise vs. Density of Receptors

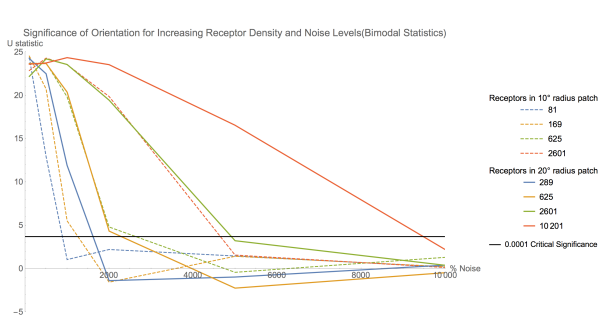

(a) Quality of Orientation for many density of receptors and noise levels

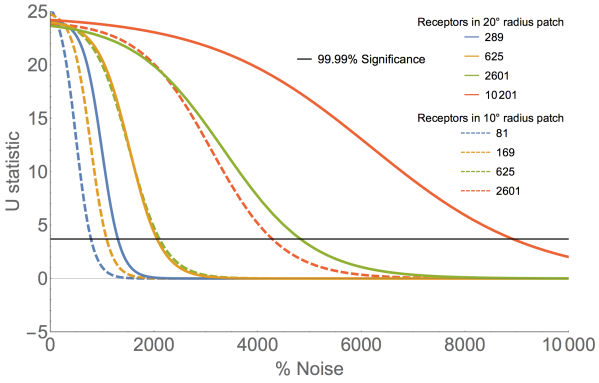

(b) Logistic Best Fit Curves

Figure 2.30: Quality of Orientation for various receptor densities and noise levels. The magnetic field is horizontal, and the receptor patch is located behind the retina. The receptor patch is 20° in radius and contains between 289 and 10,000 receptors. The tested noise levels range from 100% to 10,000%. The starting points are evenly distributed. The gain and initial step size are set to critical values. The line of 99.99% significance is displayed. The best fit curve is a logitic fit defined by equation 3.

The simulation expects that quality of orientation will increase as more receptors are added, but decrease as more noise is applied. In order for this simulation to scale up to a biological system properly, we must find a relationship between the number of receptors, the noise level, and their effect on the orientation. The quality of orientation will remain unchanged as long as the increase in noise is the same as the increase in the number of receptors. This is expected as the variance of the signal will decrease by $(\sqrt{N})$, while increasing the noise level will increase the variance by $(\sqrt{N})$. This means that a biological system with thousands or millions of receptors may possibly be extremely robust to noise in the system.

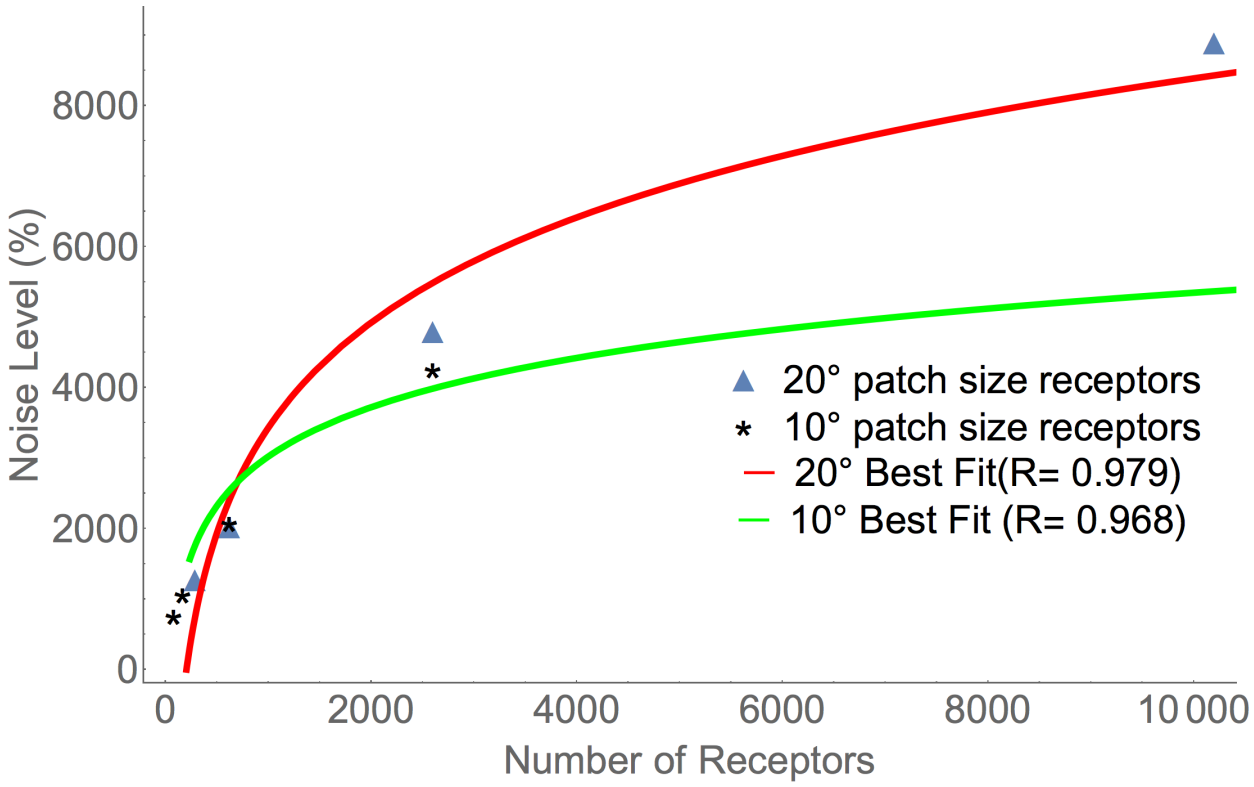

Figure 2.31: For the above plots, the relation between density and noise is quantified by a log fit that shows the receptor density required to be robust with 99.99% certainty up to a level of noise. There are approximately 10,000 cone cells within a 20° radius patch size. According to the fit, if every cone cell were also contained a magnetically sensitive radical pair, the head would be able to orient up to 8000% noise.

Effect of Gain and Step Size

To replicate real world conditions, particularly those of the bird studies performed in Frankfurt, Germany, [54] the magnetic field vector must be at 66°. The location of the patch on the retina should be located at 66° above the center in order to achieve maximal contrast as the head turns. As shown above, as the magnetic field vector changes angle, the possible range of anisotropic singlet yield changes. Because of this smaller range, the same amount of noise will distort the signal more. To compensate for this, the gain and initial step size can be modified to attempt to amplify the decreased signal and continue to orient.

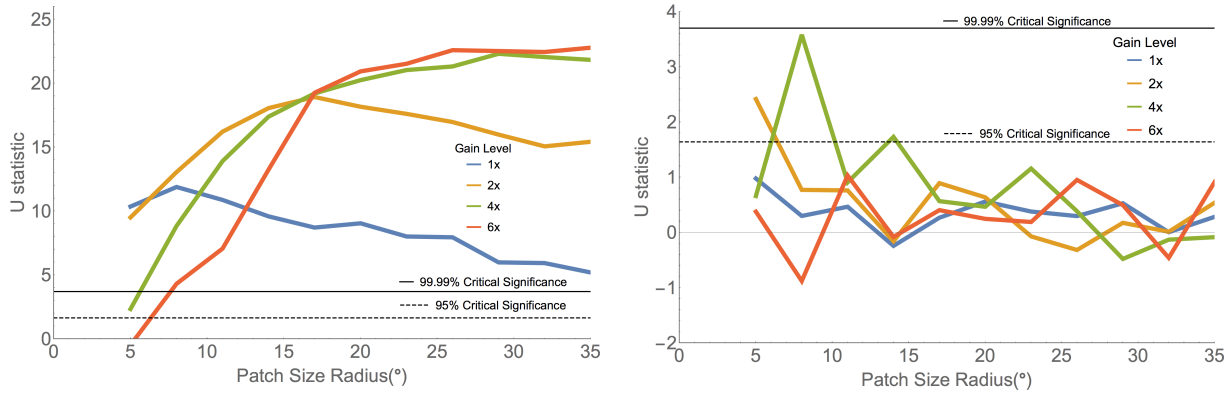

(a) Bimodal Quality of Orientation

(b) Unimodal Quality of Orientation

Figure 2.32: Quality of Orientation for four gain levels at magnetic field inclination of 0° with 100% noise. The patch is also located at 0°.

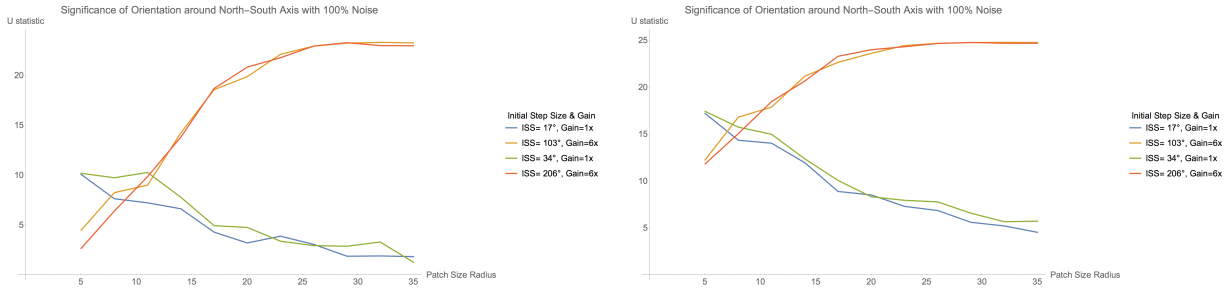

(a) Bimodal Quality of Orientation for two gain and initial step sizes

(b) Unimodal Quality of Orientation for two gain and initial step sizes

Figure 2.33: Quality of Orientation for gain and step sizes under 100% noise. Magnetic Field is at an inclination angle of 66°, and the patch is also located at 66°.

The gain is the more important feature that aids in orientation. Because the range in singlet yield decreases by roughly a factor of five, the remaining signal needs to be amplified in order to achieve significant orientation. The small patch sizes under low gain is actually better at achieving good orientation than larger patch sizes because small patch sizes will give bigger contrast as the head turns. The high gain at low patch sizes distorts the signal because the noise that occurs at the few receptors is amplified and can disorient the head, but once the patch sizes get larger, the head is able to average out those receptors and use the higher gain to properly act on the signal it receives.

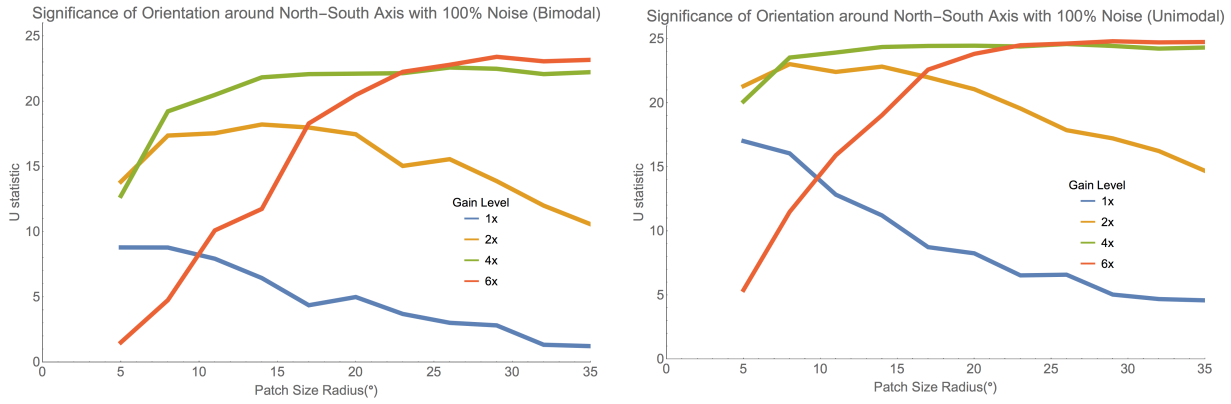

(a) Bimodal Quality of Orientation for two gain and initial step sizes

(b) Unimodal Quality of Orientation for two gain and initial step sizes

Figure 2.34: Quality of Orientation for four gain levels under 100% noise. Magnetic Field is at an inclination angle of 66°, and the patch is also located at 66°.

Finding Orientation

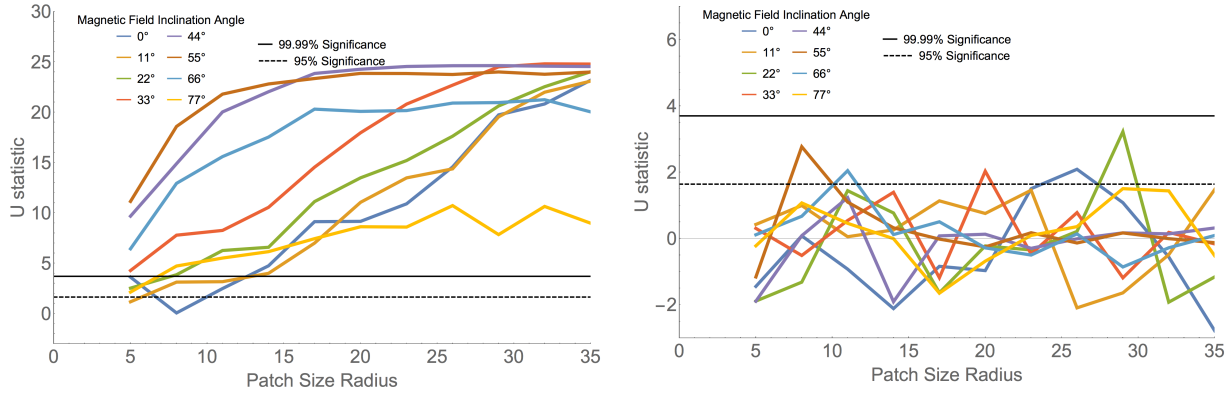

(a) Bimodal Quality of Orientation

(b) Unimodal Quality of Orientation

Figure 2.35: Quality of Alignment with when changing the magnetic field inclination at 100% Noise and 3x gain

The head is able to align itself with the north south axis at a 3x critical gain level even with a 0° patch location. The quality improves when the patch size gets larger. With unimodal statistics which measures the ability to orient north, the head is still not able to orient itself north, because with the patch at 0°, north is still indistinguishable from south.

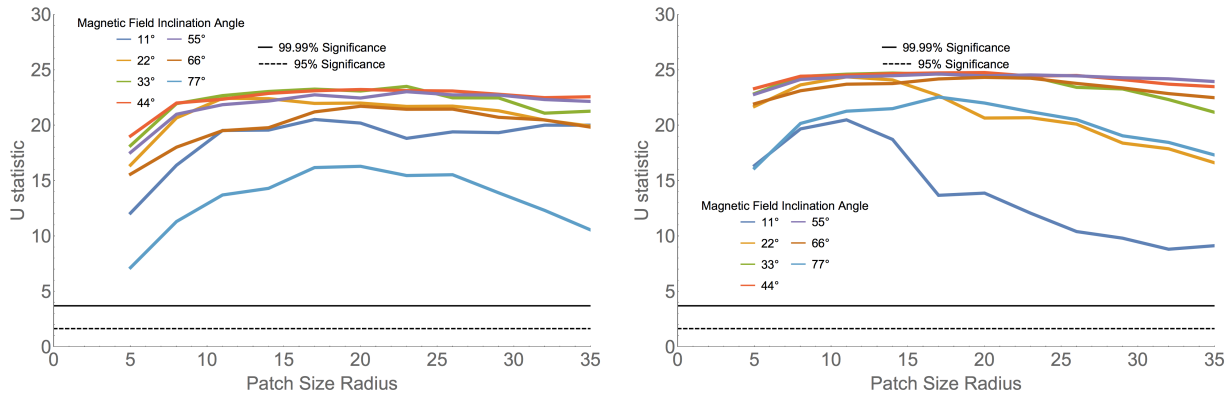

(a) Bimodal Quality of Orientation (b) Unimodal Quality of Orientation

Figure 2.36: Quality of Alignment with when changing the magnetic field inclination with 66° patch location and 100% Noise and 3x gain

Then the magnetic field has an inclination angle, and the patch of receptors is located off center, the head is able to orient north. The quality of orientation improves when the magnetic field inclination becomes closer to parallel with the z-axis of the receptors, but within the broad range of 11° to 77°, the head is able to get good orientation at all angles.

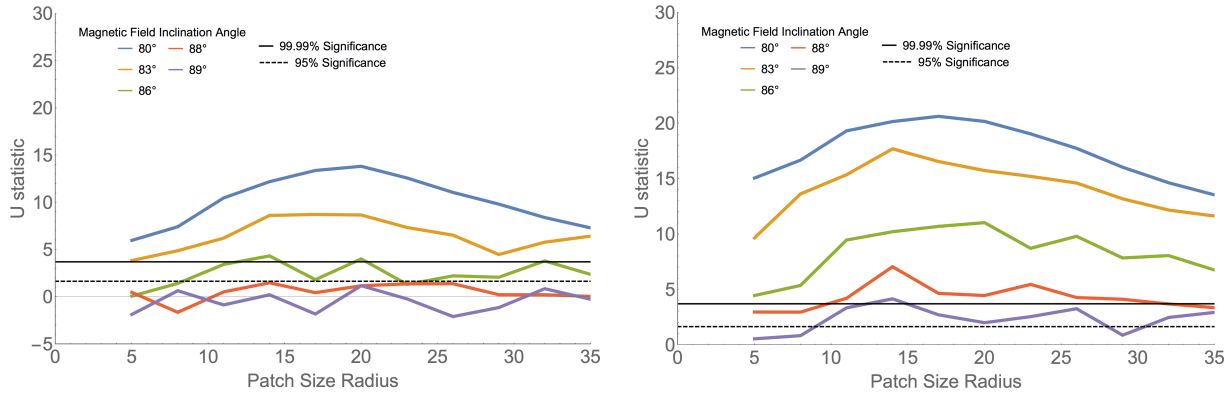

(a) Bimodal Quality of Orientation (b) Unimodal Quality of Orientation

Figure 2.37: Quality of Alignment with a steep magnetic field inclination with 66° patch location and 100% Noise and 3x gain

When changing the magnetic field to a very steep inclination angles, there exists a point where orientation is much more significant. The interesting part is that studies by Susanne Akesson [1] brought birds to areas of Earth with an extremely high inclination angle. The

birds were able to orient themselves up to an inclination level of 87°. The breakdown in quality of orientation seems to occur at 86° in my simulation.

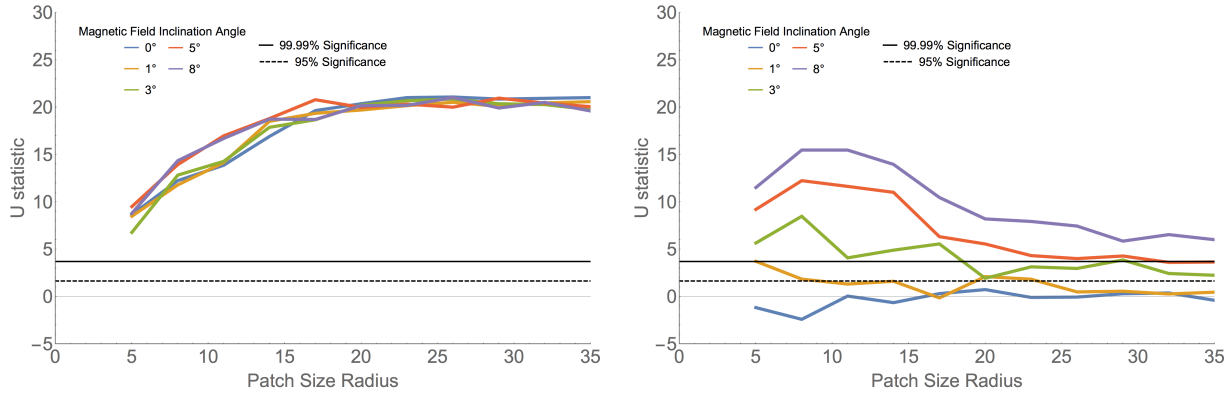

(a) Bimodal Quality of Orientation

(b) Unimodal Quality of Orientation

Figure 2.38: Quality of Alignment with a very gradual magnetic field inclination with 66° patch location and 100% Noise and 3x gain

There is no anecdotal evidence of studies done in areas of near 0° inclination magnetic field, but these set of trials show that alignment is highly significant at low inclination angles, and orientation may only be possible at inclination angles above 5°.

2.3 Conclusions

This model attempts to replicate some basic mechanics of an eye and show that its feasible to use the magnetic field to be able to orient oneself through the radical pair mechanism. Although the lifetime of the radical pair may be small, the signal may be weak and susceptible to noise, and a host of environmental conditions may be in play, with enough receptors, it is possible through a simple algorithm to use the information provided by radical pairs at enough receptor sites to gradually orient oneself with the axis of the magnetic field with a single eye. We've constructed a model that contains features of a head that takes into account the magnetic field vector, head direction, eye direction, receptor location, and keeps

track of necessary Euler angles. Although the magnetic field permeates the hemisphere of the retina, the retina is modeled as a spherical shell with points on the shell acting as receptor cells. The lattice structure of the receptor cells creates a signal similar to one as if every infinitesimal point on the spherical shell reacted as a radical pair mechanism, and the lattice structure signal improves as more receptors are added, and the distance between receptors decreases. The most basic simulation is one where a head has a single eye pointing forward on its head, like a human. The variables that can be tweaked are the density of receptors in the eye, choosing which area of the retina to receive and process signal, and gain to amplify the radical pair signal. What angle the head begins at and the number of the degrees that the head should initially turn affect the outcome of the algorithm, and the method by which the algorithm ends will create variance in its actual orientation. Finally when noise is applied and distorts the signal, and ideal set of conditions can be found to create consistent and accurate orientation based off of principles of the radical pair mechanism.

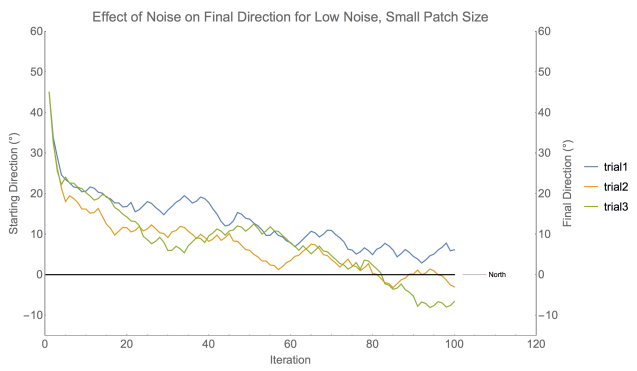

(a) low noise, small patch direction

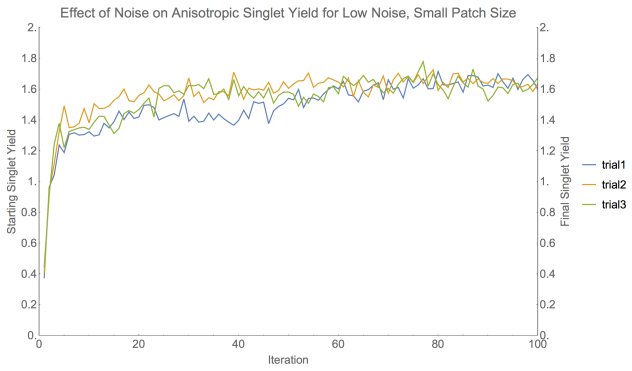

(b) low noise, small patch yield

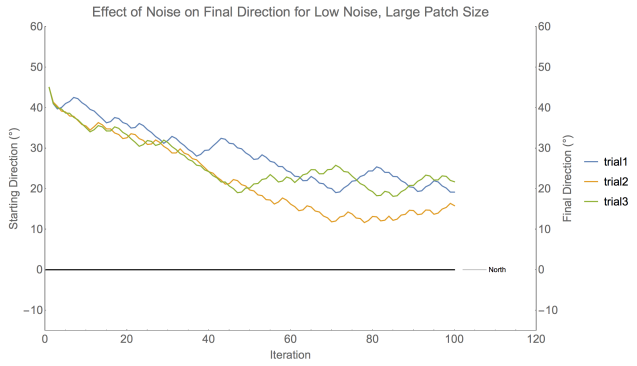

(c) low noise, large patch direction

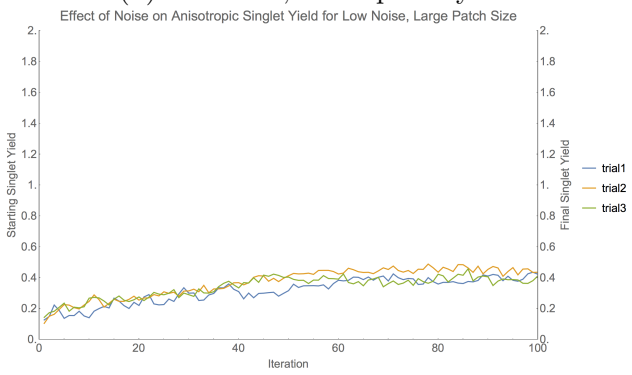

(d) low noise, large patch yield

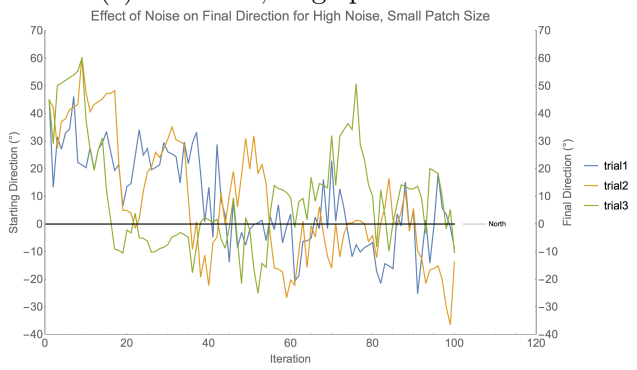

(e) high noise, small patch direction

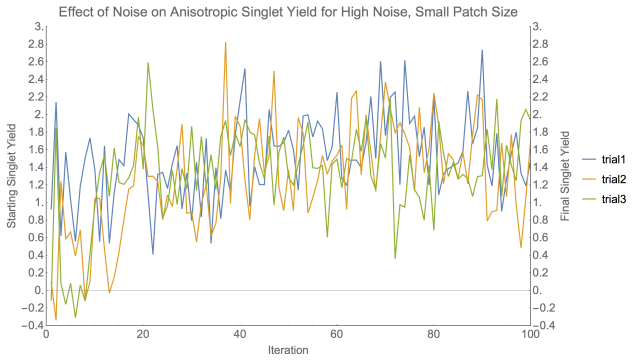

(f) high noise, small patch yield

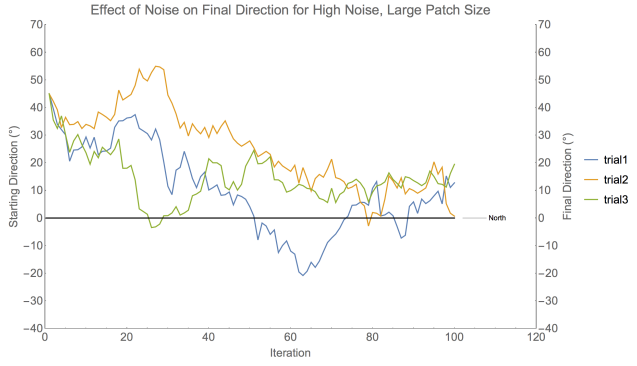

(g) high noise, large patch direction

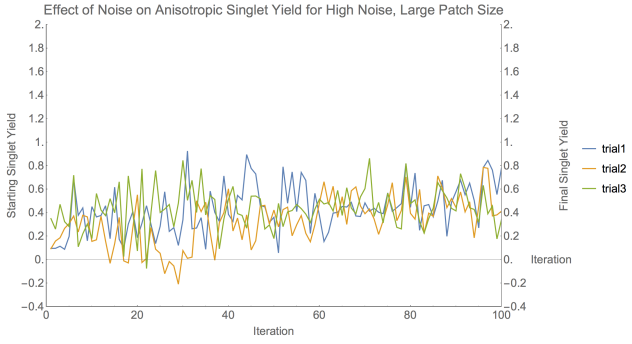

(h) high noise, large patch yield

Figure 2.25: Example trials. The magnetic field is horizontal, and the receptor patch is located behind the retina. The receptor patch is 70° in radius for large cases and 30° in small cases. The noise is 20% for low noise, and 200% for high noise. The density of receptors is constant at 133 receptors per steradian. The starting direction is 45° northeast.

Chapter 3

Magnetoreception Virtual Reality Simulation

3.1 Introduction

There has been previous work done that show what a potential magnetic image might look like if there existed the ability to see magnetic fields. However, these are typically only for a few important directions such as the cardinal and ordinal directions as well as looking directly into or perpendicular to the magnetic field. There has been limited work on the analysis of the effectiveness of having two side facing eyes and the combination of the data received that may aid in navigation. A simulation of an environment that incorporates this magnetic image was created for both human forward-facing eyes, and bird side-facing eyes.

3.2 Creating a Magnetic Image

3.2.1 Phyics to Consider behind the Image

Getting to a magnetic image starts from this formula 1.16 [48]for the singlet state yield from a radical pair mechanism. The strength of the magnetic field is contained the in the term omega. M is the total number of nuclear spin configurations (2 for the most simple one proton case). The k rate constant takes into account the rate at which the transitions from the radical pair back to singlet or triplet states occur and is essentially the lifetime of the radical pair. The P term dictates the amount of singlet state that exists within the now mixed eigenstates that all contain a different mix of states.

There are many ways to simplify the cases to determine singlet yield. Under a high rate k, as soon as the radical pair enters the singlet state, it immediately gets converted to a product, so the singlet yield is 100%. The rate k must be at a value that enables sufficient mixing of states. Under a very high magnetic field, the higher and lower triplet states move extremely far away from the zero triplet and singlet state, so the chance that the radical pair is in the singlet state is 50%.

An isotropic case means that the radical pair reacts only to the intensity of the magnetic field and not the direction. This is not particularly interesting for a magnetic sense. Under a high field, the chance that the radical pair is in the singlet state is still 50%. Under a zero field, there is still some degenerate splitting because the electron and the nucleus still precess around each other. The interesting regime is in the low field where an external magnetic field interferes with the natural precession of the electron and nucleus, but not too high in which the strong magnetic field completely polarizes the radical pair.

The anisotropic case is the interesting case because the anisotropy creates a system where the direction of the external magnetic field makes a difference. Under cases the anisotropy is

much greater than the external magnetic field which is greater than the rate k, the limiting amount of singlet yield is 5/8 and when the anisotropy is much greater than the rate k which is greater than the external magnetic field, the singlet yield is 3/8.

If the radical pair is the mechanism that is in the eye, the molecule must be ordered in such a way that all of the receptors have a common radial direction that is perpendicular with the retina. It would not matter if the radical pairs behavior were anisotropic and the molecules had random directions. This would give random noise. The radical pair needs to be organized similarly to the current photoreceptors in the eye which all face the center of the eyeball. Under this assumption, all of the radical pairs that line the surface of the retina would have different singlet yields under the exposure to a uniform magnetic field. The radical pair would only react to the component of the magnetic field which is parallel with its own anisotropy. This means that there could be a gradient of singlet yield product across the retina. When this gradient of signals is sent through the nervous signal to the brain and processed, a magnetic image could be formed.

3.2.2 Normalizing the Image

The magnetic image, which is created by differences in singlet yield product has maximum and minimum values that are determined by the interactions that affect the radical pair. In the most basic radical pair under the low field regime and ideal k constant will create singlet yield products between 3/8 and 5/8 which depend on the angle that the external magnetic field makes with the radical pair. For the basic radical pair that considers only the external field and one anisotropic hyperfine interaction, any image is essentially a Cos[2 theta] image. The rate k, strength of the external magnetic field, and the anisotropy determine the maximum and minimum singlet yields. Similar to the way that the iris and the brain are able to process and regulate images, the simulation is able to normalize images to create

contrast and amplify a small magnetic affect. If the magnetic image were initially shades of gray, the brain and the simulation could stretch the values of the image from black to white.

Colors

Instead of using just black and white and shades of gray to show what a magnetic image could look like, colors can be substituted. A typical rainbow gradient with red for the area of the retina with the most singlet yield product and purple for the least.

3.2.3 Blending with VR simulation

Types of Overlay and Blending

Because its unknown how a magnetic image could be interpreted, two candidate options can be offered. The first one is a common blending of normal vision and the magnetic image. In this method, the magnetic image is transparent and overlaid on top of normal vision. The amount of transparency can be varied from 0% or no magnetic image to 100% which would be only magnetic vision. In this method, an organism would be able to simultaneously use both senses at once. An organism would see a lighter shade of gray along the north-south axis.

A second method involves affecting the sensitivity by which normal photoreceptors operate. Instead of two signals being sent to the brain which overlap, the two signals could be multiplied into one. This means that photoreceptors with the most singlet product send a higher amplitude of normal visual signal to the brain, and the receptors with less singlet product provide a weaker signal to the brain. What this means is that areas of the retina with high singlet yield would appear brightest.

Localized Field

The simulation only takes a local field into account. When animals navigate over thousands of miles, the magnetic field can vary both in intensity and angle. Though if an animal is migrating from Mexico to Canada, the inclination would change by only approximately 30 degrees. The strength of the magnetic field in that range changes from 0.4 Gauss to 0.55 Gauss. While these changes are significant, a normal bird migration takes 2-3 weeks, so the change hour to hour or even day to day are slow. So the simulation only takes into account a uniform field with a set inclination angle and set strength.

3.3 Simulation Creation

3.3.1 All components

While the pattern of the magnetic field was created in Mathematica, the simulation is put together through a popular game engine, Unity. It is supported on many platforms including PCs and mobile devices. The program controls many aspects of the simulation that are commonly associated with video games. Some example assets that are manipulatable are lighting, terrain, user interface, movement, and camera angles. The program allows for many customizable assets through javascript or c# to be manually controlled.

Cameras

As a visual simulation, the camera is essential to replicating the eye. Different animals have different eye characteristics such as distance between the eyes, the angle that the normal makes in relation with respect to the head, field of view, and viewing distance. On top of that in the later section, there is discussion on virtual reality and what adjustments must

be made in order to properly get a 3D image from two eyes. The cameras can also be fitted with different lenses such as fisheye which is useful for an animal to have in order to increase their field of view.

Magnetic Image

The magnetic image is created in a mathematical computation program, such as Mathematica, must be mapped out to a rectangular image because the Unity program accepts two dimensional textures. This projection is called an equirectangular projection. The magnetic image is initially spherical such as the Earth. This image must be flattened into a format that is able to be wrapped in the Unity program. To convert the spherical magnetic image, longitudinal axes which are normally the same length and meet at the poles become equal length parallel vertical lines on the map. Latitudinal axes which are normally parallel but also vary in length, becoming shorter towards the poles, again become parallel, equal length lines.

The equation for this transformation is x= longitude Cos (latitude) y= latitude

This produces an image with an aspect ratio where the horizontal is twice as long as the vertical. This image is then saved and imported into the Unity program and correctly wraps around a sphere which is centered on the head.

The magnetic image is now on a sphere that must maintain its orientation because the local field does not change, only the animals head and eyes do. The animal is constantly inside this magnetic image sphere.

Lighting and shadows

Because the simulation is outdoors, its safe to assume that the light coming from the sun approaches our environment in parallel rays. Therefore the choice in directional light applies instead of spot or point lights where light emanates from a close source that allows shadows to disperse. It should be noted however, that calculating light and shadows can easily take up a majority of processing power and memory usage, so lowering light settings can make the simulation run smoother. Also, the program can calculate how light bounces off of one surface onto another surface, and turning off this option called illumination greatly alleviates build time and increases smoothness of the simulation. The directional light is applied at a 45° angle from the west, imitating approximately 3 PM.

Terrain

The most obvious portion of an environment is the terrain which is either stood on or flown about. A free terrain was downloaded and inserted into the simulation. A mountainous region was chosen in order to create some variety and to imitate a bird or other animal using the magnetic field to traverse the terrain. Some magnetoreception theories include the use of the natural landmarks along with using the magnetic field with navigation to remember and locate specific areas such as a nest for birds or storage areas for nuts and food for rodents. Detail in the terrain was mostly turned down again to speed up loading times and lower processing usage. The terrain also needed to be turned into a mesh collider which means that other objects cannot cross into the terrain such as falling through the ground or running through a mountain. While wind and grass are possible options, they are ignored because there is no evidence that would point to being an assistant or hinderance to magnetoreception.

Pilot marker

Because the magnetic sense is not a natural sense for humans, an indicator needs to be created to assist people understand how to use the magnetic image. Various compasses are used in video games, but as this simulation resembles a flight simulator, a horizontal compass is used so that the player can know what direction they are looking at as well as how far away they are from looking north. This was created by making an image of a horizontal ruler which was spaced by cardinal directions and angle numbers. This image has to repeat so that as the head turns this line stays continuous. The image should only change if the head moves along the azimuth but not along the elevation above the horizon. For forward facing eyes where the head and the cameras are pointed in the same direction, there doesnt need to be any initial offset between the image and the eye, but to simulate bird eyes, there needs to be an offset so that as the left eye might be pointed 70 degrees west of north, the head is still pointed north, and therefore the horizontal compass indicator must still show north.

3.3.2 Computer Movement and Viewing Controls

To include complete freedom of movement in our three dimensional space, two major motions must be considered. The player is allowed to change position by translation. The player can move up/down, left/right, and forward/backward. The player is then allowed to rotate allow the x-axis, y-axis, and z-axis, which are commonly known as roll, pitch, and yaw respectively. There are potentially two more degrees of freedom for our simulation that incorporates two eyes. To simulate different animals, it could be valuable to change the distance between the eyes and change the field of view of the eyes. For this simulation, those options are not adjustable. While its possible to have the eyes rotate and translate in perpendicular motions independently of each other, those are not practical options.

To create a simulation that resembles the flight of a bird however, the translational options should be limited to only the direction that the bird is pointed at. Therefore in the simulation, the player can only move in a forward direction but the player can rotate along all three axes.

3.3.3 VR implementation

Google released a Google Cardboard SDK for the Unity platform in order to create virtual reality programs for Google cardboard headsets through smartphones. The SDK allows the ability to read a smartphones gyroscope information, interact with its screen, and correct distortion caused by lenses, as well as other features that enhance a virtual reality experience.

Because virtual reality headsets use a lens that creates a wide field of view, a normal image coming through the headset will be distorted. Creating images that are warped beforehand and then are subsequently distorted so that they look clear to the viewer negates this effect. The entirety of the simulation goes through this post-process because it is a feature of virtual reality and not of the actual simulation.

Movement Controls

All of the Google cardboard headsets have a single button that simulates a tap on a smartphone screen. For the simulation, pushing this button corresponds with moving forward. The accelerometers and gyroscopes enable the use of head tracking to change the players view of the environment. The player has all degrees of rotation including roll, pitch, and yaw.

Sliders

Sliders were built into the simulation to control the amount of blending of the magnetic image and normal vision. For the blending of the black/white overlay or color overlay with the normal vision, the slider controls how much of each image is scene. When the slider is all the way left, there is only normal vision, but as the slider moves right, the magnetic image begins to take over until the magnetic image is the only thing visible when its all the way right. The second type of blending changes the brightness of certain parts of the image. The slider changes the amount that certain areas of normal vision are darkened by. The magnetic image is a grayscale image, and the normal vision remains bright in areas of white magnetic image and becomes darkened in areas of black magnetic image. When the slider is all the way right in areas where the magnetic image is dark, there is no vision, though where the magnetic image is bright, the vision remains unchanged.

Variables in Eye Offset Angle and Field of View

Animals who are preyed upon generally want the widest field of view, so their eyes are located at the sides of their head. Predatory animals have their eyes positioned in front of their head which results in less field of view but allows for stereoscopic vision which enables depth perception. Most of the preyed upon animals have similar field of views with each other. Horses have eyes angled at 65° from the front of their head, while pigeons are at 70°. However, because anatomy of an eye varies between animals, the total field of view, amount of monocular and binocular view, and blind spots also varies between animals.

The vertical field of view of humans is approximate 135° from superior(up) to inferior(down). The horizontal field of view for a single eye stretches 60° towards the nose to 110° towards the temple. This means that the total horizontal field of view is 220° but only the center 120° of that is stereoscopic. Of that stereoscopic vision, only 60° is generally considered peripheral

vision. The Cardboard SDK for Unity presets a total field of view of near 90°. The program is able to slightly this field of view for slight variations depending on the objects in the environment. It needs to balance the field of view with focus. There is no angle difference as both eyes are pointed exactly forward and are simply separated by a small distance in the simulation.

For the bird simulation, the eyes are each angled 70° away from the head with 160° of both horizontal and vertical field of views. This results in a horizontal 300° field of view and 20° of binocular vision. Hawks and pigeons have a horizontal 300° field of view, but the American woodcock actually has 360° field of view because of its protruding eyes and small body.

3.4 Magnetic VR iPhone Application

3.4.1 iPhone Application

As of 2017, the iPhone application is downloadable on the Apple App Store under the title MagneticVR. Upon launch, the app has eight scenes. Six of the scenes are meant to work with human eyes, and the last two are built for bird eyes.

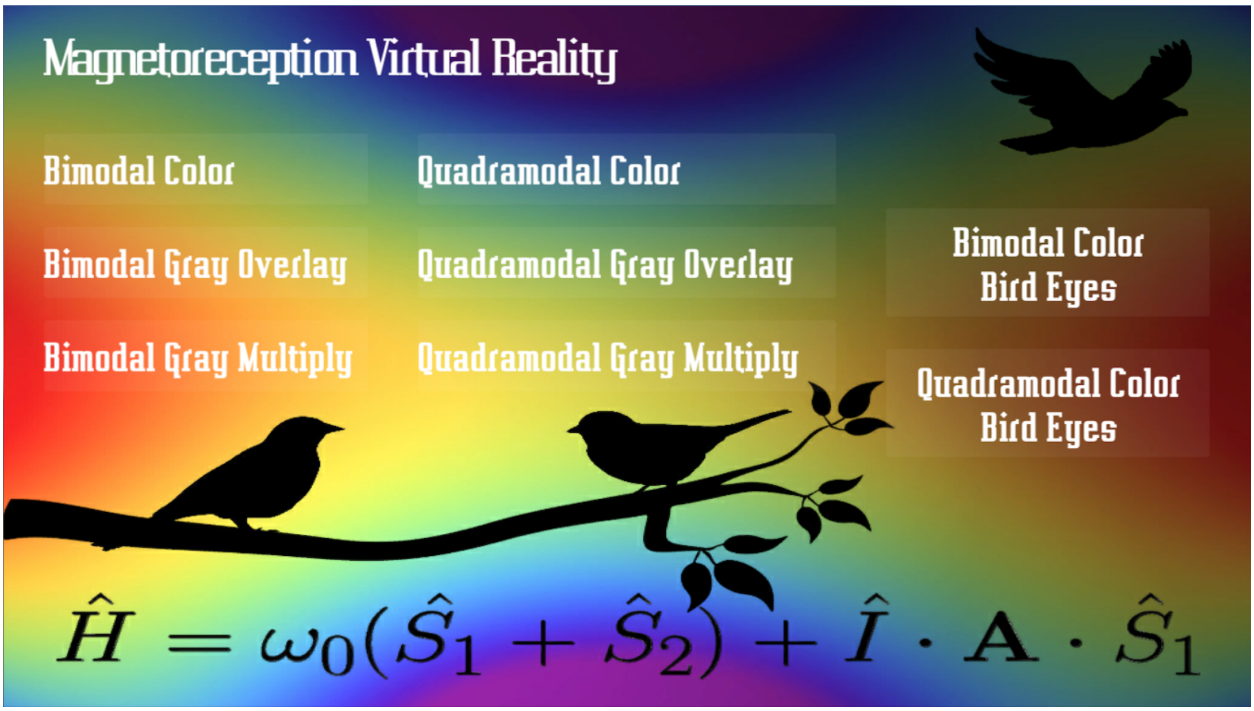

Figure 3.1: Main Menu

3.4.2 Human Eye Scenes

There are three scenes each with a bimodal and quadramodal radical pair model. These three scenes are color overlay, gray overlay, and gray multiply. Each of these scenes uses the same pattern, but is applied in a different way as explained above. The shape on the screen is warped in such a way that it becomes corrected once inserted into a Google Cardboard headset. To orient oneself north under the human eye configuration for the bimodal case, one is simply looking to find the red spot/white spot/bright spot in the downward direction depending on which scene was selected.

The quadramodal case is slightly trickier in that instead of looking for the brightest spot, north can be found by looking for the bright, narrow "x". Along the plane that is perpendicular to the magnetic field vector, there are four more spots that contain a fat "x", and those must be learned to be ignored.

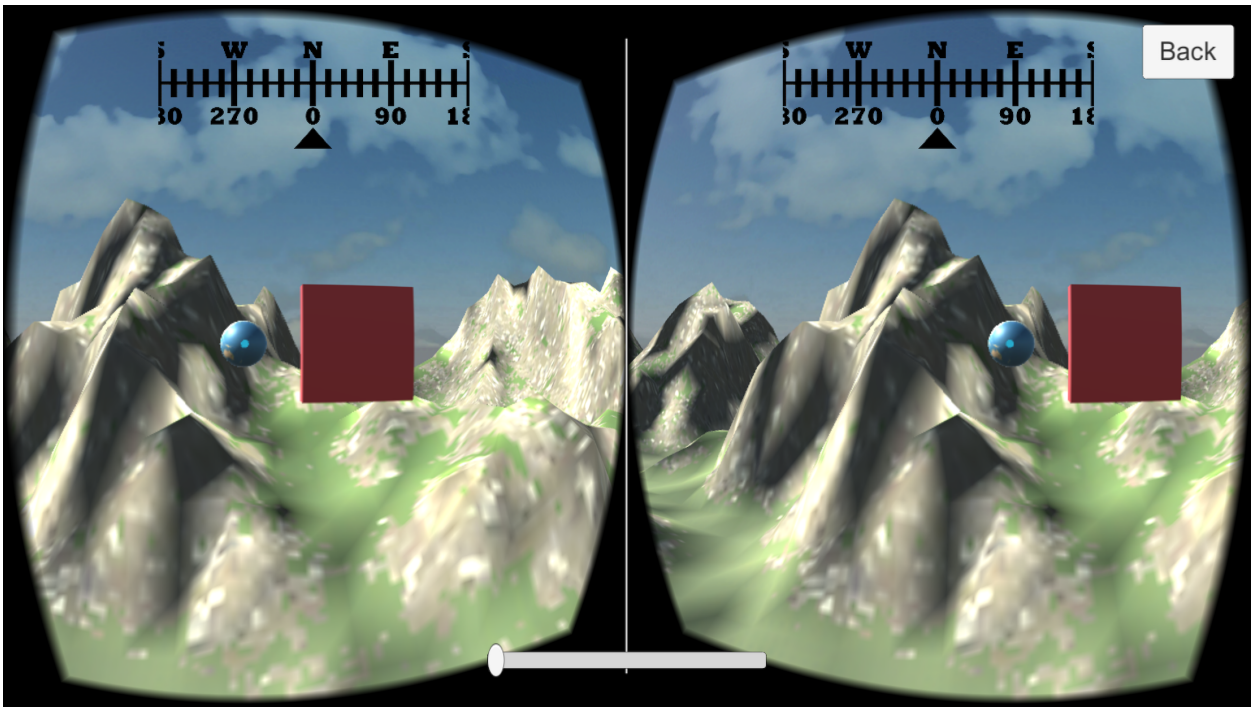

Figure 3.2: Virtual Reality World with no Magnetic Field

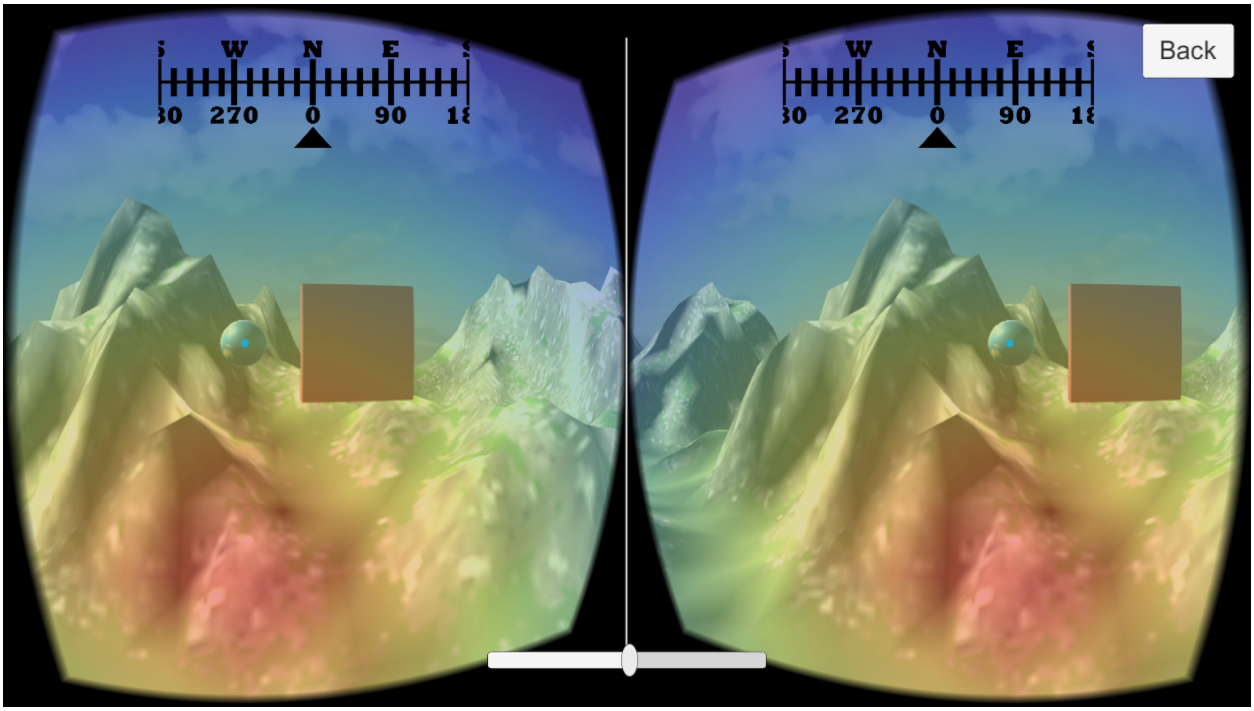

Figure 3.3: Virtual Reality World with Magnetic Field

3.4.3 Bird Eye Scenes

There are only two bird eye scenes because this app is more useful as a demonstration rather than a real model of what a bird may perceive. Google Cardboard or any sort of virtual reality only enables 60° of vision because that is what human eyes perceive. The 180° vision that a single bird's eye is known to have is just like a human's eye because 180° is achieved by rotating the eyeball in the eye socket. To replicate a bird's eye, a large solid angle of 170° in both horizontal and vertical directions must be warped into a flat square shape. Because of this, 3D effects are removed (they don't apply anyway since both eyes are looking in completely different directions). The warping is such that objects on the side of the screen look much larger than objects in the middle of the screen despite being the same size.

In the bimodal case, north can be found when areas of least anisotropic singlet yield are found across diagonals from the top inner parts of the image to the bottom outer parts of the image. When the bird head is pointed west or east, then one eye is pointed north and the other is pointed south, so each eye sees an area of maximum yield. When the head is pointed south, then the diagonals of least singlet yield are most symmetric but along the opposite of north such that they run from the top outer part of eye to the bottom inner portion of the eye.

In the quadramodal case, alignment is achieved by find a symmetric image between the left and right eye. There is a subtle difference between north and south and it could be learned. When the head is facing east or west, then there is a vertical symmetry.

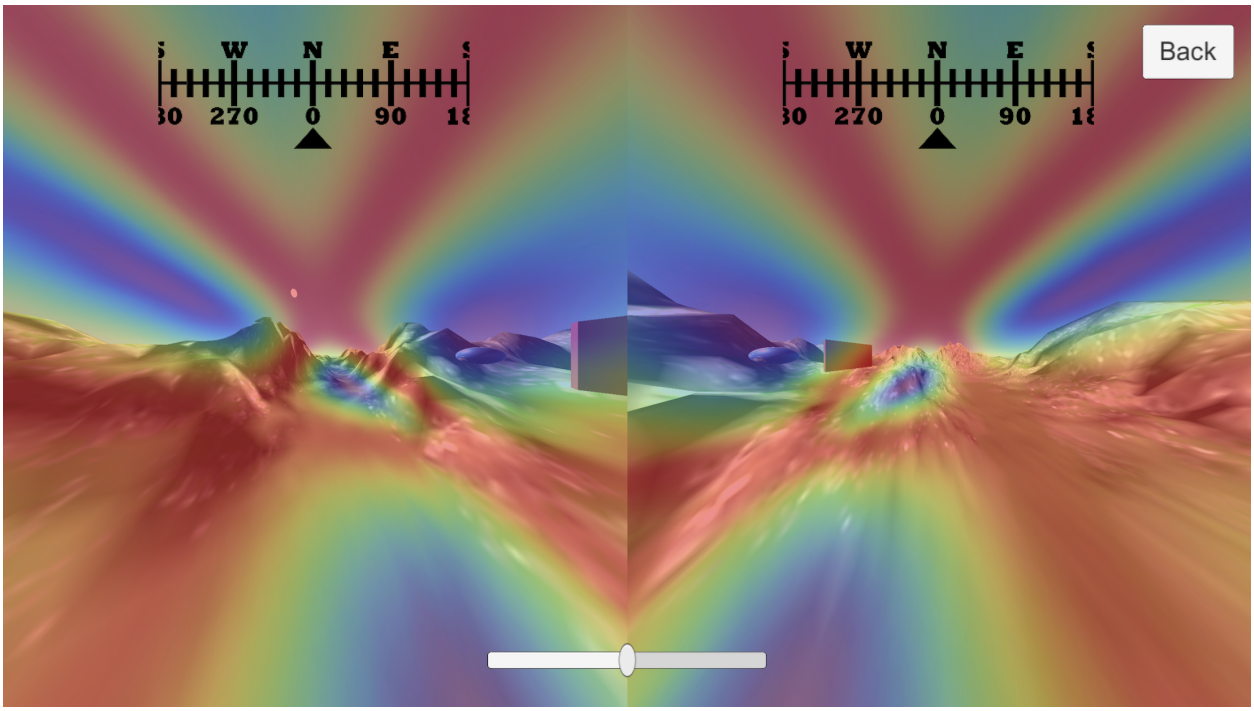

Figure 3.4: Bird's View of Virtual Reality World with Magnetic Field

Chapter 4

Experiments on Drosophila in Hirsch Maze

4.1 Introduction

Magnetoreception is a fascinating problem because it is a sense where the underlying mechanisms are still unknown. A wide range of organisms from birds, mammals, amphibians, fish, bacteria, and insects have been tested and documented to detect the geomagnetic field ([54], [55], [12], [6], [7], [21], [35], [11], [45], [15]). The extent to which organisms display behaviors such as migration, navigation, and alignment is varied along with reasons for why they might exhibit this behavior. Despite evidence that a magnetic sense exists, the mechanism is still not known. Due to evidence that the magnetic sense is connected to the ability to receive 502 nm turquoise light [55], the cryptochrome photoreceptor is a candidate to house the physics behind the mechanism. To explore this theory, biological experiments are needed to detail the biological models which can explain the decisions animals make in different magnetic field conditions.

Most of the current, good behavioral models do not explore difference in genetics whether by looking at known differences within the same species or looking at different generations of a species. The most convincing evidence of magnetoreception such as European robins [52] and sea turtles [25]do not look at differences within their own sub-family because these animals have long lifetimes and do not reproduce quickly. Also, affecting the gene expression in these animals is much more difficult than simpler insects or bacteria. The genetic models in Drosophila Melanogaster are reasonably well known. The cryptochromes in Drosophila can be engineered to have strains of flies that completely lack cryptochrome or only have certain portions of the cryptochrome mutated. Drosophilae are the easiest organisms to explore magnetic behavior while noting these differences in cryptochrome genetics.

Testing magnetoreception in Drosophila is not new. There have been many experiments in many assays with different ways of evaluating the effects of magnetic fields. Early experiments found that after being trained to associate the angle between the direction of a light motive and direction of a magnetic field, Drosophila were entered into a radial maze where they could choose one of eight directions to proceed. Male Drosophila displayed a strong magnetic response with respect to the magnetic field while females did not show any response. This behavior continues under blue light; under red light, the response was rotated by 90 degrees clockwise [36]. The Reppert lab showed a nave avoidance response in many strains of Drosophila but most prominently in Canton-S flies. These flies were able to be trained to move towards a magnetic gradient under full spectrum and blue light, but not red light. More importantly, there was a direct link to cryptochrome as the nave magnetic response was impaired and then recovered in certain mutations of cryptochrome and disappeared altogether in other mutations of cryptochrome [16], [15].

In addition to traveling towards magnetic fields, magnetic fields have been recorded to affect other behaviors. Exposure to magnetic fields raises the circadian rhythm period of Drosophila from 24 hours to 27 hours. This behavior continued under weak blue light, but was non-

existent under red light [57]. The tendency for flies to climb up inside a plexiglass cylinder was found to be inhibited by a magnetic field. Drosophila continued this negative geotaxis behavior under blue light [14].

The ability for Drosophila larvae has been hypothesized to be useful as larvae could use the magnetic field to orient themselves while burrowing. When larvae were tested, they seemed to prefer anti-cardinal quadramodal behavior. This means there was a tendency to not traverse North, South, East, or West, but rather NW, NE, SW, and SE [34]. Drosophila can be induced to experience a seizure by a constant pulse of light. Flies seizure duration was found to be extended when exposed to magnetic fields under blue light as compared to orange light, blue light, and magnetic fields separately [29].

Despite a great deal of work done in magnetoreception, theres been a low amount of incorporation with the even more extensive geotaxis research. Research done in geotaxis behaviors of Drosophila is much older starting from the 1960s when Drosophila were selected through Hirsch mazes by geotaxis behavior [56]. Eventually the Drosophilae were engineered into strains that preferred moving with or against Earths gravity. Later, the gene expression difference for these strains of flies compared to a control Canton-S fly was found [49](Toma, 2002). The strains of flies with extreme geotaxis behavior showed increased expression of cryptochrome. This organization is the basis for our exploration of magnetic field effects on Drosophila in a geotaxis setup.

The Hirsch maze is two dimensional which allows an external magnetic field the flexibility to intersect with the assay at many angles and directions. While many assays collect data after the fly has made a single decision, our assay allows for a longer amount of time per test and multiple movement decisions. On top of this, we need an assay that not only tells whether or not a magnetic sense exists but can provide a metric to measure the extent of magnetic sensitivity. Having steps allows us to make conclusions not just that Drosophila can or cannot respond to magnetic stimuli but the degree to which each fly moved towards

or away from a magnetic field gradient. When collecting data in the Hirsh maze, the results are quantized because the fly must end up in a tube. The Hirsch maze is a medium between T-mazes where the fly moves strictly towards or away from a field and radial assays where the fly can make a choice with initially 360° of motion. The Hirsh maze guides the flies in one direction with a light source but allows many choices in a perpendicular direction. This means that we can count not only the number of Drosophila that move towards a magnetic field, but the extent to which each fly moved. This setup enables us to tell what magnetic field conditions provide the largest magnetic response. Testing Drosophila in magnetic field effects has been notoriously difficult to reproduce. Its important to try to create an assay that can produce the most consistent results by minimizing the effect of as many extraneous variables as possible. Being able to see the degree to which each magnetic field condition affects the fly enables us hone in on the possible physics theories to understand the magnetoreception mechanism.

4.2 Geotaxis Maze

4.2.1 Hirsch Maze Overview

Hirsch mazes are a multiple unit classification assay. Typically used for selecting Drosophila with differences in geotactic and phototactic behavior, this assay can be used to test effects from other stimuli. The assay itself is two-dimensional while stimuli can be applied in all three directions. The assay used in these experiments uses a modified nine-step Hirsch-type maze which means Drosophilae make eight decisions to end up in nine final tubes.

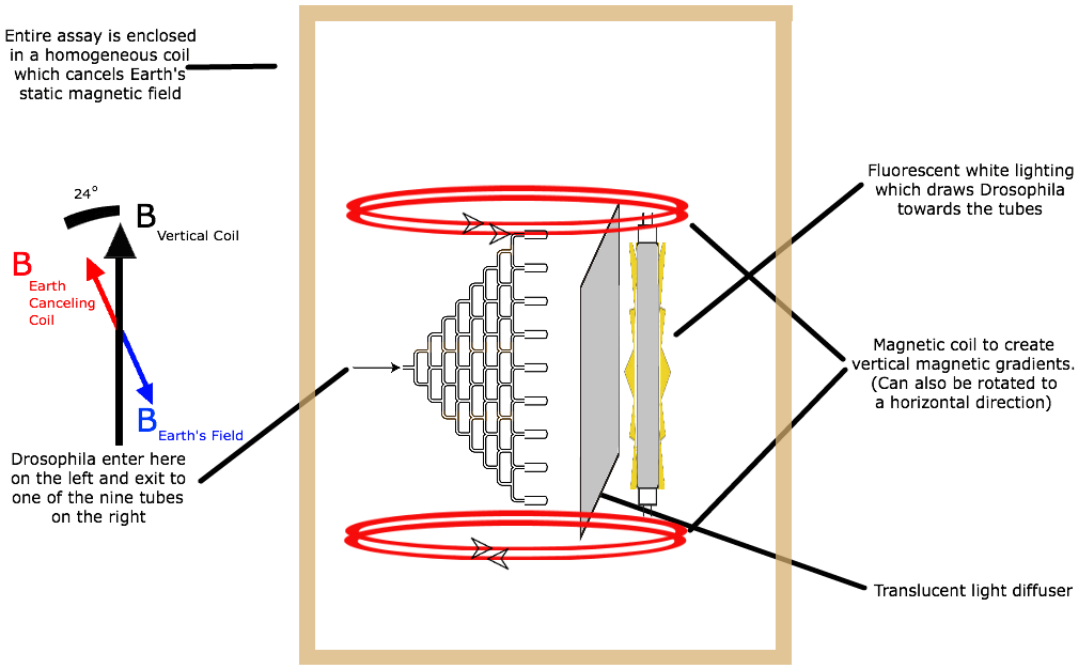

Figure 4.1: Schematic showing experimental apparatus. In vertical testing, Drosophila are loaded into the maze from the left entry point and traverse the maze from left to right towards the diffused, flourescent light source. Exit tubes are numbered from 1 to 9, starting from the lowest exit. The system is enclosed in a (brown) Merritt coil which is aligned with and cancels the local geomagnetic field, while the inner,red, 2-loop system produces a magnetic field gradient.

4.2.2 Development of Assay

Hirsch mazes were first made in 1959 to select Drosophila for geotaxis properties and to take a further look at chromosome differences. The first Hirsch maze constructed in our lab was made of 1/8 inner diameter tygon tubing ,Nalgene 1/8 inner diameter Y-type, and T-type polypropylene connectors. This structure was not rigid, so the assay needed to be mounted on plywood for consistent alignment and leveling. This assays largest problem was cleaning the maze as Drosophila would get stuck and die in the maze. This meant the maze needed to be taken apart and cleaned. The next maze design consists of two patterned halves of plexiglass bolted together [49]. These pieces are machined by a computer aided a plastic mill.

The two slabs contain screw holes so that these two pieces can be easily bolted together and taken apart to clean. Plexi-glass is optically translucent and structurally rigid for consistent experiments. The first iteration of this maze used unpolished plexi-glass which had the unexpected consequence of flies not being able to grip the walls of the maze resulting in flies slipping and getting stuck. The second iteration (see figure 2) used fire-polished mazes which rectifies this problem. As Drosophila walk into the end glass tube, they must pass through a hollow plastic cone which prevents the Drosophila from moving backward out of the tube. The maze is 16 cm across from the start to any final tube and 22 cm between the furthest end tubes.

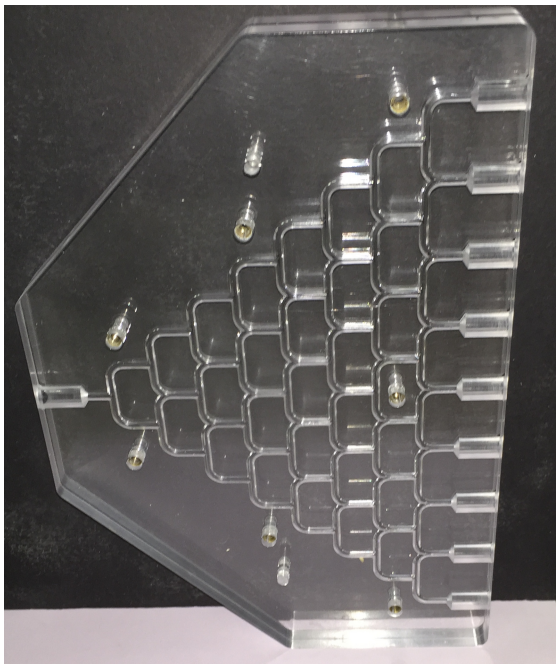

Figure 4.2: Second iteration of Hirsch-style maze, made of machined plexiglass

4.2.3 Motive for this Assay

The nine-step Hirsch maze is unique in comparison to other assays for magnetic testing. Drosophila travel perpendicular with respect to the direction of the magnetic field versus other assays where the head is either pointed in the direction of the magnetic field or the

Drosophila has free choice of what direction to face. Our assay requires all Drosophila to initially move in the same direction towards the light source. In nine steps, Drosophilae have eight opportunities to make directional decisions. T-maze or cross assays where the organism is inserted into the center of the maze must deal with a bias in that the organism is initially pointed in a certain direction. Assays with one or two steps also typically take less time for the Drosophilae to complete.

4.2.4 Scoring and Statistics

A positive geotaxis response means that an organism follows the force of gravity. Negative geotaxis indicates movement away from a gravitational force. Each experimental run is given a score by taking a weighted average of the number of Drosophila in each of the end tubes, with the bottom tube given value 1, and the top tube value 9. Thus, a score of 9 would correspond to extreme negative geotaxis, and a score of 1 would correspond to extreme positive geotaxis. In the horizontal configuration, a score of 1 would correspond to the left most tube, and 9 would correspond to the right most tube. The unit of statistical analysis was the average score for one set of Drosophila in one maze. Drosophila tested over two generations to ensure results are reproducible. Scores were tested using ANOVA and the Dunnett procedure for control group comparisons. Calculations were performed in Wolfram Mathematica 8.0 (Wolfram Research Inc, Champaign, IL USA).

4.3 Magnetic Field Systems

4.3.1 Canceling Earth's Static Field

Throughout all of the experiments in this paper, Earths static magnetic field was canceled by creating an equal and opposite magnetic field in the opposite direction by use of a Merritt coil. It consists of four square loops with side length of 1.5m, and wound with ratio 26:11:11:26, tilted to align with the local field [30]. The field inside the testing region was measured to be constant within 5% using an Integrity Design & Research IDR-321 geomagnetometer (Integrity Design and Research, Burington, VT) and was able to reduce Earths magnetic field by a factor of 100 from μT to .5 μT.

4.3.2 Magnetic Field Gradient Specifications

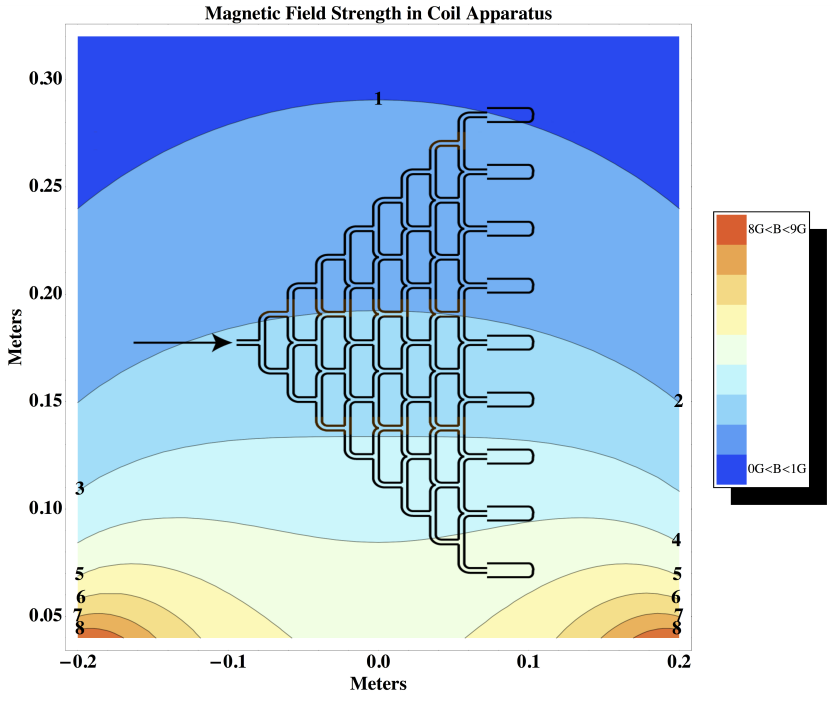

Figure 4.3: Magnetic gradient field from a circle loop with a magnitude of 5G at the center of the bottom loop

The magnetic gradient field is formed by two circle coil loops (see red coils in figure 1). Each one of these coil loops is double-wound [5]. This allows two currents to be run independently with a choice in clockwise or counterclockwise. In parallel, each coil loop can therefore create a field pointed in either direction, or in anti-parallel, the currents can cancel and create a net zero field. With two of these coil loops oriented parallel to each other, there is great flexibility in magnetic conditions with the intention of bio-electromagnetic experiments. A magnetic field can be created by both, one, or none of the coils; the field can have a general direction either towards or away from the center of the assay. Each coil loop has a circular diameter of 0.416 m and they are separated by 0.343m. To create a magnetic gradient, one coil loop has current run parallel to create the field, while the other loop is anti-parallel creating no net field. The intended field strength is calibrated so that the middle of the coil running parallel currents has a field strength of 500 μT (see figure 3). In the entire region within the coil loops, the strongest field was measured at 800 μT as close to the wire of the coil running parallel current and under 100 μT at the opposite coil. For the maze assay itself, the magnetic field strength varies from 500 μT to 100 μT between end tubes.

4.3.3 Defining Magnetic Field Conditions

In the vertical configuration as pictured in figure 1, a magnetic field is created by only either the top or bottom coil loop. When a magnetic field is created by the top coil and a net zero field by the bottom coil, a strong magnetic gradient is created from the top, and this condition is called a top field. In the opposite case a field is created from the bottom coil loop and is called a bottom field. Because we can also control the polarity of the magnetic field, the field created by a top or bottom coil which follows the right-hand rule and points up is called an up field. The same follows for a down field. In the horizontal direction, the condition created by the coil loop on the right side running parallel current and the left side producing no net field is named a right field. The opposite condition is a left field. For both

experiments in the vertical and horizontal directions, a control field is defined as a net zero magnetic field where both coil loops produce a net zero magnetic field.

4.4 Results

4.4.1 Geotaxis with Magnetic Field Gradient

The first experiment conducted was the comparison between "top field," "control field," and "bottom field" conditions with runs consisting of 75 males and females at one time. These magnetic field conditions were chosen in order to reproduce the naïve avoidance of 500 μT magnetic fields by Canton-S Drosophila in a T-Maze [15]. The difference in geotaxis maze scores between "top field" vs. " bottom field" ($F=6.41$ $P < 0.03$) are significant. This indicates that under a "top field," Drosophila ended up in a lower tube than " bottom field". This Canton-S strain set of data shows naive behaviors with respect to externally applied magnetic field gradients that are consistent with what was seen in T-mazes [15]. However, there's no difference between "top field" vs, "control field" & "bottom field" vs. "control field." For an attempt to confirm the above results, this experiment was repeated at a separate time and by a different experimentalist. From other labs working in this field and this lab's previous experience, the Canton-S strain of Drosophila have been the most responsive to magnetic fields [15]. 50 males and 50 females were tested across the same conditions. Again, between "top field" vs. "control field" & "bottom field" vs. "control field" conditions, both show no significant difference in maze scores. ($F=0.82$ & $P=0.372$, $F=0.845$ & $P=0.366$, respectively). However the difference in score between "top field" and "bottom field" was not significant ($F=3.37$, $P=0.076$) for this set of data. When the data of these two experiments were combined, the levels of significance mirror the first set of data in that the Drosophila show a significant naive avoidance response to a vertical gradient field

(F=4.57, P<0.05).

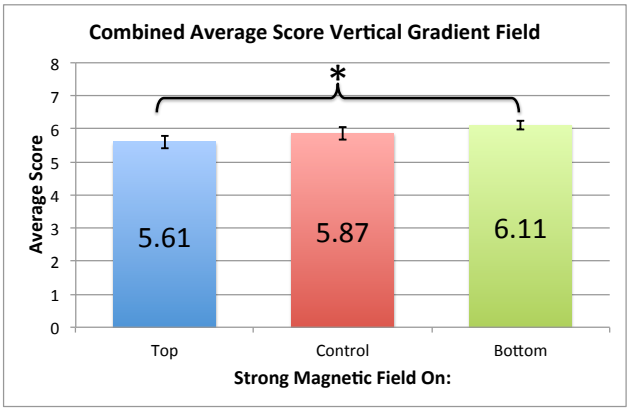

(a) low noise, small patch direction

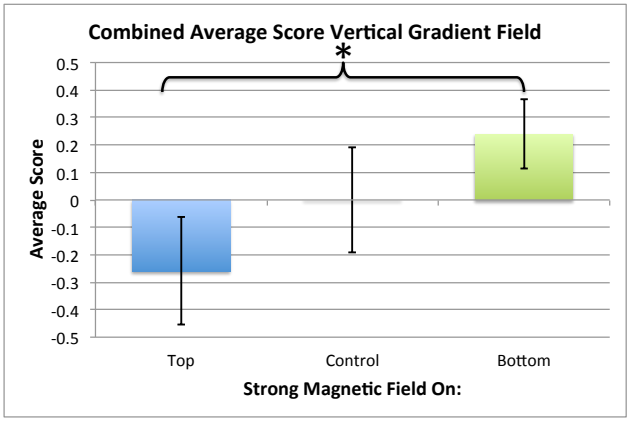

(b) low noise, small patch yield

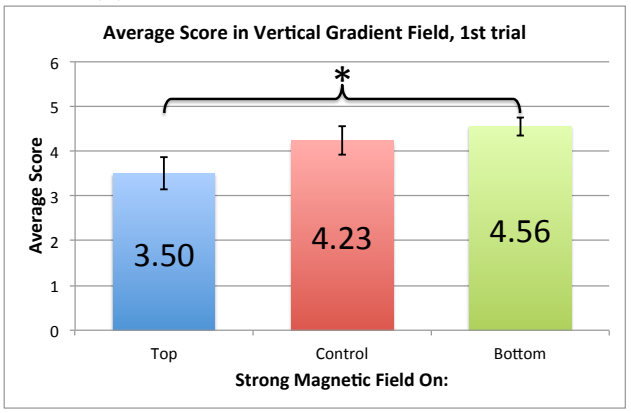

(c) low noise, large patch direction

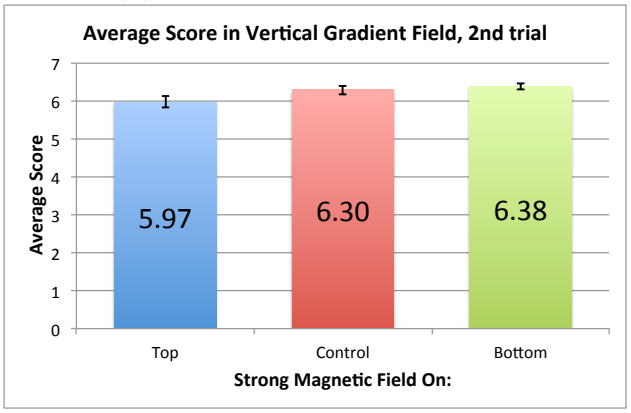

(d) low noise, large patch yield

Figure 4.4: a)With the maze in a vertical direction, over 5000 flies were tested in gradient fields stronger from the bottom or top, or a control zero net field. *=P<0.05. From the combined data, there is medium significance that the scores from a "top field" vs "bottom field" are different b) The score difference from control c) results from the first experiment conducted in May of 2011, of 1223 flies of generation 24 and 25 Canton-S flies d) results from the second experiment conducted in September of 2014, of 4134 flies of generation 60 and 61 Canton-S flies.

4.4.2 Horizontal Assay with Magnetic Field Gradient

In the horizontal setup, Drosophila have the option to travel left or right. This experiment compares "right field," "control field," and "left field" conditions by testing 75 males & females at a time and 50 males & females at a time by another experimenter. During the

first set of tests, there was no significant difference between any of the conditions. A "right field" is almost identical with the "control field", and the "left field" is not significant with the other conditions.

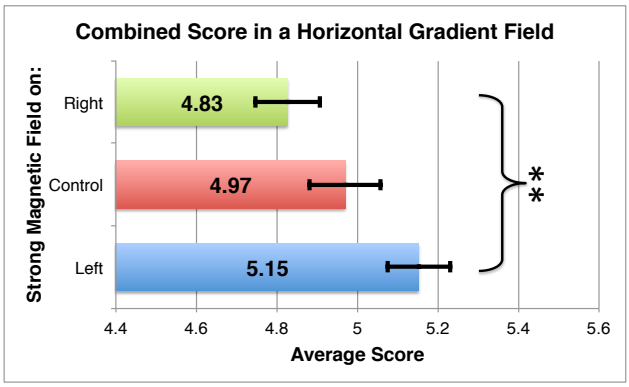

(a) low noise, small patch direction

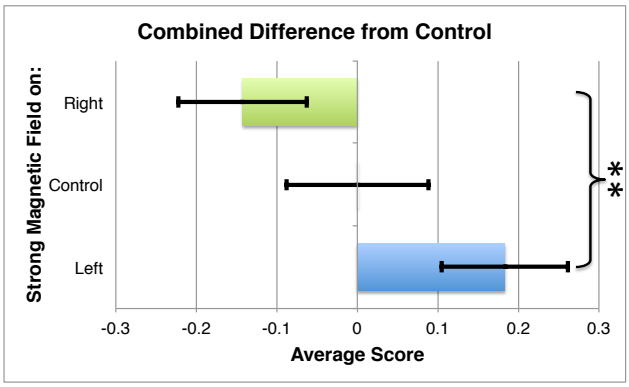

(b) low noise, small patch yield

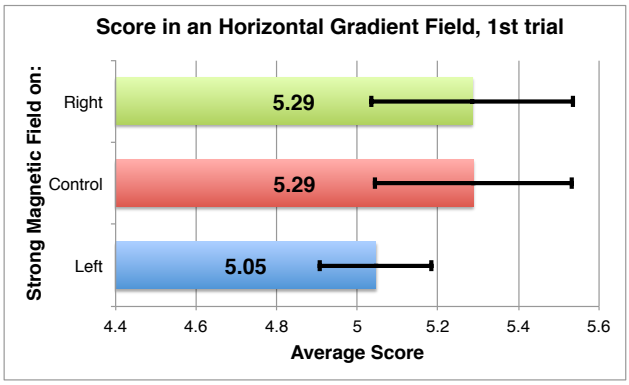

(c) low noise, large patch direction

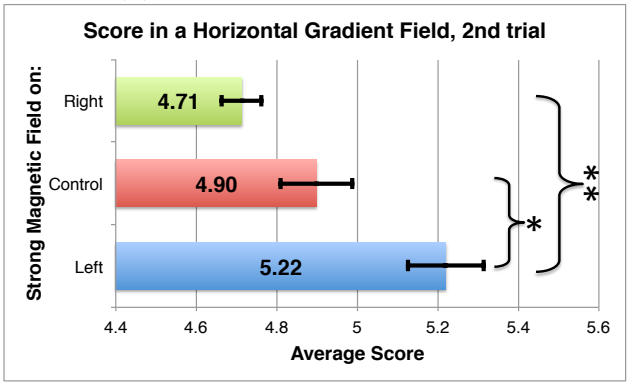

(d) low noise, large patch yield

Figure 4.5: a)With the maze in a horizontal direction, over 3437 flies were tested in "left field," "right field," and "control field" . *=P<0.05 and **=P<0.0005. From the combined data, there is very high significance that the scores from a "left field" vs. a "right field" are different b) The score difference from control c) results from the first experiment conducted in February of 2011, of 1122 flies of generation 22 and 23 Canton-S flies. There was no significant difference between any conditions d) results from the second experiment conducted in August of 2014, of 2315 flies flies of generation 58 Canton-S flies. There is a significance of *=P<0.05 between the "left field" vs. the "control field" and a very high significance of **=P<0.0005 between the "right field" vs. the "left field."

However, a second repetition of this experiment produced different results. Under a "left field", the Drosophila have a high score, indicating they prefered to move to the right. The opposite is true that under a "right field" the Drosophila scored lower and prefered the left side. There is no significance between "right field" and "control field" (F=3.12, P<0.1) but

between "control field" and "left field" there is a significant difference (F=6.14, P<0.02). When comparing the scores of "left field" vs "right field" there is very high significance (F=22.44, P<0.00005) that these mean scores are different. When this data from the two horizontal experiments was combined, Drosophila show a highly significant naive avoidance response to a horizontal gradient field (F= 8.17, P<0.01)

4.4.3 Vertical Assay with a Magnetic Field Gradient and Focusing on Polarity

In this assay, it's also possible to test if Drosophila respond to a different magnetic polarity in the gradient field. Equal number of tests were done for both top and bottom coils creating fields with positive and negative polarity refered to as "up field" and "down field" in a previous section. There is no difference between the "control field" and the "up field" and there was no significant difference between the "down field" compared to both the "control field" and "up field." The lack of of significance in difference of maze score for "up field" and "down field" (F=2.89 P<0.1) indicates that in this assay, polarity of magnetic field had no affect on Drosophila behavior.

4.5 Discussion

Our results describe a new behavioral assay that shows a magnetic response in Drosophila as well as providing additional insight into the scope and power of this sensory system. From these experiments alone, it's unclear whether Drosophila are sensitive to the intensity of the magnetic field or to the change or steepness of the magnetic field gradient. Canton-S Drosophila overall show a natural avoidance to the magnetic field from both vertical and horizontal orientations. The geotaxis behavior exhibitied by Drosophila can be influenced

by a magnetic field gradient. Horiztonally, Canton-S Drosophila respond almost symmetrically from oppositely applied magnetic fields. There was no indication that Drosophila respond to the polarity of the field. The radical pair mechanism, a magnetite based mechanism, or an unknown mechanism may be responsible for the magnetic sensitivity of geotaxis. Although there is no direct connection established between the magnetic field effects and cryptochrome at this time, a working theory is in progress. Our nine-step Hirsch maze provides an alternate degree of motion for Drosophila to move while changing the method by which a score is collected and calculated. Lengthening the testing time allows more room for a magnetic response rather than a sensory impulse. These alternates can be further useful in more experiments in exploring magnetoreception and other behavioral characteristics of Drosophila.

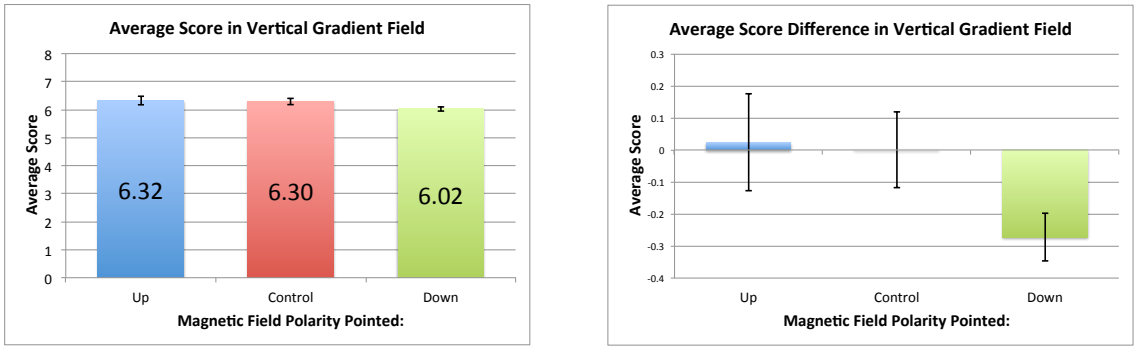

Figure 4.6: Under a 5G vertical gradient field that came from either the top or bottom coil, but with a consistent polarity in the magnetic field pointed up or down, there was no level of significant difference between any of the conditions

4.6 Methods Summary

4.6.1 D. melanogaster cultures and stocks

All Drosophila were raised on standard media at 22°C, with a 12h:12h light/dark cycle. Canton-S wildtype Drosophila obtained from Bloomington Fly Store. The Drosophila pro-

cedures are a summary of the more extensive information available in the book Drosophila Protocols, by William (UCSC) Sullivan, Michael Ashburner (Cambridge), and R. Scott Hawley (UCD). The experiments conducted in the vertical orientation were done first in May of 2011, testing 1223 flies of generation 24 and 25 Canton-S flies and then again in September of 2014 testing 4134 flies of generation 60 and 61 Canton-S flies. The experiments conducted in the horizontal orientation were done in February of 2011, testing 1122 flies of generation 22 and 23 Canton-S flies and then again in August of 2014, testing 2315 flies of generation 58 Canton-S flies.

4.6.2 Experimental Conditions

One test consists of a set number of males and females run through the two mazes simultaneously. The number of males & females were either 75 or 50 at one time. The Drosophila are aged 3-6 days, loaded into separate mazes placed side-by-side in the magnetic field exposure system until all Drosophila complete the maze. A typical run through the assay takes approximately 120 minutes for most Canton-S Drosophila to reach a tube at the end of the maze. A fluorescent tube light bulb is placed 30 cm from the end of the maze as motivation for the Drosophila to move forward. 10 cm in front of the lightbulb is a uniform diffuser. Light intensity is measured to be 15 μmol/cm^3 with a Li-Cor Biosceiences LI-250A light meter (Li-Cor Biosceinces Lincoln, NE). In the horizontal setup, the maze lies on its side, and to prevent a light bias, the maze is covered above and below with a nonmagnetic stiff black sheet. Mazes were cleaned gently with dilute Alconox, rinsed thoroughly with DI water, and vacuum dried at the end of each day.

Bibliography

[1] S. Åkesson, J. Morin, R. Muheim, and U. Ottosson. Avian orientation at steep angles of inclination: experiments with migratory white–crowned sparrows at the magnetic North Pole. *Proceedings of the Royal Society of London B: Biological Sciences*, 268(1479):1907–1913, Sept. 2001.

[2] E. Batschelet. *Recent statistical methods for orientation data*. Jan. 1972.

[3] R. Beason and J. Nichols. Magnetic orientation and magnetically sensitive material in a transequatorial migratory bird. *Nature*, 309:151–153, May 1984.

[4] R. Beason and P. Semm. Does the Avian Ophthalmic Nerve Carry Magnetic Navigational Information? *Journal of Experimental Biology*, (199):1241–1244, 1996.

[5] J. P. Beaugrand. An attempt to confirm magnetic sensitivity in the pigeon,Columba livia. *Journal of Comparative Physiology A*, 110(3):343–355, 1976.

[6] S. Begall, E. P. Malkemper, J. Červený, P. Němec, and H. Burda. Magnetic alignment in mammals and other animals. *Mammalian Biology - Zeitschrift für Säugetierkunde*, 78(1):10–20, Jan. 2013.

[7] H. Burda, S. Marhold, T. Westenberger, R. Wiltschko, and W. Wiltschko. Magnetic compass orientation in the subterranean rodentCryptomys hottentotus (Bathyergidae). *Experientia*, 46(5):528–530, May 1990.

[8] A. R. Cashmore. Cryptochromes: Blue Light Receptors for Plants and Animals. *Science*, 284(5415):760–765, Apr. 1999.

[9] J. Cerveny, S. Begall, P. Koubek, P. Novakova, and H. Burda. Directional preference may enhance hunting accuracy in foraging foxes. *Biology Letters*, 7(3):355–357, May 2011.

[10] M. E. Deutschlander, J. Phillips, and S. C. Borland. Extraocular magneticcompass in newts. *Nature*, 400:322–324, July 1999.

[11] F. J. Diego-Rasilla, R. M. Luengo, and J. B. Phillips. Light-dependent magnetic compass in Iberian green frog tadpoles. *Naturwissenschaften*, 97(12):1077–1088, Oct. 2010.

[12] D. H. Dommer, P. J. Gazzolo, M. S. Painter, and J. B. Phillips. Magnetic compass orientation by larval Drosophila melanogaster. *Journal of Insect Physiology*, 54(4):719–726, Apr. 2008.

[13] D. T. Edmonds. A Sensitive Optically Detected Magnetic Compass for Animals. *Proceedings of the Royal Society of London B: Biological Sciences*, 263(1368):295–298, Mar. 1996.

[14] G. Fedele, E. W. Green, E. Rosato, and C. P. Kyriacou. An electromagnetic field disrupts negative geotaxis in Drosophila via a CRY-dependent pathway. *Nature Communications*, 5:1–6, 1.

[15] R. J. Gegear, A. Casselman, S. Waddell, and S. M. Reppert. Cryptochrome mediates light-dependent magnetosensitivity in Drosophila. *Nature*, 454(7207):1014–1018, July 2008.

[16] R. J. Gegear, L. E. Foley, A. Casselman, and S. M. Reppert. Animal cryptochromes mediate magnetoreception by an unconventional photochemical mechanism. *Nature*, 463(7282):804–807, Nov. 2010.

[17] N. S. Hart, J. C. Partridge, and I. C. Cuthill. Visual pigments, oil droplets and cone photoreceptor distribution in the european starling (Sturnus vulgaris). *Journal of Experimental Biology*, 201(9):1433–1446, May 1998.

[18] V. Hart, P. Nováková, E. Malkemper, S. Begall, V. Hanzal, M. Ježek, T. Kušta, V. Němcová, J. Adámková, K. Benediktová, J. Červený, and H. Burda. Dogs are sensitive to small variations of the Earth's magnetic field. *Frontiers in Zoology*, 10(1):80, 2013.

[19] S. Healy. Vision, brain and behavior in birds. *Trends in Ecology & Evolution*, 9(9):351, Sept. 1994.

[20] A. J. Kalmijn. The Electric Sense of Sharks and Rays. *Journal of Experimental Biology*, (55):371–383, 1971.

[21] T. Kimchi and J. Terkel. Magnetic compass orientation in the blind mole rat Spalax ehrenbergi. *Journal of Experimental Biology*, 204(4):751–758, Feb. 2001.

[22] J. L. KIRSCHVINK. South-Seeking Magnetic Bacteria: Short Communications. *Journal of Experimental Biology*, 86(1):345–347, June 1980.

[23] J. L. Kirschvink and J. L. Gould. Biogenic magnetite as a basis for magnetic field detection in animals. *Bio Systems*, 13(3):181–201, Jan. 1981.

[24] J. C. S. Lau, C. T. Rodgers, and P. J. Hore. Compass magnetoreception in birds arising from photo-induced radical pairs in rotationally disordered cryptochromes. *Journal of The Royal Society Interface*, 9(77):3329–3337, Oct. 2012.

[25] K. J. Lohmann and C. M. F. Lohmann. Detection of magnetic field intensity by sea turtles. *Nature*, 380(6569):59–61, Mar. 1996.

[26] K. Maeda. Magnetically sensitive light-induced reactionsin cryptochrome are consistent with its proposed role as a magnetoreceptor. pages 1–6, Mar. 2012.

[27] K. Maeda, K. B. Henbest, F. Cintolesi, I. Kuprov, C. T. Rodgers, P. A. Liddell, D. Gust, C. R. Timmel, and P. J. Hore. Chemical compass model of avian magnetoreception. *Nature*, 453(7193):387–390, Apr. 2008.

[28] E. J. Maier and J. K. Bowmaker. Colour vision in the passeriform bird, Leiothrix lutea: correlation of visual pigment absorbance and oil droplet transmission with spectral sensitivity. *Journal of Comparative Physiology A*, 172(3):295–301, Apr. 1993.

[29] R. Marley, C. N. G. Giachello, N. S. Scrutton, R. A. Baines, and A. R. Jones. Cryptochrome-dependent magnetic field effect on seizure response in Drosophila larvae. *Scientific Reports*, 4, July 2014.

[30] R. Merritt, C. Purcell, and G. Stroink. Uniform magnetic field produced by three, four, and five square coils. *Review of Scientific Instruments*, 54(7):879–882, July 1983.

[31] R. W. MURRAY. The Response of the Ampullae of Lorenzini of Elasmobranchs to Electrical Stimulation. *Journal of Experimental Biology*, 39(1):119–128, Mar. 1962.

[32] A. R. O'Dea, A. F. Curtis, N. J. B. Green, C. R. Timmel, and P. J. Hore. Influence of Dipolar Interactions on Radical Pair Recombination Reactions Subject to Weak Magnetic Fields. *The Journal of Physical Chemistry A*, 109(5):869–873, Feb. 2005.

[33] P. J. H. Olga Efimova. Role of Exchange and Dipolar Interactions in the Radical Pair Model of the Avian Magnetic Compass. *Biophysical Journal*, 94(5):1565–1574, Mar. 2008.

[34] M. S. Painter, D. H. Dommer, W. W. Altizer, R. Muheim, and Phil. Spontaneous magnetic orientation in larval Drosophila shares properties with learned magnetic compass responses in adult flies and mice. *Journal of Experimental Biology*, 216(7):1307–1316, Mar. 2013.

[35] Phil, R. Muheim, and P. E. Jorge. A behavioral perspective on the biophysics of the light-dependent magnetic compass: a link between directional and spatial perception? *Journal of Experimental Biology*, 213(19):3247–3255, Sept. 2010.

[36] J. B. Phillips and O. Sayeed. Wavelength-dependent effects of light on magnetic compass orientation in Drosophila melanogaster. pages 1–6, May 2004.

[37] J. B. Phillips, P. W. Youmans, R. Muheim, K. A. Sloan, L. Landler, M. S. Painter, and C. R. Anderson. Rapid Learning of Magnetic Compass Direction by C57BL/6 Mice in a 4-Armed 'Plus' Water Maze. *PLoS ONE*, 8(8):e73112, Aug. 2013.

[38] T. Ritz. Quantum effects in biology: Bird navigation. *Procedia Chemistry*, 3(1):262–275, Jan. 2011.

[39] T. Ritz, S. Adem, and K. Schulten. A Model for Photoreceptor-Based Magnetoreception in Birds. *Biophysical Journal*, 78(2):707–718, Feb. 2000.

[40] T. Ritz, P. Thalau, J. B. Phillips, R. Wiltschko, and W. Wiltschko. Resonance effects indicate a radical-pair mechanism for avian magnetic compass. *Nature*, 429(6988):177–180, May 2004.

[41] C. T. Rodgers. Magnetic field effects in chemical systems. *Pure and Applied Chemistry*, 81(1):19–43, 2009.

[42] C. T. Rodgers and P. J. Hore. Chemical magnetoreception in birds: The radical pair mechanism. pages 1–8, Jan. 2009.

[43] V. P. Shcherbakov and M. Winklhofer. The osmotic magnetometer: A new model for magnetite-based magnetoreceptors in animals. *European Biophysics Journal*, 28(5):380–392, June 1999.

[44] I. A. Solov'yov, H. Mouritsen, and K. Schulten. Acuity of a Cryptochrome and Vision-Based Magnetoreception System in Birds. *Biophysj*, 99(1):40–49, July 2010.

[45] A. Stabrowski and P. M. Nollen. The responses of Philophthalmus gralli and P. megalurus miracidia to light, gravity and magnetic fields. *International Journal for Parasitology*, 15(5):551–555, Oct. 1985.

[46] P. Thalau, T. Ritz, K. Stapput, R. Wiltschko, and W. Wiltschko. Magnetic compass orientation of migratory birds in the presence of a 1.315MHz oscillating field. *Naturwissenschaften*, 92(2):86–90, Dec. 2004.

[47] C. R. Timmel and K. B. Henbest. A study of spin chemistry in weak magnetic fields. *Philosophical Transactions of the Royal Society A: Mathematical, Physical and Engineering Sciences*, 362(1825):2573–2589, Dec. 2004.

[48] C. R. Timmel, U. Till, B. Brocklehurst, K. A. Mclauchlan, and P. J. Hore. Effects of weak magnetic fields on free radical recombination reactions. *Molecular Physics*, 95(1):71–89, Sept. 1998.

[49] D. P. Toma, K. P. White, J. Hirsch, and R. J. Greenspan. Identification of genes involved in Drosophila melanogaster geotaxis, a complex behavioral trait. *Nature Genetics*, June 2002.

[50] T. Válková and M. Vácha. How do honeybees use their magnetic compass? Can they see the North? *Bulletin of Entomological Research*, 102(4):461–467, Aug. 2012.

[51] C. Walcott, J. L. Gould, and J. L. KIRSCHVINK. Pigeons have magnets. *Science*, 205(4410):1027–9, Oct. 1979.

[52] R. Wiltschko and W. Wiltschko. Magnetoreception. *BioEssays*, 28(2):157–168, Feb. 2006.

[53] W. Wiltschko, U. Munro, H. Ford, and R. Wiltschko. Red light disrupts magnetic orientation of migratory birds. *Nature*, 364(6437):525–527, Aug. 1993.

[54] W. Wiltschko and R. Wiltschko. Magnetic Compass of European Robins. *Science*, 176(4030):62–64, Apr. 1972.

[55] W. Wiltschko and R. Wiltschko. Magnetic orientation and magnetoreception in birds and other animals. *Journal of Comparative Physiology A*, 191(8):675–693, May 2005.

[56] C. M. Woolf, H. M. Sasmor, and T. A. Markow. Positive and negative geotaxis: Sex-linked traits inDrosophila pseudoobscura. *Behavior Genetics*, 8(1):65–71, Jan. 1978.

[57] T. Yoshii, M. Ahmad, and C. Helfrich-Förster. Cryptochrome Mediates Light-Dependent Magnetosensitivity of Drosophila's Circadian Clock. *PLoS Biology*, 7(4):e86, 2009.